

1. Report No. <b>FHWA/TX-10/0-6132-1</b>		2. Government Accession No.		3. Recipient's Catalog No.	
4. Title and Subtitle <b>NEW GENERATION MIX-DESIGNS: LABORATORY TESTING AND CONSTRUCTION OF THE APT TEST SECTIONS</b>				5. Report Date <b>December 2009</b> <b>Published: March 2010</b>	
				6. Performing Organization Code	
7. Author(s) <b>Lubinda F. Walubita, Vivekram Umashankar, Xiaodi Hu, Brandon Jamison, Fujie Zhou, Tom Scullion, Amy Epps Martin, and Samer Dessouky</b>				8. Performing Organization Report No. <b>Report 0-6132-1</b>	
9. Performing Organization Name and Address <b>Texas Transportation Institute, The Texas A&amp;M University System College Station, Texas 77843-3135 and The University of Texas at San Antonio, San Antonio, TX 78249.</b>				10. Work Unit No. (TRAIS)	
				11. Contract or Grant No. <b>Project 0-6132</b>	
12. Sponsoring Agency Name and Address <b>Texas Department of Transportation Research and Technology Implementation Office P. O. Box 5080 Austin, Texas 78763-5080</b>				13. Type of Report and Period Covered <b>Technical Report: September 2008-September 2009</b>	
				14. Sponsoring Agency Code	
15. Supplementary Notes Project performed in cooperation with the Texas Department of Transportation and the Federal Highway Administration. Project Title: Development and Field Evaluation of the Next Generation of HMA Mix Design Procedures URL: <a href="http://tti.tamu.edu/documents/0-6132-1.pdf">http://tti.tamu.edu/documents/0-6132-1.pdf</a>					
16. Abstract Recent changes to the Texas HMA mix-design procedures such as adaption of the higher PG asphalt-binder grades and the Hamburg test have ensured that the mixes routinely used on the Texas highways are not prone to rutting. However, performance concerns have been raised about these mixes, which are now "drier", more difficult to compact, and more susceptible to cracking. This is particularly problematic with the dense-graded Type C and D mixes that are widely used throughout the State of Texas. Consequently, several new ideas are under consideration to either modify the existing mix-design criteria (target densities, VMA requirements, etc.) and/or to include new and simpler cracking test procedures. Of primary focus in this research project is the comparative evaluation of the following three mix-design procedures and making recommendations thereof: (1) the modified volumetric mix-design procedure; (2) the Hamburg (rutting) and Overlay (cracking) test based balanced mix-design procedure; and (3) a simplified balanced mix-design procedure with a simpler alternative cracking test. The research methodology and scope of work incorporates extensive literature review of the existing mix-design procedures, laboratory testing, and field validation including accelerated pavement testing (APT) and performance monitoring. This interim report provides a preliminary overview of the mix-designs and laboratory test evaluations of three commonly used Texas mixes (namely Type B, Type C, and Type D) based on the Texas gyratory, volumetric, and balanced mix-design procedures. As well as conducting round-robin tests in six different Texas laboratories to quantify the Overlay test variability and repeatability, the laboratory tests also included comparative evaluation of various cracking tests such as the indirect tension, direct uniaxial tension, and semi-circular bending. HMA mix workability and compactability tests for quantifying the constructability aspects of the mixes were also conducted and are discussed in this report. Construction details of the APT test sections are also discussed in this interim report.					
17. Key Words <b>Mix-Design, Volumetric, Balanced, Texas Gyratory Compactor, Hamburg, Rutting, Overlay, Cracking, APT, Infra-Red, Thermal Imaging, X-Ray CT, GPR, FWD, ALF, Workability, Compactability</b>			18. Distribution Statement <b>No restrictions. This document is available to the public through NTIS: National Technical Information Service Springfield, Virginia 22161 <a href="http://www.ntis.gov">http://www.ntis.gov</a></b>		
19. Security Classif.(of this report) <b>Unclassified</b>		20. Security Classif.(of this page) <b>Unclassified</b>		21. No. of Pages <b>180</b>	
				22. Price	



**NEW GENERATION MIX-DESIGNS:  
LABORATORY TESTING AND CONSTRUCTION OF THE APT TEST  
SECTIONS**

by

Lubinda F. Walubita, Vivekram Umashankar, Xiaodi Hu,  
Brandon Jamison, Fujie Zhou, Tom Scullion, Amy Epps Martin

Texas Transportation Institute  
Texas A&M University System

and

Samer Dessouky

University of Texas at San Antonio

Report 0-6132-1

Project 0-6132

Project Title: Development and Field Evaluation of the Next Generation of  
HMA Mix Design Procedures

Performed in cooperation with the  
Texas Department of Transportation  
and the  
Federal Highway Administration

December 2009

Published: March 2010

TEXAS TRANSPORTATION INSTITUTE  
The Texas A&M University System  
College Station, Texas 77843-3135

University of Texas at San Antonio  
San Antonio, Texas 78249



## **DISCLAIMER**

The contents of this report reflect the views of the authors, who are responsible for the facts and the accuracy of the data presented herein. The contents do not necessarily reflect the official view or policies of the Federal Highway Administration (FHWA) or the Texas Department of Transportation (TxDOT). This report does not constitute a standard, specification, or regulation, nor is it intended for construction, bidding, or permit purposes. The United States Government and the State of Texas do not endorse products or manufacturers. Trade or manufacturers' names appear herein solely because they are considered essential to the object of this report. The engineer in charge was Tom Scullion, P.E. (Texas No. 62683).

## **ACKNOWLEDGMENTS**

This project was conducted for TxDOT, and the authors thank TxDOT and FHWA for their support in funding this research project. In particular, the guidance and technical assistance provided by the project director (PD) Dale Rand, P.E., of TxDOT, proved invaluable. The following project advisors also provided valuable input throughout the course of the project: Hector Cantu, Miles Garrison, and Robert Lee.

Special thanks are also extended to Lee Gustavus, Rick Canatella, and Tony Barbosa from the Texas Transportation Institute (TTI) for their help with laboratory and field work. A word of gratitude is also conveyed to the Louisiana Transportation Research Center and the Louisiana State University for their help with the accelerated pavement testing.

## TABLE OF CONTENTS

LIST OF FIGURES .....	xii
LIST OF TABLES .....	xiv
LIST OF NOTATIONS AND SYMBOLS.....	xvi
CHAPTER 1. INTRODUCTION .....	1-1
BACKGROUND .....	1-1
The Proposed Modified Volumetric Mix-Design Procedure.....	1-1
The Proposed Balanced Mix-Design Procedure .....	1-2
The Proposed Simplified Balanced Mix-Design Procedure .....	1-2
HMA Workability and Compactability Evaluation .....	1-3
ACCELERATED PAVEMENT TESTING .....	1-3
RESEARCH OBJECTIVES AND SCOPE OF WORK.....	1-3
DESCRIPTION OF THE REPORT CONTENTS .....	1-5
SUMMARY .....	1-5
CHAPTER 2. LITERATURE REVIEW .....	2-1
PREVIOUS RESEARCH ON CRACK MODELING IN TEXAS .....	2-1
THE INDIRECT TENSION TEST METHOD .....	2-2
IDT Data Analysis .....	2-3
IDT Test Evaluation.....	2-6
THE SEMICIRCULAR BENDING TEST METHOD .....	2-6
SCB Data Analysis .....	2-7
SCB Test Evaluation.....	2-9
THE DIRECT TENSION TEST METHOD.....	2-10
DT Data Analysis.....	2-10
DT Test Evaluation.....	2-11
THE OVERLAY TESTER METHOD .....	2-12
OT Data Analysis.....	2-12
OT Test Evaluation.....	2-13
THE MODIFIED OVERLAY TESTER METHOD .....	2-13
SUMMARY .....	2-15

## TABLE OF CONTENTS (CONTINUED)

CHAPTER 3. MATERIALS, MIX TYPES, AND EXPERIMENTAL DESIGN .....	3-1
MATERIALS AND MIX-DESIGNS .....	3-1
Mix-Design Modifications.....	3-2
Aggregate Gradations .....	3-3
Aggregate Sieve Analysis .....	3-4
LAB TEST PLANS AND HMA SPECIMEN MATRIX.....	3-5
HMA SPECIMEN FABRICATION.....	3-8
Short-Term Oven Aging and Molding.....	3-9
Cutting and Coring of the Specimens .....	3-9
SUMMARY .....	3-10
CHAPTER 4. AIR VOID CHARACTERIZATION WITH X-RAY CT	
SCANNING TESTS .....	4-1
THE X-RAY CT SCANNER .....	4-1
X-RAY CT TEST RESULTS.....	4-3
AV Distribution in 6-Inch Diameter by 6.9-Inch high DT Molded Samples .....	4-3
AV Uniformity and Variability- 6-versus 4-Inch High DT Test Specimens.....	4-5
Effects of the SGC Molds on the 6.9-Inch High DT Samples .....	4-5
AV Distribution in 6-Inch Diameter by 4.5-Inch High OT Molded Samples .....	4-6
AV Distribution versus Sample Molding Height .....	4-7
HMA Mix Comparisons–Type B versus Type D Mix .....	4-7
Sample Trimming Distance .....	4-9
SUMMARY .....	4-10
CHAPTER 5. LABORATORY CRACKING TESTS, RESULTS, AND	
COMPARATIVE EVALUATION OF THE TEST METHODS .....	5-1
LABORATORY CRACKING TEST PROTOCOLS .....	5-1
HMA MIXES EVALUATED.....	5-3
REPEATED-LOADING OT TEST RESULTS .....	5-3
MONOTONIC-LOADING DT TEST RESULTS .....	5-5
MONOTONIC-LOADING IDT TEST RESULTS .....	5-9



MONOTONIC-LOADING SCB TEST RESULTS .....	5-11
REPEATED-LOADING IDT (R-IDT) TESTING .....	5-13
Selection of the R-IDT Input Loads .....	5-13
Preliminary R-IDT Test Results for Type B Mix .....	5-13
REPEATED LOADING SCB (R-SCB) TESTING .....	5-15
Selection of the R-IDT Input Loads .....	5-15
Preliminary R-SCB Test Results for Type B Mix .....	5-15
EVALUATION AND COMPARISON OF THE CRACKING TEST METHODS .....	5-17
MIX AND TEST METHOD RANKING .....	5-17
SUMMARY .....	5-21
CHAPTER 6. OVERLAY ROUND-ROBIN TESTING AND VARIABILITY-	
REPEATABILITY EVALUATION .....	6-1
THE OT TEST METHOD.....	6-1
HMA MIX AND SPECIMEN FABRICATION .....	6-2
OT ROUND-ROBIN TEST PLAN .....	6-3
OT ROUND-ROBIN TEST RESULTS .....	6-4
Specimen Air-Voids.....	6-4
Initial Tensile Peak Loads.....	6-5
Number of OT Cycles to Failure .....	6-5
GENERAL OBSERVATIONS AND DISCREPANCIES .....	6-10
OT Software.....	6-10
OT Machine Calibration and Load Rate.....	6-10
Initial Start Loads.....	6-12
Sample Drying and Gluing .....	6-13
Specimen Geometry.....	6-13
Glue Curing and Weights.....	6-13
Sample Test Setup.....	6-14
RECOMENDATIONS.....	6-14
SUMMARY .....	6-15
CHAPTER 7. DEVELOPMENT OF WORKABILITY AND COMPACTABILITY	
INDICATORS FOR HMA .....	7-1

INTRODUCTION .....	7-1
LITERATURE REVIEW .....	7-2
Energy Indices Parameters.....	7-2
Compaction Curve Characteristics .....	7-2
Shear Stress Measurements.....	7-3
DESCRIPTION OF SAMPLES .....	7-14
Compaction Curve .....	7-15
TESTING RESULTS AND ANALYSIS .....	7-17
Effect of Apparatus .....	7-17
Effect Binder Content .....	7-18
Effect Mix Design.....	7-22
SUMMARY AND FINDING.....	7-23
FUTURE WORK.....	7-23
CHAPTER 8. MIX-DESIGN EVALUATIONS AND CONSTRUCTION OF	
THE APT TEST SECTIONS .....	8-1
MIX-DESIGN METHODS AND HMA MIX EVALUATED .....	8-1
The Texas Gyrotory Mix-Design Method.....	8-1
The Proposed Balance Mix-Design Method.....	8-2
The HMA Mix Utilized for APT Testing .....	8-3
DESCRIPTION OF THE APT FACILITY AND THE ALF MACHINE .....	8-4
CONSTRUCTION OF THE APT TEST SECTIONS .....	8-5
Subgrade, Subbase, and Base Materials .....	8-5
Construction of Joints in the JCP Sections .....	8-7
HMA Placement, Paving, and Compaction Process .....	8-8
CONSTRUCTION QUALITY CONTROL-ASSURANCE TESTS .....	8-9
IR Thermal Imaging .....	8-9
Nuclear Density Measurements .....	8-10
QC Asphalt-Binder Tests .....	8-10
GPR Measurements .....	8-11
Raw Materials, Plant Mixes, and Cores .....	8-12
APT TEST PLAN .....	8-12

SUMMARY .....	8-13
CHAPTER 9. SUMMARY OF FINDINGS .....	9-1
MAJOR FINDINGS TO DATE .....	9-1
Research Overview and Laboratory Mix-Design Evaluations .....	9-1
Literature Review on Cracking Tests .....	9-2
Air Voids and X-Ray CT Scanning Tests .....	9-3
Cracking Test Evaluation .....	9-3
Overlay Round-Robin Tests .....	9-4
Workability and Compactability Indicator Tests .....	9-5
Field Mix-Design Evaluations and APT Testing .....	9-6
ONGOING AND FUTURE PLANNED WORKS.....	9-7
PRODUCT DELIVERABLES .....	9-7
REFERENCES .....	R-1
APPENDIX A: AGGREGATE GRADATIONS .....	A-1
APPENDIX B: AIR VOID DISTRIBUTION .....	B-1
APPENDIX C: CRACKING TEST RESULTS .....	C-1
APPENDIX D: OT ROUND-ROBIN TEST RESULTS.....	D-1
APPENDIX E: MIX-DESIGN DETAILS FOR WORKABILITY AND COMPACTABILITY INDICATOR TESTS .....	E-1
APPENDIX F: APT CONSTRUCTION DETAILS .....	F-1

## LIST OF FIGURES

Figure	Page
3-1 Aggregate Gradations .....	3-4
4-1 Pictorial Setup of TTI's X-Ray CT Scanner .....	4-2
4-2 Original SGC Compaction Cylinders .....	4-2
4-3 Typical AV Distribution in 6"φ by 6.9" High DT Molded Sample.....	4-3
4-4 Comparison of DT Failure Zones and Vertical AV Distribution .....	4-4
4-5 AV Percentage and Size Distribution in a 4.5-Inch High Molded Sample .....	4-6
4-6 AV Distribution versus Molding Height .....	4-7
4-7 AV Size Comparisons for DT Samples–Type B versus Type D Mix .....	4-8
5-1 Example of Typical OT Crack Failure with a Single Crack.....	5-4
5-2 Example of DT Failure Modes .....	5-7
5-3 Example of End Cap Failure .....	5-7
5-4 DT Stress-Strain Response Curves and Typical Crack Failure Mode.....	5-8
5-5 IDT Stress-Deformation Curves and Typical Crack Failure Mode.....	5-10
5-6 SCB Stress-Displacement Curves and Typical Crack Failure Mode .....	5-12
5-7 Type D R-IDT Percent Load Relationship Curves.....	5-14
5-8 Type B R-SCB Percent Load Relationship Curves .....	5-16
6-1 Aggregate Gradation for the Type D Mix .....	6-2
6-2 Comparison of Air Voids .....	6-4
6-3 Comparison of Initial Tensile Peak Loads .....	6-5
6-4 Number of OT Cycles to Failure .....	6-6
6-5 OT Results for All Labs (30 Specimens).....	6-7
6-6 Single versus Double Cracking (Lab# 2 Type D Mix).....	6-8
6-7 Single versus Double Cracking (Lab# 5 Type D Mix).....	6-8
6-8 Example of Double Cracking in OT Specimen .....	6-9
6-9 Effects of Different Displacement Loading Rates (Lab# 4 Type D Mix) .....	6-11
6-10 In-Built Dial Gauge .....	6-12
6-11 Comparison of OT Start Loads.....	6-12
6-12 Example of Inconsistent Curing Weights.....	6-14

## LIST OF FIGURES (CONTINUED)

7-1	Parameters Used for Calculating the Shear Stress.....	7-4
7-2	Typical GTM Densification Results.....	7-6
7-3	Parameters for the Calculation of Shear Stress .....	7-7
7-4	Shear Stress Measurements at Different Compaction Levels: (a) AC14 (Soft Asphalt), (b) AC 20 (Stiff Asphalt) .....	7-8
7-5	The Change in Percent Air Voids at Maximum Shear Stress.....	7-9
7-6	French Maximum Shear Stress by Moutier .....	7-10
7-7	Gyratory Load Cell Plate Assembly .....	7-11
7-8	Gyratory Load Cell Plate Assembly Placed on the Mold during Gyration Process .....	7-12
7-9	Applied External Forces and the Stress Distributions Used in Energy Relations .....	7-13
7-10	Aggregate Gradation for B and D Mixes.....	7-14
7-11	A Schematic Diagram Shows the Two Zones of the Compaction Curve .....	7-16
7-12	The Effect of Pine and Servopac in B and D Compaction .....	7-17
7-13	Effect of Binder Content on Compaction Indices of B Mix.....	7-18
7-14	Effect of Binder Content on Compaction Indices of D Mix.....	7-21
7-15	Preliminary Energy Indices for B and D Mixes .....	7-22
8-1	Graphical Illustration of the Balanced Mix-Design Concept .....	8-2
8-2	Aggregate Gradation for the Type C Mix .....	8-3
8-3	LTRC's ALF Device .....	8-4
8-4	LTRC-APT Experimental Test Sections .....	8-6
8-5	Construction of the Low LTE at the LTRC-APT Test Site.....	8-7
8-6	HMA Placement and Compaction Operations .....	8-8
8-7	Finished HMA Mat at the LTRC-APT Test Site.....	8-8
8-8	IR Thermal Imaging of the HMA Mat .....	8-9
8-9	GPR Measurements .....	8-11
8-10	TTI's Mobile Lab .....	8-12

## LIST OF TABLES

Table	Page
2-1	Variability Comparison of Fatigue (Crack) Test Methods (SHRP, 1994)..... 2-14
3-1	Materials and Mix-Design Characteristics ..... 3-2
3-2	Type C Mix (Hunter) – Original versus Modified Mix-Design..... 3-3
3-3	Type C Mix (Beaumont) – Original versus Modified Mix-Design ..... 3-3
3-4	Test Plan and Aggregate Specimen Matrix for the OT Round-Robin Testing ..... 3-5
3-5	Test Plan and HMA Specimen Matrix for the Workability Indicator Tests ..... 3-6
3-6	Test Plan and HMA Specimen Matrix for APT Mix-Design Evaluation ..... 3-6
3-7	Test Plan and HMA Specimen Matrix for the Crack Evaluation Tests ..... 3-7
3-8	HMA Mixing and Compaction Temperatures ..... 3-8
3-9	HMA Specimen Molding, Cutting, and Coring ..... 3-10
4-1	Test Plan and HMA Specimen Matrix for X-Ray CT Scanning Tests ..... 4-1
4-2	Mix AV Comparisons as a Function of Sample Height ..... 4-9
5-1	Laboratory Cracking Test Protocols ..... 5-2
5-2	Average OT Test Results ..... 5-3
5-3	Average DT Test Results ..... 5-6
5-4	Average IDT Test Results ..... 5-10
5-5	Average SCB Test Results ..... 5-11
5-6	R-IDT Test Results at Various Load Levels for the Type D Mix..... 5-14
5-7	R-SCB Test Results at Various Load Levels for the Type B Mix ..... 5-16
5-8	Preliminary Comparison of the Cracking Test Methods..... 5-18
5-9	Test Method Discriminatory Ratios ..... 5-19
5-10	Preliminary Ranking of the Cracking Test Methods..... 5-20
5-11	Overall Test Method Utility Rank ..... 5-21
6-1	Mix-Design Characteristics for OT Round-Robin Testing ..... 6-2
7-1	Maximum Shear Resistance at Different Angles and Binder Type ..... 7-9
7-2	Compaction Parameters Determined from Conventional Compaction Curve ..... 7-16
8-1	HMA Mix-Design Details for APT Testing..... 8-3

**LIST OF TABLES (CONTINUED)**

8-2    QC Nuclear Density Measurements ..... 8-10

8-3    QC Asphalt-Binder Content Measurements..... 8-10

9-1    List of Currently Ongoing and Future Planned Works ..... 9-8

## LIST OF NOTATIONS AND SYMBOLS

AASHTO	American Association of State Highway and Transportation Officials
FWD	Falling weight deflectometer
GPR	Ground penetrating radar
HMA	Hot-mix asphalt
HMAC	Hot-mix asphalt concrete
HWTT	Hamburg wheel tracking test
IR	Infrared
MTD	Material transfer device
NDT	Non-destructive test (ing)
NMAS	Nominal maximum aggregate size
OT	Overlay tester
PG	Performance grade
QA	Quality assurance
QC	Quality control
$\varepsilon_t$	Horizontal tensile strain measured in microns ( $\mu\varepsilon$ )
$\varepsilon_v$	Vertical compressive strain measured in microns ( $\mu\varepsilon$ )
$\phi$	Symbol phi used to mean diameter



# **CHAPTER 1**

## **INTRODUCTION**

Recent changes to the Texas HMA mix design procedures such as adaption of the higher PG asphalt-binder grades and the Hamburg test have ensured that the HMA mixes that are routinely used on the Texas highways are not prone to rutting. However, performance concerns have been raised about these mixes, which are now “drier”, more difficult to compact, and more susceptible to both reflective and fatigue cracking. This is particularly problematic with the dense-graded Type C and D mixes that are widely used throughout the State of Texas. Several new ideas are under consideration to either modify the existing mix-design criteria (target densities, VMA requirements, etc.) and/or to include new and simpler cracking test procedures.

### **BACKGROUND**

Based on the literature review, the primary focus of this research is to comparatively evaluate the following three mix-design procedures and make recommendations thereof:

- The modified volumetric mix-design procedure proposed by TxDOT’s construction division,
- The balanced mix-design procedure that is based on meeting both the Hamburg (rutting resistance) and Overlay (cracking resistance) prescribed test criteria, and
- A simplified balanced mix-design procedure with a simpler alternative cracking test.

A brief description of these proposed mix-design procedures is discussed in the subsequent text.

### **The Proposed Modified Volumetric Mix-Design Procedure**

The basic approach of the proposed modified volumetric mix-design procedure involves starting with HMA mixes compacted at 50 gyrations in the gyratory press and then checking both the VMA and Hamburg criteria ( $\leq 12.5$  mm rutting at 50 °C). This is ideally an iterative

process and the low number of gyrations will ensure that more asphalt-binder is added in the first test series.

TxDOT is evaluating this procedure on a trial basis and its postulated advantages include the use of the current test equipment with minimal changes to the already existing test procedures. Its anticipated weaknesses include the possibilities to take substantially longer time than existing methods particularly if several iterations are required to arrive at an acceptable design OAC. Furthermore, there is also no guarantee that the designed mix will have adequate cracking resistance.

### **The Proposed Balanced Mix-Design Procedure**

The concept of the balanced mix-design method is fundamentally centered on ensuring adequate rutting and cracking resistance for the HMA mixes (Zhou et al., 2007). The idea is to design an HMA mix that is at least both rutting-and cracking-resistant. With this concept, the design philosophy is based on designing and selecting an OAC that simultaneously meets certain prescribed laboratory rutting and cracking requirements based on the Hamburg and Overlay tests, respectively. With the Overlay tentative failure criterion set at a minimum of 300 OT load cycles and the Hamburg rut depth at 12.5 mm (maximum), recent studies at Texas Transportation Institute (TTI) have yielded satisfactory results for CAM mixes and most of the dense-grade mixes (Zhou et al., 2007). The only mixes that could not be balanced were those that used soft asphalt-binders (i.e., lower PG grades such as PG 64-22) with low quality aggregates such as absorptive limestones.

Thus far, the observed strengths of this proposed balanced mix-design method include the potential to balance two different performance criteria (i.e., rutting and cracking resistance characterization) and that the test results can be utilized in structural designs and performance prediction analyses. Potential weaknesses include costliness, variability in the test results, need for a double blade saw, and time consuming with gluing and cleaning up processes.

### **The Proposed Simplified Balanced Mix-Design Procedure**

The proposal for a simplified balanced mix-design procedure with a simpler alternative cracking test is primarily centered on circumventing the shortfalls associated with the Overlay

test, particularly with respect to variability in the test results and the issues of specimen gluing/curing.

The idea with this approach is to devise a more practical, cost-effective, repeatable, and reliable cracking test with less variability in the test results compared to the Overlay tester. This ultimately calls for a comparative evaluation of various tests such as the indirect tension, direct tension, bending beam, semi-circular bending, etc.

### **HMA Workability and Compactability Evaluation**

As noted in the introductory paragraph, the shift to higher PG asphalt-binders and use of rut-resistant mixes also compromises the constructability properties of some mixes. Therefore, as new mix-designs are sought, workability and compactability characteristics of the mixes also need to be evaluated as well. Where possible, the new mix-design procedures should also incorporate some constructability evaluation criteria such as workability and compactability indicators or indices.

### **ACCELERATED PAVEMENT TESTING**

Based on the foregoing discussions, this study was initiated in 2008 to research, develop, and test the new generation of mix-design procedures that ensures satisfactory rutting and cracking performance as well as guaranteeing mix constructability. The intention is to run the proposed new procedures in parallel with the existing procedures and compare the results there after. Additionally, the new designs will also be evaluated on a series of test sections constructed on actual field highways.

However, one major concern is that with the current research cycles, the construction and monitoring of test sections under actual traffic loading is postulated to take a minimum of 6 to 8 years to obtain definitive information on the new mix-design performance. This factor, therefore, necessitated the incorporation of accelerated pavement testing (APT) in this study.

### **RESEARCH OBJECTIVES AND SCOPE OF WORK**

As discussed above, the primary objective of this research project is to develop new generation mix-design procedures that optimize both rutting and cracking performance, without compromising the constructability aspects of the mixes. The research methodology incorporates

extensive literature review of the existing mix-design procedures, laboratory testing, and field validation including APT testing and performance monitoring.

This interim report provides a preliminary overview of the research work completed as of summer 2009. The report's scope of work is as follows:

- Literature review of the currently available cracking tests that are or can be used in routine HMA mix-design procedures.
- Material acquisition, sieve analyses, and mix-design developments. Three mix types (Type B, C, and D) with up to nine different mix-designs were evaluated.
- Mix-design and laboratory test evaluations of the commonly used Texas mixes based on the Texas gyratory, volumetric, and balanced mix-design procedures. Mixes Type C and D were evaluated under this task.
- Round robin testing in six different Texas laboratories to quantify the Overlay test variability and repeatability. A Type D mix was utilized for this task.
- Comparative laboratory test evaluation of various cracking tests such as the indirect tension, direct uniaxial tension, and semi-circular bending based on two mixes. Mixes Type B, C, and D, were used for this task.
- HMA mix workability and compactability tests for quantifying the constructability aspects of the mixes and development of the workability/compactability criteria. Mixes Type B, C, and D as well as plant-mix from NCAT (Alabama) were tested under this task for evaluating the HMA mix workability and compactability characteristics.
- Construction of the APT test sections in Louisiana. During this reporting period, construction of the APT test site had been completed in Louisiana. A Type C mix was utilized for constructing the HMA layers. TTI researchers monitored the construction process and the details are discussed in this report.

The APT testing is being performed on the Texas mix (Type C) under a cooperative agreement with the LTRC and LSU in the State of Louisiana. As the State of Texas lacks such APT facilities, this cooperative venture will provide the research team with the ability to test the Texas mixes in a similar environment. The Texas and Louisiana climatic conditions do not differ significantly. Note that the LTRC's APT has been running successfully for almost one

decade and that experience will ensure that the accelerated testing of the Texas materials will be both successfully and efficiently completed.

## **DESCRIPTION OF THE REPORT CONTENTS**

This interim report consists of nine chapters including this chapter (Chapter 1) that provides the background, the research objectives, methodology, and scope of work. Chapter 2 is the literature review and is predominantly focused on evaluating the currently existing laboratory cracking tests that are used in mix-design procedures. The materials and mix-design evaluations including the experimental design and HMA specimen fabrication are discussed in Chapter 3. This is then followed by air void characterization based on X-ray CT scanning tests in Chapter 4.

Chapters 5 and 6 present and discuss the laboratory evaluation of the various cracking and OT round-robin (variability/repeatability assessment of the Overlay tester) tests, respectively. HMA mix workability and compactability evaluation is discussed in Chapter 7, while the APT test section construction is discussed in Chapter 8.

Chapter 9 then provides a summation of the interim report with a list of the major findings and recommendations. Ongoing and future planned works are also discussed in this chapter. Some appendices of important data are also included at the end of the report.

## **SUMMARY**

In this introductory chapter, the background and the research objectives were discussed. The research methodology and scope of work were then described followed by a description of the report contents. Note in this interim report that as some of the laboratory tests such as the Hamburg, X-ray CT, and Dynamic Shear Rheometer use standard metric (SI) units, some of the test results have consequently been reported in metric units.



## **CHAPTER 2**

### **LITERATURE REVIEW**

A literature review consisting of an extensive information search of electronic databases and their resulting publications was conducted to gather data on the currently available cracking tests that are in use. The findings of this literature review are discussed in this chapter and include the direct-tension, indirect-tension, semi-circular bending, and the Overlay cracking tests. A brief background on the previously conducted research on HMA mix cracking-resistance characterization in Texas is presented first followed by a detailed description of each test (direct-tension, indirect-tension, semi-circular bending, and the Overlay). A summary of key findings is then presented to wrap-up the chapter.

#### **PREVIOUS RESEARCH ON CRACK MODELING IN TEXAS**

In 2004, a research study under TxDOT Project 0-4468 was performed to evaluate and recommend a fatigue HMA mix-design and analysis system that ensures adequate performance under specified environmental and traffic loading conditions in a particular pavement structure (Walubita et al., 2006). The results of this study proved that the Calibrated Mechanistic with Surface Energy (CMSE) approach provides a rational methodology for fundamentally characterizing the fatigue resistance of HMA mixes. Together with surface energy measurements, this CMSE approach requires direct-tension (DT), relaxation modulus (RM), and repeated direct tension (RDT) testing to comprehensively characterize the HMA mix fatigue (cracking) resistance.

The CMSE analysis models are based on the HMA fundamental material properties and incorporate most of the influencing variables such as asphalt-binder oxidative aging, traffic loading, and environmental conditions. Therefore, it is a very rational and reliable methodology for characterizing the HMA mix fatigue resistance at a fundamental level. However, this approach is impractical for routine mix-design applications due to the numerous laboratory tests that are required, among others. In addition, the required input data for the CMSE analysis models are very comprehensive and relatively complex. Consequently, while this approach maybe very ideal for research purposes, it is unfeasible for routine industry application.

However, comparative evaluations of the CMSE laboratory tests (DT, RM, and RDT) indicated that the DT test alone could be used as a surrogate fatigue-cracking test in lieu of the entire CMSE approach. A follow up study was subsequently performed through the TxDOT Project 408006 to further investigate the DT as a surrogate fatigue-cracking test (Walubita and Epps Martin, 2007). The results obtained were promising and substantiated the potential use of the DT as a surrogate test protocol for rapid routine HMA mix-design and mix screening for fatigue-cracking resistance. Concurrently, investigations into utilizing the SCB test as a surrogate fatigue-cracking test were also initiated. However, the study was terminated prematurely due to inadequate funding and thus, no conclusive findings were realized.

Therefore, one of the primary goals of this study will be to continue and expand upon these previous research findings by evaluating various cracking test methods and recommending one that is simple and robust, especially for ranking the commonly used Texas mixes. The DT, IDT, SCB, and OT tests will be evaluated; both in static monotonic and repeated loading modes. A minimum of three different mix types will be investigated for their cracking resistance properties and compared using each of these test methods. Concurrently, the study is also intended to continue full CMSE testing (DT, RM, and RDT) for HMA fatigue resistance characterization and comparison with the surrogate test results. This aspect will be further explored in this study.

In the subsequent sections, the DT, IDT, SCB, and OT are described and discussed in greater details. At the time of this report, however, the literature review and testing development for repeated loading modes had not been thoroughly investigated. Consequently, the information search for these test modes is excluded from this interim report.

## **THE INDIRECT TENSION TEST METHOD**

Indirect-tension testing has been used to characterize the properties of HMA mixes for over 30 years and has exhibited potential for accurately predicting the fatigue resistance properties of HMA mixes (Walubita et al., 2002). The typical IDT setup requires a servo-hydraulic closed-loop testing machine capable of axial compression (Huang et al., 2005). Several publications recommend using a loading rate of 2 in/min, most notably are the standard procedures in Tex-226-F (TxDOT, 2004) and ASTM D6931 (ASTM, 2005).



The specimen is typically loaded diametrically in compression and this indirectly induces horizontal tensile stresses in the middle zone of the specimen that ultimately causes cracking. For the evaluation of the tensile properties of the HMA mixes, the permanent deformation under the loading strip is undesirable (Huang et al., 2005). Therefore, the compressive load is distributed using loading strips, which are curved at the interface to fit the radius of curvature of the specimen.

The fracture energy of the IDT specimen is calculated using the strain at the center of specimen, which is determined from the displacements with a 2-inch gauge length using linear viscoelastic solutions (Kim et al., 2002). However, one issue that may be problematic with the IDT set-up is the gauge length of the Linear Variable Displacement Transducers (LVDTs). The existence of large aggregates, particularly for coarse-graded mixes, in the middle of the specimen can affect the displacement measurements between gauge points if the length is too short. So caution must be exercised to watch out for such potential problems and account for them in the subsequent data analyses and interpretation of the results.

Typical test temperatures range from -20 °C (Buttlar et al., 1996) to 25 °C (Huang et al., 2005). The data captured during IDT testing include time, applied load and horizontal and vertical specimen deformation.

## **IDT Data Analysis**

Various models have been developed to analyze and interpret the data from IDT testing since its inception. It is important to choose or develop the model that most accurately and appropriately represents the properties of the material being tested and the manner in which it is being tested. Fatigue cracking (stress) and fracture energy analysis models constitute some of commonly used models for analyzing IDT data. However, previous research has indicated that the relationship between fracture energy and fatigue cracking should not be represented by linear or power equations because this can lead to an erroneous relationship and unrealistic prediction of fatigue cracking (Kim et al., 2002). According to Kim and Wen (2002), the fracture energy of an IDT specimen can be characterized using the following equation:

$$F = e^{\frac{\ln(100-C)}{C} - b} \quad \text{(Equation 2-1)}$$

where,

- F = fracture energy, Pa,
- C = fatigue cracking percentage, %,
- a = 11.9 (regression coefficient), and
- b = 91 (regression coefficient).

Based on the IDT testing of WestTrack cores, the fracture energy calculated from a specimen tested at 68 °F proved to be an excellent indicator of fatigue cracking resistance of a mix (Kim et al., 2002).

On the other hand, stress analysis models are considered simpler and were more prevalent in the literature reviewed, but they usually require certain conditions to be met for the model to be applicable. According to Buttlar et al. (1996), the tensile stress in the center of an IDT specimen can be calculated using Equation 2-2.

$$\sigma_t = \frac{2P}{\pi t D} \quad (\text{Equation 2-2})$$

where,

- $\sigma_t$  = IDT strength,
- P = maximum axial load,
- t = specimen thickness, and
- D = specimen diameter.

Based on the research by Buttlar et al. (1996), Equation 2-2 holds only when plane stress conditions are met. However, plane stress conditions only apply for thin disks, whereas the HMA specimen thickness is generally greater than 2 inches. Therefore, tensile strengths computations based on conventional analysis methods maybe erroneous. The IDT strength calculated by Equation 2-2 generally overestimates the true tensile strength of the HMA, and this overestimation is variable among different mixes.

However, some researchers are skeptical of the IDT test as a predictor of fatigue cracking resistance in field pavements. Huang et al. (2005) states that the stress state during diametrical testing on a specimen under loading is complicated and not a realistic representation of the stress state in the whole pavement structure. However, the diametrical stress provides some insight onto the stress state itself.

The maximum horizontal tensile stress at the center of the specimen is generally one third of the vertical compressive stress at the same point (Huang et al., 2005). Huang et al. also presented models for horizontal stress and strain calculations at the center of the specimen as follows:

$$\sigma_T = \frac{2P_{ult}}{\pi t D} \quad \text{(Equation 2-3)}$$

$$\varepsilon_T = 13.2H_T \quad \text{(Equation 3-4)}$$

where,

- $\sigma_T$  = tensile strength, kPa,
- $P_{ult}$  = peak load, N,
- $t$  = specimen thickness, mm,
- $D$  = specimen diameter, mm,
- $\varepsilon_T$  = horizontal tensile strain at failure, and
- $H_T$  = horizontal deformation at failure.

In this study, plane stress conditions were assumed to have been met in the IDT specimen set-up. Therefore, Equations 2-3 and 2-4 were utilized to characterize the tensile and fracture properties of the HMA mixes, i.e., the tensile strength ( $\sigma_T$ ) and strain at failure ( $\varepsilon_T$ ) were the IDT parameters that were utilized as indicative measures of the HMA fracture strength and cracking resistance.

## **IDT Test Evaluation**

The IDT test has an advantage over the other tests in that the specimen preparation is very simple and easy. The test duration is also very short. However, the stress state in the specimen tends to be very complex thus, causing analysis problems. This makes the accuracy of the IDT results subjective. Therefore, better IDT analysis models still need to be developed. However, the IDT test is still accurately being applied for comparative HMA mix evaluation and screening for cracking resistance.

## **THE SEMICIRCULAR BENDING TEST METHOD**

The development of SCB as a predictor of cracking resistance in HMA mixes has appeared relatively recent in the field of pavement engineering. The SCB specimen is a half disk, typically 4-6-inch in diameter and 1.5-2-inch thick (Huang et al., 2009), that is loaded in compression using a three-point flexural apparatus. The same equipment that is used with the IDT can be used for the SCB. However, an additional apparatus (described in Chapter 4) must be utilized to achieve the three-point bending mode. The rate at which the specimen is loaded is not very well specified, but Walubita et al. (2002) had success when using 0.05 in/min loading rate.

Specimen fabrication and preparation for the SCB test is very simple and quick. Many researchers cut a notch in the base of the specimen to ensure that the crack initiates in the center of the specimen. Notch depths vary depending on many factors such as specimen thickness, diameter, loading rate, test temperature, mix type, etc.

At a first glance, the calculation of stiffness in the middle point of the lower specimen surface may seem difficult because affixing the strain gauges onto the specimen is time and resource consuming. In the case of the current study, however, HMA stiffness determination may become an important parameter to explore. The SCB test accommodates this requirement in that the stiffness can be obtained by replacing the horizontal strain with vertical deflections, as in the flexural bending beam fatigue (FBBF) analysis (Huang et al., 2009).

For analysis purposes, the spacing between the supports is typically 0.8 times the specimen diameter. From the literature search, the typical test temperatures for the SCB test are between 10 °C (Huang et al., 2009) and 25 °C (Molenaar et al., 2002). Data recorded during IDT testing include the following: time, applied load, and horizontal displacement at the crack (Molenaar et al., 2009) or vertical deflection in the specimen.

## SCB Data Analysis

As with IDT, SCB analysis cannot be completely analyzed using simple geometry-based models due to its non uniform stress distribution and the heterogeneity of HMA. For example, Molenaar et al. (2002) states that SCB tensile stress can be obtained as follows:

$$\sigma_t = 4.8 \frac{F}{D} \quad (\text{Equation 2-5})$$

where,

$\sigma_t$  = maximum tensile stress at the bottom of the specimen,

F = load per unit width of the specimen at failure, and

D = specimen diameter.

Based on Molenaar et al. (2002), Equation 2-5 is only an indicator and not a true measure of the tensile characteristics of the HMA material. As mentioned by Huang et al. (2009), Equation 2-5 must be adjusted based on consideration of idealized conditions, as follows:

$$\sigma = \frac{3PL}{2th^2} = \frac{6PL}{tD^2} \quad (\text{Equation 2-6})$$

where,

$\sigma$  = SCB tensile stress at the middle point of the lower surface,

P = load,

L = spacing between the supports,

t = specimen thickness,

h = D/2, specimen height, and

D = specimen diameter.

In Equation 2-6, when the load reaches the maximum value,  $\sigma$  represents the material strength. However, this is assuming ideal stress distribution within the specimen (Huang et al., 2009). By contrast, Equation 2-5 is valid only if the distance between the supports is  $0.8 \cdot D$  (Molenaar et al., 2002). Considering both Equations 2-5 and 2-6, SCB has an advantage over the IDT because tension cracking is the dominant failure mode.

Furthermore, the HMA tensile strength determined from the SCB test is nearly 3.8 and 1.5 times higher than that determined from the IDT and FBBF (Huang et al., 2005, 2009), respectively. In addition to the significant differences in the specimen geometry, this high tensile strength is in part attributed due to complexities in stress and strain states, nonlinearity, and visco-elasticity of the HMA material. Based on elasticity theory, Huang et al. (2009) postulates that the relationship between vertical deflection and stiffness should be as given in Equation 2-7:

$$S = c \left( \frac{L}{D} \right) * \left( \frac{P}{td} \right) = c \left( \frac{L}{D} \right) * \left( \frac{p}{d} \right) \quad (\text{Equation 2-7})$$

where,

- S = stiffness modulus,
- c = dimensionless function of relative spacing between support, L/D,
- L = spacing between supports,
- D = specimen diameter,
- P = load,
- t = specimen thickness,
- d = deflection at the middle point of the lower surface of the specimen, and
- p = P/t.

The fitting equation for the dimensionless function, c, was determined to be:

$$c \left( \frac{L}{D} \right) = a * \left( e^{\frac{bL}{D}} - 1 \right) = 1.977 * \left( e^{\frac{1.175L}{D}} - 1 \right) \quad (\text{Equation 2-8})$$

So Equation 2-7 becomes:

$$S = 1.977 * \left( e^{\frac{1.175L}{D}} - 1 \right) * \left( \frac{p}{d} \right) \quad (\text{Equation 2-9})$$

Equation 2-9 is important because stiffness may prove to be one of the comparison aspects between the cracking tests to be evaluated in this study.

However, many other researchers have developed tensile stress equations based on plane stress-state conditions with modifications to make them more applicable to the SCB specimen geometry. In any event, it is postulated that the most appropriate SCB equation should closely correspond to the tensile strength measured in direct (pure) tension mode. For this reason, the equation by Hofman et al. (2003) was utilized for the SCB data analysis in this study:

$$\sigma_T = \frac{4.263P}{tD} \quad (\text{Equation 2-10})$$

where,

- $\sigma_T$  = tensile strength, kPa,
- $P$  = maximum axial load, N,
- $t$  = specimen thickness, mm, and
- $D$  = specimen diameter, mm.

According to Hofman et al. (2003), Equation 2-10 is valid for SCB stress computation with notched specimens. In this study, comparisons of the SCB stress computations with the direct-tension test were reasonable.

## SCB Test Evaluation

The SCB test has its advantages and disadvantages much like any other test method. One advantage of the SCB over the IDT is the development of a predictable crack without wedging near the loading strip (Molenaar et al., 2002). In fact, the SCB test could significantly reduce the loading strip-induced permanent deformation; thus, it may be more suitable than the IDT for evaluating the tensile properties of HMA mixes (Huang et al., 2005). Nonetheless, the main advantages of the SCB test are two-fold. The specimen is very easy to fabricate (requires no gluing) and prepare for testing (Marasteanu et al., 2008). The loading configuration is also fairly simple and easy to set-up. The SCB tensile stress measured in the specimen is direct in that it is created by direct bending of the specimen compared for instance to the IDT test.

However, the SCB has its shortfalls as well. Notching has been highlighted in previous studies as a source of variability and repeatability problems with the test. The validity of the analysis models, particularly when considering the complexity of the induced stress-state and specimen geometry, is still questionable. Further research is thus still needed in this area.

## **THE DIRECT TENSION TEST METHOD**

The DT test has recently become popular for fatigue cracking analysis. It is the most straightforward test and has the simplest analysis equation of all the test methods because the specimen is tested in direct-tension loading mode. The specimen is typically a cylinder of 6-inch in height and 4 inches in diameter (Walubita, 2006). This geometry is in part based on the ease of specimen fabrication using the Superpave gyratory compactor. The loading rate is typically 0.05 in/min (Walubita et al., 2006).

However, the specimen set-up process requires gluing end plates to the specimen ends that are in turn attached to the MTS hydraulic system. This is a very critical process for this test and it requires meticulous work to ensure reliable results. Gluing time can also be a hindrance to testing efficiency, as the process usually requires 24 hours for curing.

In addition, the failure of the specimen must be closely monitored as cracking near the ends can be an indicator that end effects may be introduced into the data and resulting analysis. In fact, proper gluing techniques must be ensured, otherwise the specimen may fail in the glued area. This also means that the HMA may not have failed before the test actually terminates and therefore, the calculated stresses and strains will be erroneous. As the LVDTs are generally attached to the specimen, HMA stiffness determination is thus possible with this test.

The DT test can be run at either 68 °F or room temperature. The data that are captured during DT testing include the load, vertical displacement, and time.

### **DT Data Analysis**

Because the stress state in a DT specimen are less complicated compared to the SCB or IDT, the stress equation for the DT test is simply (Walubita, 2006):

$$\sigma_t = \frac{P}{(\pi r^2)} = \frac{P}{\pi \frac{D^2}{4}} \quad (\text{Equation 2-11})$$



where,

$\sigma_t$  = maximum tensile stress,

$P$  = load,

$r$  = specimen radius, and

$D$  = specimen diameter.

Therefore, the HMA stiffness becomes:

$$S_T = \frac{\sigma_t}{\epsilon_T} \quad (\text{Equation 2-12})$$

where,

$\sigma_t$  = maximum tensile stress, and

$\epsilon_T$  = tensile strain at maximum axial load.

### **DT Test Evaluation**

The DT test is simple and practical because it is loaded in direct tension (Walubita et al., 2006). Data analysis is straight forward and simple. Variability in the test results and test repeatability are also reasonable.

However, both specimen preparation and set-up are tedious and comparatively time consuming processes that require meticulous attention to every detail. In general, custom guidance for specimen fabrication, gluing, and set-up is necessary, which may at times be very costly. Consequently, these shortfalls may be a hindrance toward practical application and routine use of the DT test in HMA mix-designs. Additionally, the DT test is not readily applicable for testing field cores due to the nature of the specimen geometry and dimensions.

## **THE OVERLAY TESTER METHOD**

The OT has been used pervasively and routinely in many TxDOT mix-designs for mix screening and as an indicator of cracking (reflective) resistance for HMA pavements. To date, four TxDOT district labs have OT machines that they use routinely in their HMA mix-designs and screening for cracking resistance. TxDOT has adapted a laboratory standard test procedure, Tex-248-F, for the OT test (TxDOT, 2009). Accordingly, Tex-248-F will be the basis for evaluating the OT test method in this study.

Due to its proven correlation with field performance, this test will be used as the benchmark for the comparative evaluation of other test methods. This comparison includes but not limited to the following: test duration, repeatability, and the ability to predict cracking resistance in terms of HMA mix ranking. The OT test method was also successfully applied for fatigue crack modeling in a TTI study by Zhou and Scullion (2007). Satisfactory results were obtained and indicated the potential of using the OT in M-E structural designs as well.

Generally, the OT is run in a controlled-displacement mode at a loading rate of one cycle per 10 sec (5 sec to open, 5 sec to close) with a fixed opening displacement (Zhou et al., 2007). The standard maximum opening displacement rate, according to the standard test specification Tex-248-F (TxDOT, 2009) is 0.025-inch. The test is typically run at room temperature. The data that are recorded automatically during the test include the load, displacement, and temperature. Just like the DT test, OT specimens require gluing. Thus there is a relatively long time lag between specimen fabrication and actual testing due to the gluing and curing processes, about 2 days of waiting. Similar to the DT test, this is unfavorable, particularly for industry applications.

### **OT Data Analysis**

The OT specimen is typically tested until the initial load decreases by 93 percent. The number of cycles to this load reduction (i.e., 93 percent) constitutes the number of cycles to failure and is the indicative measure of the HMA mix's cracking resistance. The current tentative failure criterion is 300 cycles (minimum) for dense-graded mixes and 750 cycles (minimum) for the fine-graded CAM mixes (Zhou et al., 2007). Therefore, it is simple to make a comparison between a better and poor crack-resistant mix by simply analyzing their number of cycles to OT failure.

## **OT Test Evaluation**

According to Zhou et al. (2007), the advantages of the OT test are that the test correlates well with field core performance. The test is fairly simple and practical. Field cores can also be easily tested in the Overlay test. Recently, however, the issues of the test's variability and repeatability have come into question. An acceptable level of variability is typically considered a coefficient of variation of about 25 percent or less.

By contrast, some laboratories have complained of the OT's high variability in the test results and poor repeatability. This OT variability issue is in fact one of the reasons for evaluating other cracking test methods in this study. The OT test has other disadvantages as well. The specimen fabrication and test preparation procedure is very wasteful in that it renders much of the molded specimen to be discarded after cutting (TxDOT, 2009). The recommended sample molding height is 4.5-inch while the final OT test specimen is only 1.5-inch thick. This in turn means making larger mix batches, which is both material and labor intensive.

## **THE MODIFIED OVERLAY TESTER METHOD**

The proposition for the modified OT<sub>2</sub> test is primarily based on the need to address the high variability and non-repeatability associated with the standard OT test. Based on readily available TxDOT data, the OT tends to be rather variable especially with coarse-graded mixes; over 30 percent COV values have been reported. The premise is to have COV values of around or less than 30 percent. Nonetheless, it should be emphasized that most (if not all) of the cracking tests, by nature of their loading configuration and failure mode, are typically associated with high variability in the test results.

From literature review, most of the cracking tests such as the flexural and diametral fatigue were found to exhibit higher COV values of over 50 percent; see Table 2-1 (SHRP, 1994). According to SHRP (1994), the results in Table 2-1 represent a minimum of 32 replicated specimens per test type. The least COV magnitude shown is 65.5 percent for the diametral fatigue test, twice the 30 percent benchmark. Evidently, these results are indicative of high variability in the crack test methods evaluated in Table 2-1. Theoretically, it can therefore be inferred from these results that it should not be unusual to observe high variability with COV greater than 30 percent in laboratory cracking tests.

**Table 2-1. Variability Comparison of Fatigue (Crack) Test Methods (SHRP, 1994).**

	Flexural Beam Fatigue	Flexural Trapezoidal Fatigue	Diametral Fatigue
Stiffness			
Coefficient of Variation (%)	12.3	11.4	19.7
Sample Variance (ln psi)	0.010	0.014	0.015
Cycles to Failure			
Coefficient of Variation (%)	98.7	171.8	65.5
Sample Variance (ln cycles to failure)	0.282	1.696	0.213

Compared to compression tests such as the Hamburg, the failure zone or point of failure in tensile crack tests such as the Overlay or the bending beam is highly localized and predetermined, i.e., at the center of the specimen. This is one potential cause of variability in most cracking tests because the weakest point in any given test specimen may not necessarily be the middle zone. For some specimens, the middle zone may actually turn up to be the strongest point, and thus, would perform completely different from specimens whose weakest area is the middle point.

Therefore, one of the objectives of this study is to attempt to modify the OT test protocol so as to improve its variability and repeatability as well as its applicability to coarse-graded mixes. In this regard, proposals to modify the displacement rate and/or the failure criterion will be explored. For instance, reducing the displacement to 0.020, 0.015, or 0.0125 inches may potentially improve the OT's applicability to coarse-graded mixes as well as variability. In fact, TxDOT's recent investigative study of varying (decreasing) the maximum opening displacement indicated a decrease in variability; i.e., the computed COV values were lower in magnitude compared to the standard OT test. On this basis, this aspect can be explored further in this study. Other aspects of possible modifications to the standard OT test protocol include the OT specimen set-up and the gluing/curing processes.

## **SUMMARY**

This chapter presented a review of the literature of the currently available cracking tests that have potential to be used in routine HMA mix-designs and mix screening for cracking resistance. In particular, the focus of the literature review was on the direct-tension, indirect-tension, semi-circular bending, and Overlay tests. These tests will be central basis of this study. Previous research on characterizing HMA mix fatigue-cracking resistance with respect to CMSE method was also reviewed and discussed in the chapter.



# **CHAPTER 3**

## **MATERIALS, MIX TYPES, AND EXPERIMENTAL DESIGN**

Three mix types (Type B, C, and D) with up to nine different mix-designs were evaluated and are discussed in this chapter. The experimental design including the test plan, HMA specimen fabrication, and AV distributional characterization are also discussed in this chapter. To wrap-up the chapter, a summary of key points is provided at the end.

### **MATERIALS AND MIX-DESIGNS**

As a minimum, the intent of the experimental design for this study was as follows:

- Evaluate at least two commonly used Texas dense-graded mixes, with known poor and good field cracking performance, respectively; preferably a Type B (typically poor crack-resistant) and D (good crack-resistant) mix.
- Evaluate at least two asphalt-binder contents, OAC and OAC plus 5 percent.
- Evaluate at least two asphalt-binder types, with a PG 76-22 included in the matrix.
- Evaluate at least two commonly used Texas aggregates types, typically limestone and crushed gravel.

On the basis of above experimental design proposal, three commonly used Texas mixes (Type B, C, and D) with up to nine different mix-designs were utilized and are discussed in this interim report. Table 3-1 lists these mixes and include the material type, material sources, and the asphalt-binder content (OAC). Where applicable, highway names where the mix had recently been used are also indicated in the table. In terms of usage, the selected mixes cover a reasonable geographical and climatic span of Texas, which include the central, northern, and south-western regions.

**Table 3-1. Materials and Mix-Design Characteristics.**

#	Mix Type	Asphalt-Binder	Aggregate	Gt	OAC	Hwy
1	Type B (Chico)	PG 64-22 (Valero)	Limestone (Chico)	2.497	4.3%	SH 114
2	Type D (Chico)	PG 70-22 (Valero)	Limestone (Chico)	2.452	5.0%	SH 59
3	Type C (Chico)	PG 76-22 (Valero)	Limestone (Chico)	2.475	5.0%	-
4	Type C (Hunter)	PG 70-22 (Valero)	Limestone (Hunter-Colorado Materials)	2.425	4.7%	FM 2440
5	Type C (Hunter-Modified)	PG 70-22 (Valero)	Limestone (Hunter-Colorado Materials)	2.445	4.9%	-
6	Type C (Jones)	PG 76-22 SBS (TFA)	Gravel (Black-Martin Marietta)	2.459	4.5%	IH 35
7	Type C (Beaumont)	PG 64-22 (Valero)	Limestone (Brownwood)	2.520	4.3%	-
8	Type C (Beaumont- Control)	PG 76-22 (Valero)	Limestone (Brownwood)	2.509	4.3%	-
9	Type C (Beaumont-Modified)	PG 76-22 (Valero)	Limestone (Brownwood)	2.509	5.2%	-

### Mix-Design Modifications

In order to improve laboratory performance in the Hamburg (rutting) and Overlay (cracking) tests, mix-design modifications were made to the original Type C (Hunter) and Type C (Beaumont) mixes. The Hamburg-rutting and Overlay-cracking performance on the original Type C (Hunter) mix, for instance, was not very satisfactory. The measured Hamburg rut depth of 11.1 mm was very close to the 12.5 mm threshold after 15 000 HWT load passes. Additionally, there was also visual evidence of stripping; suggesting moisture damage in the mix. Furthermore, the mix sustained only 34 load cycles in the Overlay test.

After aggregation gradation and blend modifications (i.e., removing the field sand and adding 1.0 percent lime) as shown in Table 2-1 were made, the modified mix-design exhibited significant improvements in the Hamburg test; with the measured rut depth being 4.4 mm after 15, 000 HWTT load passes. However, as evident in Table 3-2, no major improvements were observed in the Overlay test. In fact, the OT test indicated that the aggregate used in this mix was of relatively poor quality and probably absorptive. In fact, with this mix, some cracks cut through the aggregates.



**Table 3-2. Type C Mix (Hunter) – Original versus Modified Mix-Design.**

<b>Mix</b>	<b>Asphalt-Binder + Aggregate</b>	<b>OAC</b>	<b>Aggregate Blend</b>	<b>Hamburg Rut Depth</b>	<b>Overlay Results</b>
Type C (Hunter), Original	PG 70-22 + Limestone	4.7%	10% C-rock + 25% D-rock + 25% F-rock + 25% manufactured sand + 15% field sand	11.1 mm @ 15 k	34 cycles
Type C (Hunter- Modified)	PG 70-22 + Limestone	4.9%	10% C-rock + 35% D- rock + 15% F-rock + 39% manufactured sand + 1.0% lime	4.4 mm @ 15 k	38 cycles
Laboratory test benchmark utilized				≤ 12.5 mm	≥ 300 cycles

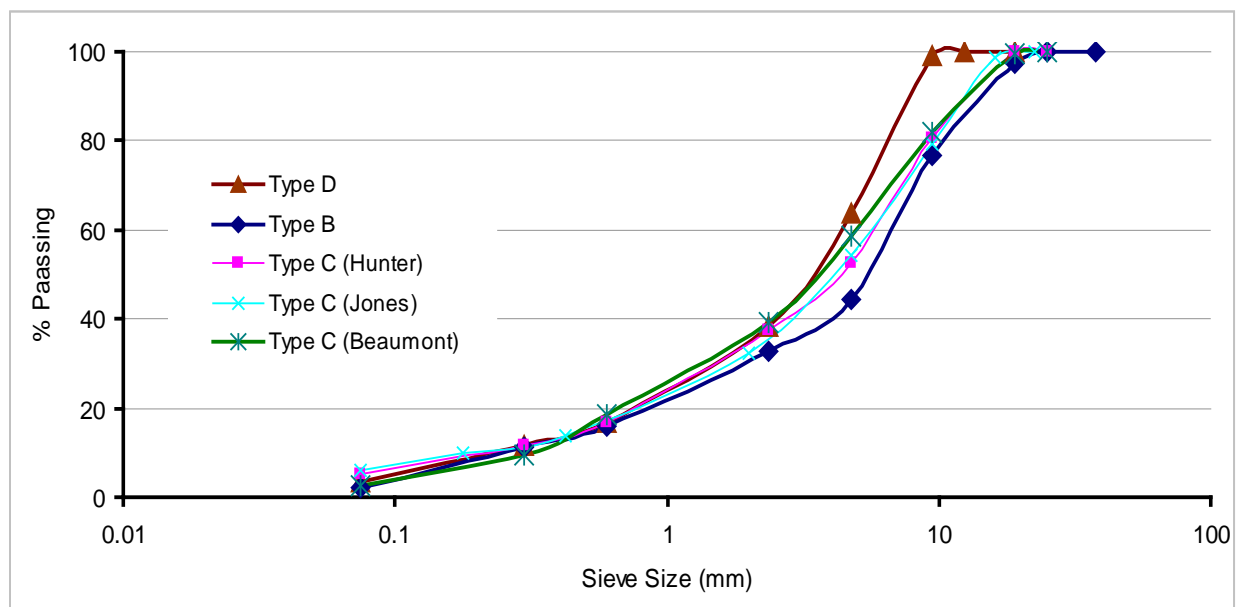
Like Type C (Hunter) mix, Type C (Beaumont) mix also performed unsatisfactorily in the Hamburg test, with the rut depth exceeding the 12.5 mm threshold after 10 000 HWTT load passes. The number of load cycles to crack failure in the OT test was also below 300. Mix-design modifications including switching to a higher PG asphalt-binder grade (i.e., PG 76-22) and changing the aggregate blend resulted in improved laboratory performance, both in the Hamburg and the Overlay tests. These modifications and the subsequent laboratory test results are shown in Table 3-3.

**Table 3-3. Type C Mix (Beaumont) – Original versus Modified Mix-Design.**

<b>Mix</b>	<b>Asphalt-Binder + Aggregate</b>	<b>OAC</b>	<b>Aggregate Gradation</b>	<b>Hamburg Rut Depth</b>	<b>Overlay Results</b>
Type C (Beaumont), Original	PG 64-22 + Limestone	4.3%	20% C-rock + 40% Grade 5 + 25% Screenings + 15% washed sand	12.8 mm @ 10 k	144 cycles
Type C (Beaumont - Modified)	PG 76-22 + Limestone	5.2%	20% C-rock + 40% Grade 5 + 30% Screenings + 10% washed sand	7.0 mm @ 20 k	600 cycles
Laboratory test benchmark utilized				≤ 12.5 mm	≥ 300 cycles

### Aggregate Gradations

Figure 3-1 is a plot of the aggregate gradations for the mixes listed in Table 3-1. As can be seen from the figure and as would be typically expected, the Type B mix gradation is the coarsest. Type D mix exhibits the finest gradation. Detailed gradation tables and graphs for each respective mix are included in Appendix A.



**Figure 3-1. Aggregate Gradations.**

### Aggregate Sieve Analysis

In order to accurately reflect the specified aggregate gradation for each mix type and account for the dust particles, adjustments were made to the original aggregate gradation based on the results of a wet sieve analysis. Wet sieve analysis is necessary when adjusting the aggregate gradation because, quite often, dust particles and the aggregate fractions passing the number 200 sieve size tend to cling to the surfaces of the particles that are larger than the number 200 sieve size. This phenomenon is often not well accounted for in a given gradation specification.

Wet sieve analysis is basically an iterative process of aggregate sieving, wetting/washing, and drying, followed by subsequent gradation adjustments based on the aggregate mass loss or gain on the individual sieve sizes. For this study, this was accomplished based on the TxDOT standard specification Tex-200-F (TxDOT, 2004). On average, three to four iterations were required prior to achieving the final adjustment. After gradation adjustment, new maximum theoretical specific gravities ( $G_t$ ) were accordingly determined using the ASTM standard D2041 (ASTM, 2003). It is important to note that a wet sieve adjustment does not change the fundamental properties of the gradation, but instead gives a more accurate representation of the specified gradation.

## LAB TEST PLANS AND HMA SPECIMEN MATRIX

The test plan and HMA specimen matrix for the five main laboratory tasks conducted during this reporting period are listed in Tables 3-4 through 3-7. These five tasks that are listed as follows:

- 1) Laboratory task 1: Comparative evaluation of defensible cracking tests based on the DT, IDT, SCB, and OT tests. The results of this task are presented in Chapter 5.
- 2) Laboratory task 2: Round-robin testing for quantifying the OT variability and repeatability. This task and the accompanying results are discussed in Chapter 6.
- 3) Laboratory task 3: Workability indicator tests based on the Servo Pac and Pine gyratory compactors. Details of this task and the lab results are discussed in Chapter 7.
- 4) Laboratory task 4: OAC mix-design evaluation/development for APT testing based on the proposed balanced mix-design and the Texas gyratory methods. This task is discussed in greater details in Chapter 8 of this interim report.
- 5) Laboratory task 5: AV distributional characterization in the compacted HMA samples based on the X-ray CT scanning tests. This task is discussed in Chapter 4.

**Table 3-4. Test Plan and HMA Specimen Matrix for the OT Round-Robin Testing  
(for Overlay Variability and Repeatability Evaluation).**

Lab	Mix	Mix-Design	HMA Specimen AV	OT Test Temperature	Replicate Specimens
Atlanta (TxDOT)	Type D (Chico)	5.0% PG 70-22 + Limestone	7±1%	77°F	≥ 4
Austin (TxDOT)	Type D (Chico)	5.0% PG 70-22 + Limestone	7±1%	77°F	≥ 4
Childress (TxDOT)	Type D (Chico)	5.0% PG 70-22 + Limestone	7±1%	77°F	≥ 4
Houston (TxDOT)	Type D (Chico)	5.0% PG 70-22 + Limestone	7±1%	77°F	≥ 4
PaveTex	Type D (Chico)	5.0% PG 70-22 + Limestone	7±1%	77°F	≥ 4
TTI	Type D (Chico)	5.0% PG 70-22 + Limestone	7±1%	77°F	≥ 4
Total HMA replicate specimens					≥ 24
*In each respective lab, at least two specimens were glued and tested by TTI researchers. Similarly, at least two specimens were glued and tested by the respective lab personnel/technician					

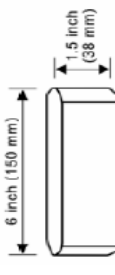

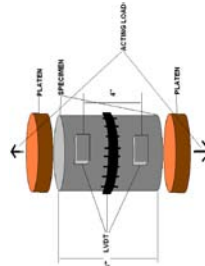
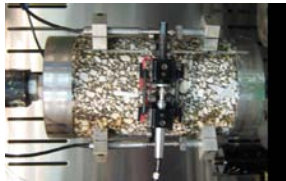
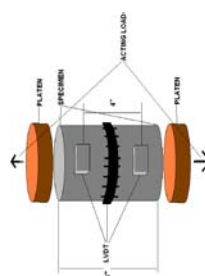
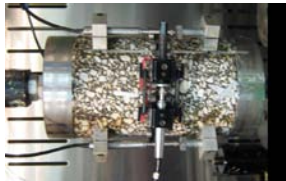
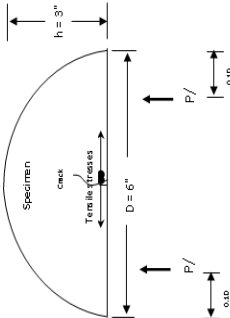
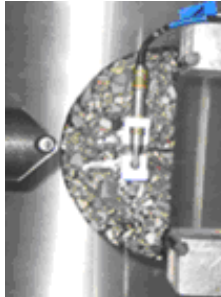
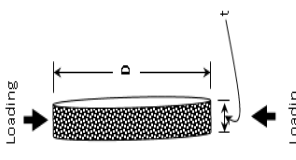

**Table 3-5. Test Plan and HMA Specimen Matrix for the Workability Indicator Tests.**

Mix Type	Mix-Design	Asphalt-Binder Content	No. of Replicate Specimens ( $\geq 28$ )	
			Servo Pac Gyratory Compactor	Pine Gyratory Compactor
Type D (Chico)	PG 70-22 + Limestone	OAC	$\geq 3$	$\geq 3$
		OAC + 0.5%	$\geq 3$	$\geq 3$
Type C (Hunter-Modified)	PG 70-22 + Limestone	OAC	$\geq 3$	$\geq 3$
		OAC + 0.5%	$\geq 3$	$\geq 3$
Type B (Chico)	PG 64-22 + Limestone	OAC	$\geq 3$	$\geq 3$
		OAC + 0.5%	$\geq 3$	$\geq 3$
Type C (Jones)	PG 76-22 SBS + Gravel	OAC	$\geq 3$	$\geq 3$
		OAC + 0.5%	$\geq 3$	$\geq 3$
Type C (Beaumont) plant-mix	PG 76-22 + Limestone	OAC <sub>1</sub> = 4.3% OAC <sub>2</sub> = 5.1%	$\geq 6$	$\geq 6$
NCAT N8&N9 plant-mix			$\geq 6$	$\geq 6$
HMA specimen dimensions (cylindrical)			6-inch diameter by 6-inch in height	6-inch diameter by 6-inch in height
Compaction parameters			600 kPa vertical pressure at 1.25° compaction angle	600 kPa vertical pressure at 1.25° compaction angle

**Table 3-6. Test Plan and HMA Specimen Matrix for APT Mix-Design Evaluation (for OAC Determination and APT Testing).**

Mix	Mix-Design	No. of Replicate Specimens ( $\geq 135$ )		
		Texas Gyratory Method	Balanced Mix-Design Hamburg	Overlay
Type C (Hunter-Modified)	PG 70-22 + Limestone	$\geq 12$	$\geq 6$	$\geq 9$
Type D (Chico)	PG 70-22 + Limestone	$\geq 12$	$\geq 6$	$\geq 9$
Type C (Chico)	PG 76-22 + Limestone	$\geq 12$	$\geq 6$	$\geq 9$
Type C (Beaumont)	PG 64-22 + Limestone	$\geq 12$	$\geq 6$	$\geq 9$
Type C (Beaumont-Modified)	PG 76-22 + Limestone	$\geq 12$	$\geq 6$	$\geq 9$

Table 3-7. Test Plan and HMA Specimen Matrix for the Crack Evaluation Tests.

Mix Type	Asphalt-Binder Content	No. of Replicate Specimens ( $\geq 192$ )					
		OT <sub>1</sub>	OT <sub>2</sub>	DT	SCB	IDT	
Test setup, specimen geometry, and dimensions							
		     	 	 	6" $\phi$ x 6" (or 4") height	6" $\phi$ x 3" high x 2" thick	6" $\phi$ x 2" thick ( <i>t</i> )
Type D (Chico)	OAC	$\geq 3$	$\geq 3$	$\geq 4$	$\geq 4$	$\geq 4$	
	OAC + 0.5%	$\geq 3$	$\geq 3$	$\geq 4$	$\geq 4$	$\geq 4$	
Type C (Hunter-Modified)	OAC	$\geq 3$	$\geq 3$	$\geq 4$	$\geq 4$	$\geq 4$	
	OAC + 0.5%	$\geq 3$	$\geq 3$	$\geq 4$	$\geq 4$	$\geq 4$	
Type B (Chico)	OAC	$\geq 3$	$\geq 3$	$\geq 4$	$\geq 4$	$\geq 4$	
	OAC + 0.5%	$\geq 3$	$\geq 3$	$\geq 4$	$\geq 4$	$\geq 4$	
Type C (Jones)	OAC	$\geq 3$	$\geq 3$	$\geq 4$	$\geq 4$	$\geq 4$	
	OAC + 0.5%	$\geq 3$	$\geq 3$	$\geq 4$	$\geq 4$	$\geq 4$	
HMA specimen AV		7 $\pm$ 1%	7 $\pm$ 1%	7 $\pm$ 1%	7 $\pm$ 1%	7 $\pm$ 1%	
Test temperature = ambient		77°F	77°F	77°F	77°F	77°F	

Note that the laboratories listed in Table 3-4 are the only ones currently having OT machines in Texas. Four of the labs (Austin, Atlanta, Childress, and Houston) listed in Table 3-4 are owned by TxDOT and the OT machines in these labs are routinely used for mix crack-resistance evaluation and screening. TTI represents an academic and research oriented lab. On the other hand, PaveTex is a private company representing the industry. This laboratory combination was, therefore, considered appropriate for OT round-robin testing.

In Table 3-5, the incorporation of plant mixes in the test plan was necessary so as to provide a means of comparing and validating the laboratory test results with field construction/performance data. N8 and N9 were the two perpetual pavements constructed at the NCAT test track in Alabama during the 2009 test cycles. TTI researchers have had access to the plant mix, laboratory test data, construction data, and field performance data of these sections (Walubita et al., 2009). Therefore, these construction and field data will be a basis for preliminarily validating the workability indicator concepts.

Note that one of the objectives of the APT testing is to compare the performance of mixes designed with the proposed balanced mix-design and the traditional Texas gyratory methods. As noted in Table 3-6, the intent of the laboratory evaluation under this task is to design and select the OAC using both methods and thereafter, comparing their field performance under APT testing, with the Texas gyratory designed mix saving as the control mix.

## HMA SPECIMEN FABRICATION

For the lab molded samples, the HMA specimen preparation procedure was consistent with the TxDOT standard specifications Tex-205-F and Tex-241-F (TxDOT, 2005, 2009). The basic procedure involved the following steps: aggregate batching, wet sieve analysis, asphalt-aggregate mixing, short-term oven aging, compaction, cutting and coring, and finally volumetric analysis to determine AV. The HMA mixing and compaction temperatures are summarized in Table 3-8.

**Table 3-8. HMA Mixing and Compaction Temperatures.**

<b>Asphalt-Binder PG Grade</b>	<b>Mixing Temperature (°F)</b>	<b>Compaction Temperature (°F)</b>
PG 76-22	325 (163 °C)	300 (149 °C)
PG 70-22	300 (149 °C)	275 (135 °C)
PG 64-22	290 (143 °C)	250 (121 °C)

The temperatures in Table 3-8 are consistent with the TxDOT Tex-205-F and Tex-241-F test specifications for PG asphalt-binders (TxDOT, 2005, 2009). Prior to mixing, the aggregates were always pre-heated at the mixing temperature for at least 8 hours to remove any moisture and facilitate ease mixing. The asphalt-binder was also heated for approximately 1 hour before mixing so as to liquefy it.

### **Short-Term Oven Aging and Molding**

HMA short-term oven aging for both lab-molded samples and plant mixes lasted for 2 hours at the compaction temperature consistent with the AASHTO PP2 aging procedure for Superpave mix performance testing (AASHTO, 2001). Note that short-term oven aging simulates the time between HMA mixing, transportation, and placement up to the time of in-situ compaction in the field.

With the exception of some of the workability indicator tests that used the Pine compactor, all the HMA specimens were gyratory compacted and molded using the standard Superpave Gyratory Compactor (SGC) according to Tex-241-F (TxDOT, 2009). All the HMA specimens were compacted to a target AV content of  $7 \pm 1$  percent.

### **Cutting and Coring of the Specimens**

DT, IDT, and SCB specimens were compacted in the SGC to a height of 6.9-inch in a 6-inch diameter mold. As per the new standard specification requirement, the OT specimens were compacted in the SGC to a height of 4.5-inch in the same mold (TxDOT, 2009). During molding, it was necessary to vary the AV of the 6.9-inch mold in order to achieve the target AV in each respective specimen type because of the differences in the geometry and AV distribution.

Based on the test specimen geometries and the required specimen dimensions shown in Table 3-8, two IDT specimens (typically cut from the middle zone) were obtainable from a one 6.9-inch long molded sample. Four SCB specimens were obtainable from the similar molded sample configuration, while only one DT specimen could be obtained. Likewise, only one OT specimen was obtainable from a 4.5-inch long molded sample. These details are further listed in Table 3-9 for more clarity.

**Table 3-9. HMA Specimen Molding, Cutting, and Coring.**

<b>Target Test Specimen</b>	<b>Test Specimen Geometry/Dimensions</b>	<b>Sample Molding Configuration</b>	<b>No. of Obtainable Test Specimens</b>	<b>Comment</b>
IDT	See Table 3-7	Cylindrically shaped = 6-inch diameter by 6.9-inch in height	2 from one molded sample	Typically cut from the middle zone, where density is considered more uniform
SCB	See Table 3-7		4 from one molded sample	
DT	See Table 3-7		1 from one molded sample	
OT	See Table 3-7	Cylindrically shaped = 6-inch diameter by 4.5-inch in height	1 from one molded sample	

After the specimens were cut and cored, volumetric analysis based on fundamental water displacement principles as specified in ASTM D2726 (ASTM, 2009) were completed to determine the exact AV content of each test specimen. HMA specimens that failed to meet AV specification (i.e.,  $7 \pm 1.0$  percent) were discarded. The good specimens were stored at ambient temperature on flat shelves in a temperature-controlled facility prior to gluing and testing.

## **SUMMARY**

This chapter provided a presentation of the materials and mix-designs used in this study. In total, three common Texas mix types (Type B, C, and D) with up to eight different mix-designs were evaluated. The experimental design including the test plans and HMA specimen matrices for each respective laboratory task were also presented in this chapter. HMA specimen fabrication including short-term oven aging and specimen cutting/coring were also discussed.



## CHAPTER 4

### AIR VOID CHARACTERIZATION WITH X-RAY CT SCANNING TESTS

This laboratory task was initiated as a means to investigate some of the possible causes of variability in the selected cracking test methods. To reduce variability in the test results, it is important to ensure uniform AV distributions in the HMA test specimens. X-ray CT scanning tests were, therefore, conducted to characterize the AV uniformity and distributional structure of the HMA specimens that were molded and compacted to different heights. The test plan and HMA specimen matrix for this task was as shown in Table 4-1.

**Table 4-1. Test Plan and HMA Specimen Matrix for X-Ray CT Scanning Tests.**

Mix	Asphalt-Binder Content	No. of Replicates for Cylindrically Molded Samples	
		6" $\phi$ $\times$ 6.9" height	6" $\phi$ $\times$ 4.5" height
Type B (more coarse-graded)	OAC	2	2
Type D (more fine-graded)	OAC	2	2
Associated test specimens		DT, IDT, SCB	OT

The X-ray CT characterizes the AV distribution (percent AV and AV size) as a function of the HMA specimen height (or depth). For this study, X-ray CT scanning tests were performed only on the original molded samples prior to cutting and/or coring. As shown in Table 4-1, two molding heights, 6.9 and 4.5-inch, respectively, were investigated, all with a mold diameter of 6-inch. As elaborated in Chapter 3, the 6.9-inch molding height was utilized for fabrication DT, IDT, and SCB test specimens. The 4.5-inch molding height was used for fabricating OT test specimens.

#### THE X-RAY CT SCANNER

The pictorial set-up for TTI's X-ray CT scanner is shown in Figure 4-1. Details of the X-ray CT scanner including the test set-up, test procedures, modes of operation, and data analysis procedures are documented elsewhere (Masad et al., 2009). In general, however, the test is typically conducted at ambient (room) temperature.



**Figure 4-1. Pictorial Set-Up of TTI's X-Ray CT Scanner.**

At the time of this report, X-ray CT scanning of cylindrical molded samples for the Type B and D mixes had been completed. As was shown in Table 4-1, two replicate samples, representing DT and OT cylinders, were scanned for each mix. An example of the DT and OT cylindrically molded samples is shown in Figure 4-2. Detailed results of X-ray CT scanning tests are included in Appendix B.



**Figure 4-2. Original SGC Compacted Cylinders (DT Left, OT Right).**

## X-RAY CT TEST RESULTS

The results of the X-ray CT tests are analyzed and interpreted herein to explain the AV distribution of the cylinders and the potential success of considering the 4-inch high DT test specimen over the 6-inch high DT test specimens. Note that the initial objective of the X-ray CT tests in this task was to ensure a uniform AV distribution throughout the trimmed portion of the specimens compacted for testing purposes. However, the analysis also proved useful in explaining the reduced variability in the results for the 4-inch-high DT test specimens versus the 6-inch high DT test specimens, discussed subsequently in Chapter 5.

### AV Distribution in 6 Inch Diameter by 6.9-Inch High DT Molded Samples.

Figure 4-3 represents a typical AV distribution in a 6-inch diameter by 6.9-inch high compacted cylinder for a Type D mix.

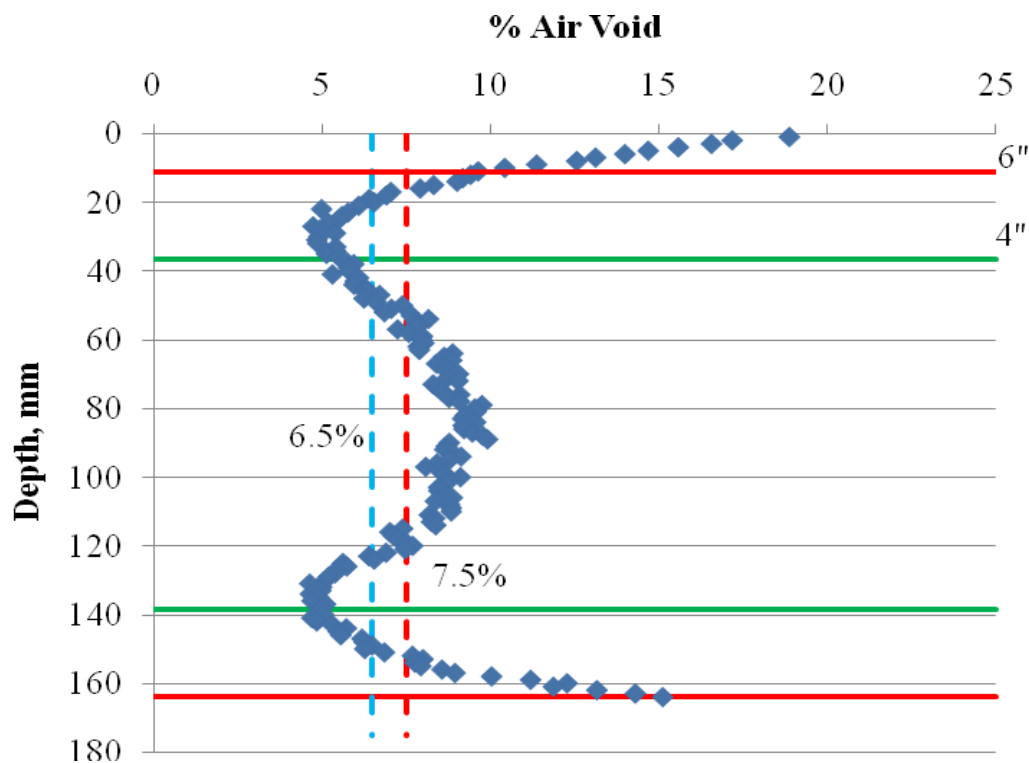
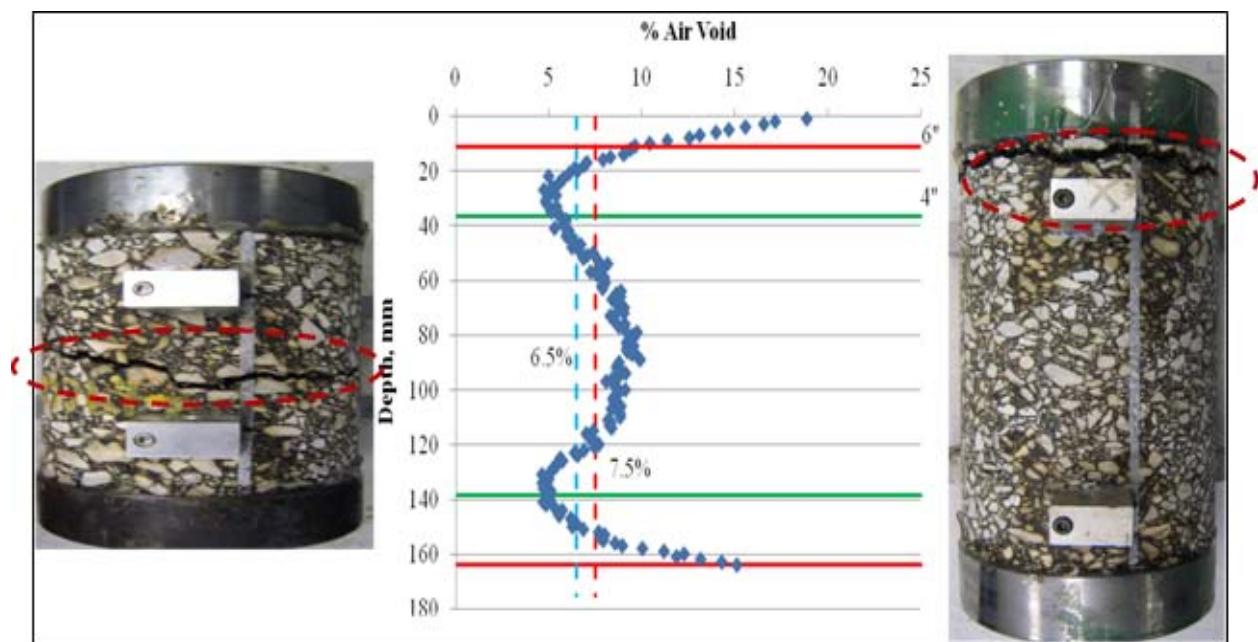


Figure 4-3. Typical AV Distribution in a 6"φ by 6.9" High DT Molded Sample.

In Figure 4-3, the red horizontal boundaries represent the AV distribution for cutting the sample to 6-inch high HMA test specimens. The green boundaries represent the AV distribution for cutting the sample to 4-inch high HMA test specimens. With respect to the target AV tolerance for this particular task, the dashed blue and red lines represent the lower and upper allowable limits, respectively. It is clear from Figure 4-3 that the AV distribution is non-uniform and considerably higher in magnitude at the ends and middle zone, representing the weaker zones where tensile failure is likely to occur if subjected to DT testing.

In the top or bottom 0.8-inch zone, the AV content is very high and significantly variable, ranging from 7.5 to about 19 percent. In the middle zone, the AV is fairly reasonable and is at least no more than 10 percent. Based on these observations, chances are, therefore, that a 6-inch high test specimen will likely fail at the end zones and in the middle zone for a 4-inch high test specimen when tested in direct-tension loading mode. Figure 4-4 shows a side by side comparison of the vertical AV distribution with the actual cut and tested DT specimens as well as the tensile failure zones for a Type D mix.



**Figure 4-4. Comparison of DT Failure Zones and Vertical AV Distribution (Type D Mix).**

For DT testing, the tensile failure zone should be in the middle as exhibited by the 4-inch high test specimen in Figure 4-4. End-failures such as the one exhibited by the 6-inch high specimens in Figure 4-4 are undesirable.

### **AV Uniformity and Variability – 6-versus 4-Inch High DT Test Specimens**

Figures 4-3 and 4-4 indicate comparatively high AV variability for the 6-inch high test specimen. The AV content decreases from about 19 percent at the outer edge to less than 5 percent just over a depth of 1-inch. As evidenced in Figure 4-4, this is a potential cause for edge failure in the 6-inch high DT specimens. For DT testing, tensile failure typically occurs at the weakest point; in this case, the least dense zones exhibiting high AV content. For the 4-inch high test specimen with a more uniform AV distribution, the weakest zone having the highest AV appears to be the middle and hence, middle-zone tensile failure as shown in Figure 4-4.

These results do indeed indicate that the AV's non-uniformity may have an impact on the variability in the cracking test results and, in the case of the DT test, 6-inch high test specimens are more vulnerable to AV related variability than the 4-inch high test specimens. This is primarily due to the fact that higher molding heights are comparatively more susceptible to aggregate segregation. In fact, it is typically not uncommon for the HMA mix to be scooped and poured in more than one lift when the molding height is greater than 5 inches.

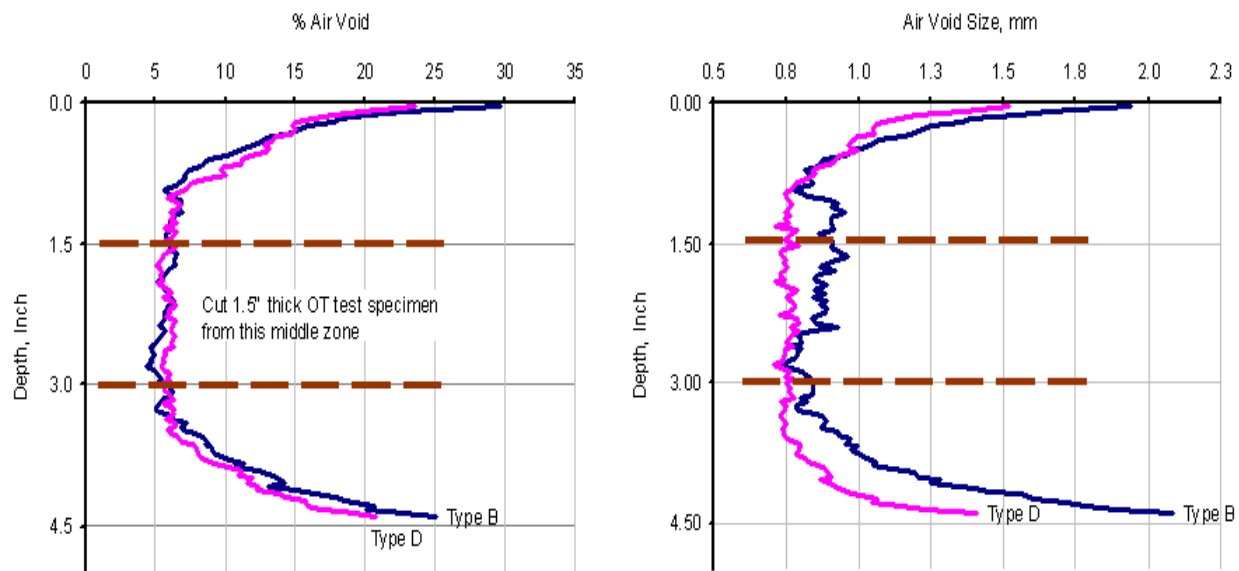
Measured in terms of the coefficient of variation (COV), the trimmed and cored 4-inch high DT test specimens also exhibited fairly acceptable variability (i.e., COV less than 25 percent) in the AV content among different test specimens compared to the 6-inch high DT test specimens. The AV test results for each individual DT test specimens are presented in Chapter 5.

### **Effects of the SGC Molds on the 6.9-Inch High DT Samples**

The AV non-uniformity and variability problem is in part attributed to the SGC mold dimensions and compaction configuration that can not adequately accommodate mold heights of more than 6.9-inch. With this current SGC molding configuration and the need to minimize variability, these X-ray CT results, therefore, support the transitioning to 4-inch high test specimen for DT tensile testing. While the final DT test specimen height should be 4-inch, the total molded sample height should still be maintained at 6.9-inch compaction height. This aspect was explored in this study and the results are presented subsequently in Chapter 5.

### AV Distribution in 6 -inch Diameter by 4.5-Inch High OT Molded Samples

As shown in Figure 4-5, the AV distribution in the 4.5-inch high OT molded samples is different from the 6.9-inch high DT molded samples. The AV distribution is uniform through out the middle zone of the sample. Only the outer edges, i.e., the top and bottom 0.8-inch, exhibited very high air voids. Thus, it is reasonable to cut 1.5-inch thick OT specimens from the middle zone of a 4.5-inch high molded sample; the AV distribution in this zone is fairly uniform.

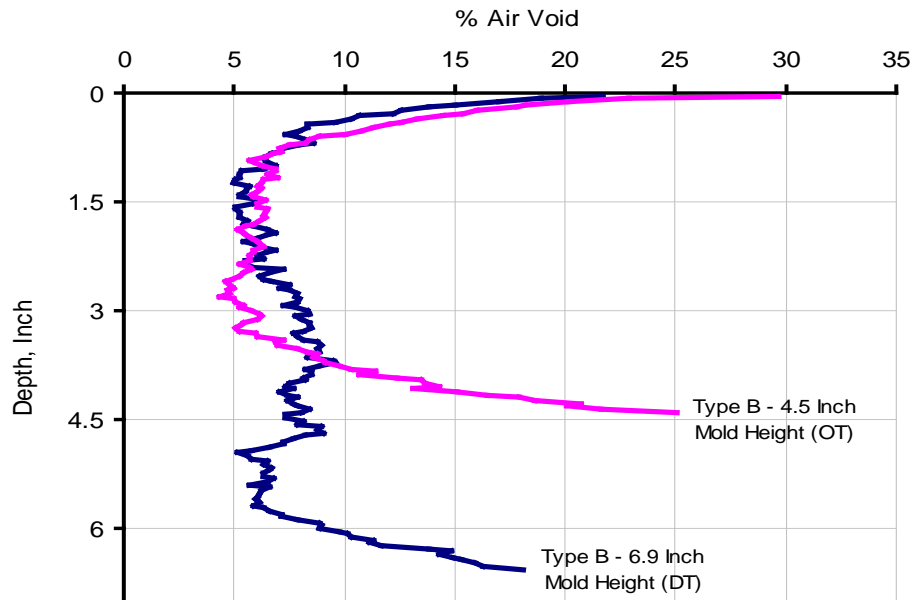


**Figure 4-5. AV Percentage and Size Distribution in a 4.5-Inch High Molded Sample.**

While the percent AV distributions as a function of depth in Figure 4-5 are insignificantly different, the AV sizes and variability (in terms of COV) for the Type B samples were larger in magnitude than those of Type D samples. In fact, the average AVs were 8.9 and 8.6 percent with COV values of 57.2 and 47.1 percent for the Type B and D sample, respectively. The AV sizes on the other hand were 1.0 mm (COV = 27.5 percent) and 0.8 mm (COV = 18.2 percent) for the Type B and D sample, respectively. This was theoretically expected because Type B mix consists of a relatively coarser aggregate gradation structure than Type D mix (see Chapter 3). In terms of the aggregate packing structure and orientation within the mix matrix, coarser aggregates often tend to create larger voids than smaller aggregates that allow a more closed packing orientation with little voiding.

### AV Distribution versus Sample Molding Height

Figure 4-6 shows a comparative plot of the AV distribution for 4.5- and 6.9-inch high molded samples.



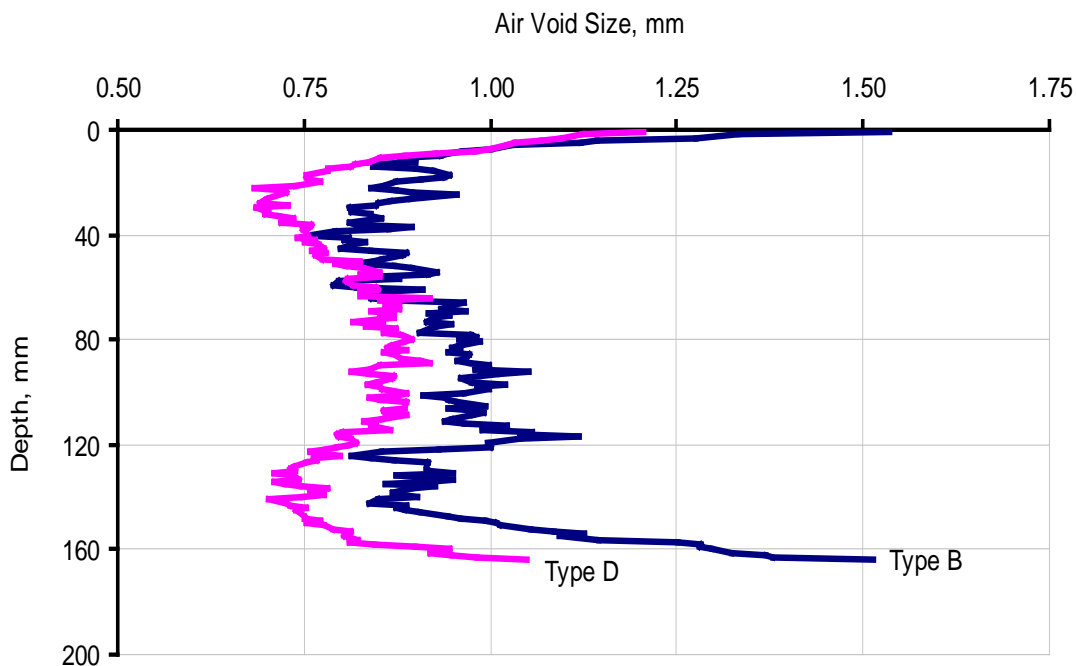
**Figure 4-6. AV Distribution versus Molding Height.**

For the mixes considered, it is clear from Figure 3-7 that molding to a shorter height leads to a better AV uniformity and distributional structure in the middle zone of the molded sample. By contrast, the figure suggests that longer molding heights would be more prone to non-uniform AV distribution and variability than shorter molding heights.

### HMA Mix Comparisons – Type B Versus Type D Mix

Interestingly, there was no significant difference in the percentage of AV distribution trend or magnitude between the two mixes; i.e., all exhibited a trend shown in Figures 4-3 through 4-6 both in terms of the percentage AV distribution and magnitude (an average of 8.3 percent). For the DT samples, and considering both mixes, the AV was typically higher at the edges and revolved between 7.5 and 10 percent in the middle zone of the specimens (see Figure 4-3). For the OT samples, the AV content for the middle zone was around 6.0 percent while the edges ranged from 7.5 to about 30 percent (see Figure 4-5).

By contrast and as was noted in Figure 4-5, there was a considerable difference in the AV sizes. The more coarser-graded Type B mix exhibited relatively larger AV sizes in magnitude compared to the more finer-graded Type D mix, as theoretically expected. Some examples of these AV size comparisons plotted as a function of DT sample depth are shown in Figure 4-7.



**Figure 4-7. AV Size Comparisons for DT Samples – Type B versus Type D Mix.**

Based on Figure 3-8, the average AV size was 0.95 and 0.82 mm for the Type B and Type D samples, respectively. Thus, the AV sizes for the Type B mix were on average 11 percent larger than those for the Type D mix. As shown in Table 4-2, variability, measured in terms of the COV magnitude, was also slightly higher for the Type B than for the Type D mix. Based on these COV numbers, it would be expected that Type B mix would be associated with more AV variability during sample fabrication compared to Type D mix. On this basis, it can intuitively be stated that coarse-graded mixes require more meticulous work and caution during sample fabrication. Notice in Table 4-2 that the average AV content for the DT samples was nearly the same for the two mixes, i.e., 8.0 and 7.9 percent for the Type B and D specimens, respectively.



**Table 4-2. Mix AV Comparisons as a Function of Sample Height  
(Percentage Content and AV Size).**

<b>Mix</b>	<b>Mix-Design</b>	<b>Sample Height</b>	<b>Avg. AV Content</b>	<b>COV for Avg. AV Content</b>	<b>Avg. AV Size</b>	<b>COV for AV Size</b>
Type B	4.3% PG 70-22 + Limestone	6.9 inches	8.0%	35.7%	0.95 mm	13.9%
Type D	5.0% PG 70-22 + Limestone	6.9 inches	7.8%	32.7%	0.82 mm	10.5%
Type B	4.3% PG 70-22 + Limestone	4.5 inches	8.9%	57.2%	1.00 mm	27.5%
Type D	5.0% PG 70-22 + Limestone	4.5 inches	8.6%	47.1%	0.84 mm	18.2%

### **Sample Trimming Distance**

To have test specimens with better AV uniformity and distributional structure, the X-ray CT results presented herein tends to favor trimming a minimum of 0.8-inch on either sides of a molded sample. This is because the sample edges were found from this study to be the weakest zones with higher AV content (i.e., lowest density) and, therefore, more prone to break failure when the sample is subjected to tensile loading. Thus, the premise is to move away from the edges as much as possible when trimming the samples.

However, 0.8 inches minimum is problematic for the 6-inch high DT specimens since the sufficiently attainable maximum mold height is only 6.9-inch. With the current SGC set-up and molding dimensions, one possible solution to this problem would be to explore shorter DT test specimens such as 4- or 5-inch high, but bearing in mind the aspect ratio and NMAS coverage requirements (Bonaquist et al., 2003; Tandon et al., 2006):

- Aspect ratio (*ar*) (longest side divided by the shortest side):  $1.5 \leq ar \leq 2.0$
- NMAS coverage (*NMAS\_C*):  $1.5 \times NMAS \leq NMAS_C \leq 3.0 \times NMAS$

In this interim report, the vertical AV distribution discussed herein did not take into account the fact that the DT specimens will be cored to 4 inches in diameter. Therefore, radial AV distribution characterization is another aspect that may be considered for exploration in the course of this research work.

## **SUMMARY**

HMA specimen AV distribution characterization based on the X-ray CT scanning test results were presented, analyzed, and discussed in the chapter. Overall, the X-ray CT test results indicated that Type B mix and the 6-inch high DT test specimens would be more likely associated with AV variability and high potential for edge failures when subjected to tensile testing, compared to the Type B mix and the 6-inch high DT test specimens, respectively. The results indicated significantly higher AV content (i.e., lowest density and weakest area) in the top and bottom 0.8-inch zone of the molded samples.

In general, there is high potential for aggregate segregation and AV variability in samples molded to higher heights. Thus, transitioning to 4-or 5-inch high DT test specimens and/or trimming a minimum of 0.8-inch on either sides of a molded sample maybe warranted. With shorter heights however, caution should be exercised to meet the specimen aspect ratio and NMAS coverage requirements

## **CHAPTER 5**

### **LABORATORY CRACKING TESTS, RESULTS, AND COMPARATIVE EVALUATION OF THE TEST METHODS**

As discussed in the preceding chapters, one of the objectives of this research study is to comparatively evaluate various laboratory cracking tests and subsequently, recommend one that is, among other desired characteristics, simpler, performance-related, repeatable, and readily applicable for routine industry use. Accordingly, this chapter addresses this objective, including describing the laboratory test protocols, presenting the laboratory cracking test results, and subsequent ranking of the test methods. The chapter then concludes with a list of key findings and recommendations.



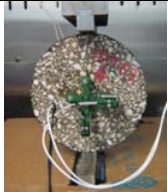

#### **LABORATORY CRACKING TEST PROTOCOLS**

Six laboratory test methods, namely (repeated loading) OT, monotonic loading DT, monotonic loading IDT, monotonic loading SCB, repeated loading IDT (R-IDT), and repeated loading SCB (R-SCB), were comparatively evaluated and are discussed in this section. The test protocols are summarily described in Table 5-1 and include the test type, loading configuration, and the output data.

Note that the OT is a standardized TxDOT cracking-performance test with the OT standard procedure described in the TxDOT test specification Tex-248-F (TxDOT, 2009). Accordingly, Tex-248-F (TxDOT, 2009) was the test procedure that was utilized for OT testing and data analyses in this interim report. IDT is both an ASTM and TxDOT standardized test procedure for characterizing the HMA mix tensile strength (indirect). For this study, the TxDOT IDT test specification Tex-226-F was utilized (TxDOT, 2004). To the authors' best knowledge at the time of this report, both DT and SCB are not standardized tests.

In addition to the monotonic loading IDT and SCB tests, preliminary investigations into their repeated loading counterparts, R-IDT and R-SCB, were also conducted. These laboratory tests (R-IDT and R-SCB) and their associated preliminary test results are also included in this interim report and are discussed in this chapter.

**Table 5-1. Laboratory Cracking Test Protocols.**

Test Type	Purpose	Pictorial/Schematic Set-Up	Specimen Prep	Test Loading Parameters	Test Stop Criteria	Output Data of Interest	Failure Criteria
OT	HMA cracking (reflective) potential		Gluing required; $\geq 8$ hrs curing time; external LVDTs optional	Repeated cyclic triangular displacement load control; max. displacement = 0.025 inches, loading rate = 10 sec/cycle; test temp = 77° F	93% load reduction or 1000 cycles, whichever comes first	Load, gap displacement, time, # of cycles to failure, test temperature	# of cycles used as measure of crack resistance.
DT	HMA tensile strength, fracture resistance, & ductility potential		Gluing required; $\geq 8$ hrs curing time; external LVDTs required	Monotonic axial tensile loading @ 0.05 in/min, 77° F test temperature, preferably capture data every 0.1s	Max load; set test to stop @ 75% load reduction or when LVDTs are maxed out	Load, time, axial deformations, max load @ failure, tensile strength ( $\sigma_t$ ), & failure tensile strain at break (max load) ( $\epsilon_t$ )	Tensile strain at max load used as indicator of ductility & cracking resistance potential
IDT	HMA tensile strength (indirect)		External LVDTs required	Monotonic axial compressive loading @ 2 in/min, 77° F test temperature	Max load or crack propagation through entire specimen	Axial load, time, max load @ failure, axial deformation, horizontal strain at max load	Max horizontal strain at max load & strength used as indicator of ductility & cracking resistance potential
SCB	HMA tensile strength, ductility, & cracking potential		Notching required = 0.25 inches, external LVDTs optional	Three-point loading configuration, monotonic axial compressive loading @ 0.05 in/min, 77° F test temperature, preferably capture data every 0.1s	Max load or crack propagation through entire specimen	Axial load, time, max load @ failure, axial deformation	Max ram displacement at max load & strength used as indicator of ductility & cracking resistance potential
R-IDT	HMA fracture strength and cracking-resistance potential	Same as IDT	Same as IDT	Repeated axial compressive loading at 1 Hz, input load is percentage of IDT max load, 77° F test temp	Still under investigation	Load, time, & # of repetitions	# of IDT load repetitions prior to crack failure utilized as indicator of crack resistance
R-SCB	HMA fracture strength and cracking-resistance potential	Same as SCB	Same as SCB	Three-point loading set-up, repeated axial compressive loading @ 10 Hz, input load is percentage of SCB max load, 77° F test temp	Still under investigation	Load, time, & # of repetitions	# of SCB load repetitions prior to crack failure utilized as indicator of crack resistance

## HMA MIXES EVALUATED

The evaluation of the test methods under this task was based on testing three mixes, namely Type B (Chico), Type C (Hunter-Modified), and Type D (Chico), at OAC design. Mix-design details for these mixes were presented previously in Chapter 3; see Table 3-1. To facilitate a level ground for comparison purposes, all the laboratory tests were conducted at ambient temperature (i.e., 77 °F). The minimum temperature conditioning time for all the test specimens was 2 hrs.

A minimum of three replicate specimens were used per test type per mix type. The target AV for the test specimens was  $7 \pm 1$  percent. As mentioned in Chapter 3, test specimens that did not meet the target AV specification were discarded and not tested. With the exception of the OT test specimens that were batched by bin percentages, test specimens for all the other cracking tests were batched by individual sieve sizes after a wet sieve analysis; refer to Chapter 3.

For the purpose of statistical analysis in this study, 30 percent COV was arbitrarily utilized as the measure of acceptable variability for all the laboratory cracking tests. Meaning, a COV less than 30 percent is considered reasonable and vice versa for COV values than 30 percent.

## THE OT TEST RESULTS

The results of standard OT testing based on mixes Type C and D are summarized in Table 5-2. Note that the results in Table 5-2 represent an average summation of a minimum of three replicate specimens per mix type. Detailed test results are included in Appendix C.

**Table 5-2. Average OT Test Results.**

<b>Mix</b>	<b>Asphalt-Binder + Aggregate</b>	<b>AV (%)</b>	<b>Initial OT Load (lb)</b>	<b># of OT Cycles of Failure (<math>N_{OT}</math>)</b>
Type C	4.9% PG 70-22 + Limestone	7.0 (COV=3.6%)	755 (COV=5.9%)	38 (COV=18.1%)
Type D	5.0% PG 70-22 + Limestone	7.3 (COV=4.2%)	633 (COV=8.1%)	274 (COV=17.05%)

With the OT test, the cracking resistance potential of a mix is measured and defined in terms of the number of OT cycles to failure, where failure is defined as 93 percent reduction in initial load. As a tentative mix screening criteria, mixes that last over 300 cycles are considered satisfactory with respect to laboratory cracking resistance. With this criteria, Table 5-2 shows better laboratory cracking performance for the Type D mix based on the higher number of OT cycles to failure. As discussed previously in Chapter 3, this result was not unexpected as the Type C mix was composed of relatively poor quality and absorptive limestone aggregates that tend to reduce the net effective asphalt-binder content. Figure 5-1 shows an example of a typical OT crack failure with a single crack.



**Figure 5-1. Example of Typical OT Crack Failure with a Single Crack.**

Statistically, the OT test results for both mixes exhibit acceptable variability, with COV values less than 30 percent; see Table 5-2. These results suggest that adherence to the Tex-248-F test procedure and exercising proper sample fabrication procedures are some of the key factors to minimizing variability and improving repeatability of the OT test. Summarily, the OT ranks Type D as a better laboratory crack-resistant mix than Type C.

## MONOTONIC-LOADING DT TEST RESULTS

For the DT test, the tensile stress and maximum tensile strain at failure (i.e., at maximum load) under a stress-strain response curve were the two parameters used as indicative measures of the HMA tensile strength, fracture resistance, and ductility potential. The ductility potential, expressed in terms of the tensile strain at maximum load (or tensile failure), was in turn utilized as an indirect measure of the HMA crack-resistance potential. Equations 5-1 and 5-2 were utilized for computing the stress and strain, respectively (Walubita, 2006):

$$S_T = P/(\pi r^2) \quad (\text{Equation 5-1})$$

$$\mu\epsilon_T = (10^6/4)*V_{avg} \quad (\text{Equation 5-2})$$

where,

$S_T$  = tensile stress, psi,

$P$  = axial load, lbf,

$r$  = specimen radius, in (4 inches in this case),

$\mu\epsilon_T$  = tensile microstrain, in/in, and

$V_{avg}$  = average vertical deformation, inch.

Evaluation of the DT test was based on two mixes, Type C and D, with specimen heights of 6 and 4 inches, respectively. Six inches is the typical height for DT test specimens (Walubita, 2006). However, based on the X-ray CT test results (i.e., AV distribution) discussed previously in Chapter 4, the intent of using two different specimen heights was to comparatively evaluate if using 4-inch high DT test specimens would be statistically beneficial in minimizing edge failures and variability in the DT test results. By nature of their geometrical dimensions, the 6-inch high DT test specimens were apparently more susceptible to the effects of non-uniform AV distribution than the 4 inch high specimens. They exhibited very high AVs at the end zones and were thus, more prone to edge failures when subjected to DT tensile loading.

The DT test results are listed in Table 5-3. The results represent an average of a minimum of three and two replicates for the 6- and 4-inch high DT test specimens, respectively. Detailed test results including individual stress-strain curves are given in Appendix C.

**Table 5-3. Average DT Test Results.**

<b>Mix</b>	<b>Mix-Design</b>	<b>AV (%)</b>	<b>Max Load (lb)</b>	<b>Tensile Stress (psi)</b>	<b>Tensile Strain @ P<sub>max</sub> (μϵ)</b>	<b>Specimen Failure</b>
Type C (6" high)	4.9% PG 70-22 + Limestone	6.7 (COV=1.7%)	839 (COV=19.1%)	71 (COV=19.1%)	2908 (COV=11.0%)	All failed at edges
Type C (4" high)	4.9% PG 70-22 + Limestone	6.1 (COV=1.5%)	1078 (COV=0.6%)	86 (COV=0.6%)	1529 (COV=16.0%)	All failed in middle
Type D (6" high)	5.0% PG 70-22 + Limestone	6.7 (COV=3.0%)	572 (COV=22.7%)	46 (COV=22.7%)	5600 (COV=19.5%)	Mostly failed at the edges
Type D (4" high)	5.0% PG 70-22 + Limestone	6.1 (COV=1.9%)	697 (COV=4.0%)	55 (COV=4.0%)	2583 (COV=13.3%)	Not exactly in middle

As evident in Table 5-3, statistical variability is reasonably acceptable for both mixes and at both test specimen heights. All the COV values are less than 30 percent in magnitude, with the Type C generally out-performing the Type D mix. With the exception of the tensile strain results for the Type C mix, variability also appears to be exhibiting a decreasing trend with a decrease in specimen height, probably due to a more uniform AV distribution, discussed previously in Chapter 4.

Furthermore, while the load and stress increased, the strain decreased as the test specimen height was decreased from 6- to 4-inch. In terms of the tensile failure modes, the majority of the 4-inch high test specimens failed in the desired middle zone. By contrast, the majority of the 6-inch high test specimens failed at the edges. Additionally, there were also instances of end cap failure, probably due to poor gluing practices and insufficient curing time. Examples of these failure modes are shown in Figures 5-2 and 5-3.

Since the majority of the failure mode was in the middle zone of the specimens, it can be theorized that the results for the 4-inch high test specimens more accurately represent the HMA tensile, fracture, and cracking-resistance properties. Therefore, consideration to using 4-inch high DT test specimens need to be explored further. However, this does not disqualify the need for being careful in the specimen preparation procedures such as gluing and curing, so as to minimize end cap failures.





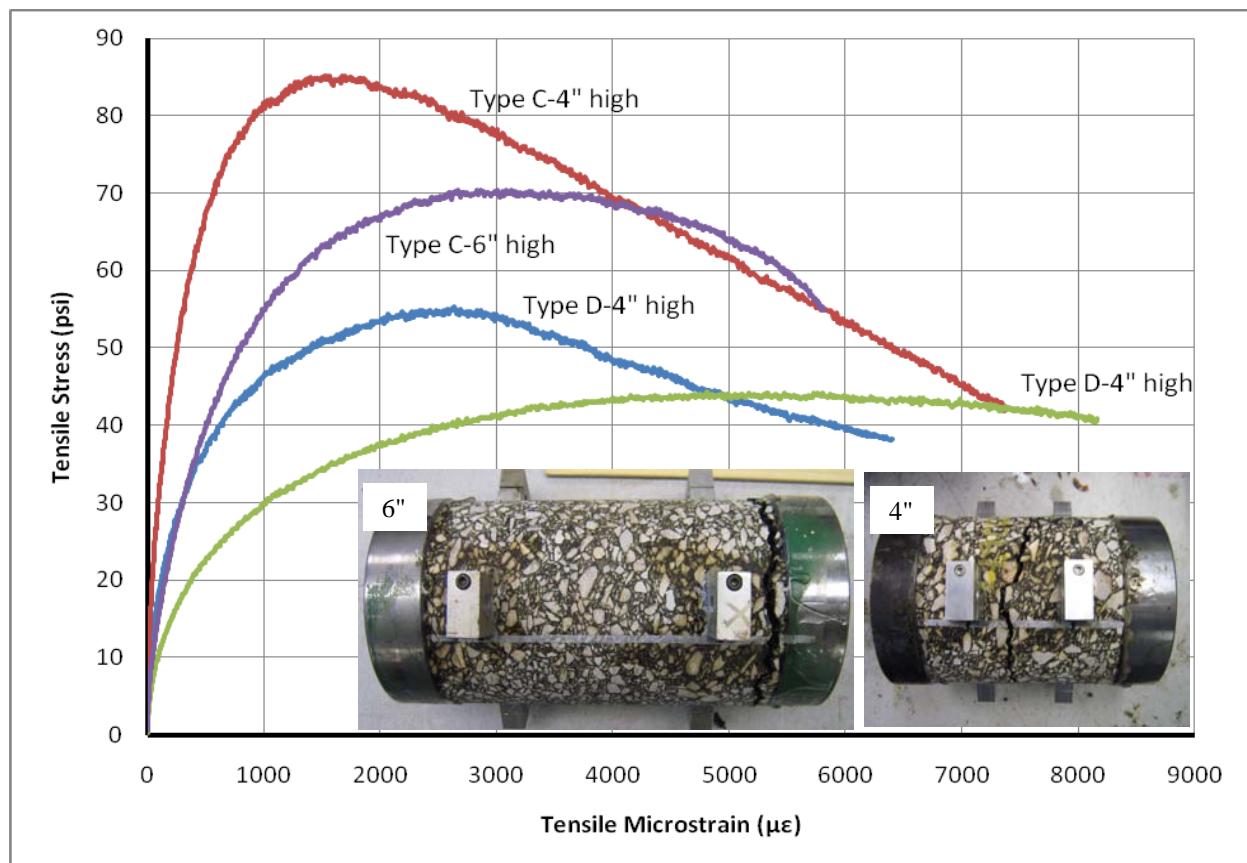
**Figure 5-2. Example of DT Failure Modes.**



**Figure 5-3. Example of End Cap Failure.**

In terms of mix comparison and using the tensile strain as an indicator of HMA ductility and cracking resistance potential, mix Type D out ranks mix Type C based on its higher strain magnitudes. For the 6-inch high test specimens, Walubita et al. (2007) previously proposed 3000  $\mu\epsilon$  as a minimum threshold for adequate laboratory cracking and fracture resistance properties. On this basis, mix Type D with 5600  $\mu\epsilon$  would be qualified as having satisfactory laboratory cracking performance. This high tensile strain at failure is indicative that the mix is fairly flexible and ductile enough to withstand load applications prior to yielding to tensile crack failure.

By contrast, mix Type C exhibits a more stiff and brittle behavior with lower tensile strains at failure. Compared to mix Type D, this mix will comparatively be more susceptible to tensile crack failure under similar loading and environmental conditions. A comparative plot of the stress-strain response curves for the two mixes and the respective specimen heights is shown in Figure 5-4.



**Figure 5-4. DT Stress-Strain Response Curves and Typical Crack Failure Mode.**

Based on the high stress magnitude, low strain magnitude at maximum stress, and the steep slope of the curve, it is clear from Figure 5-4 that mix Type C is comparatively stiffer and less ductile than mix Type D, properties that are undesirable for cracking resistance performance. If the ratio of stress to strain in the linear portion of the curves is assumed to represent the linear-elastic modulus of the mixes, it is easy to conclude that the Type C mix is the stiffer than Type D. Furthermore, it is evident that transitioning to the shorter 4-inch high DT test specimens makes the mix stiffer and more brittle with a higher tensile failure load but a much lower strain at the same failure load. Looking at Table 5-3, the strain decreased by over 47 percent when using the 4-inch high DT test specimens.

## MONOTONIC-LOADING IDT TEST RESULTS

This test was conducted according to the TxDOT test specification Tex-226-F (TxDOT, 2004). The test measures the HMA indirect tensile strength under monotonic axial compressive loading mode; see Table 5-1. The maximum load measured at failure is the parameter used to characterize the HMA indirect tensile strength and fracture resistance potential. In this interim report, the maximum horizontal deformation at maximum load (failure point) was used as the indicator of the ductility and crack-resistance potential. For the IDT data analysis, the indirect tensile stress occurring in the center of the specimen was computed as follows (Huang et al., 2005):

$$S_T = \frac{2P}{\pi t D} \quad (\text{Equation 5-3})$$

where,

$S_T$  = tensile stress, psi,

$P$  = axial load, lbf,

$t$  = specimen thickness, inch (2" in this case), and

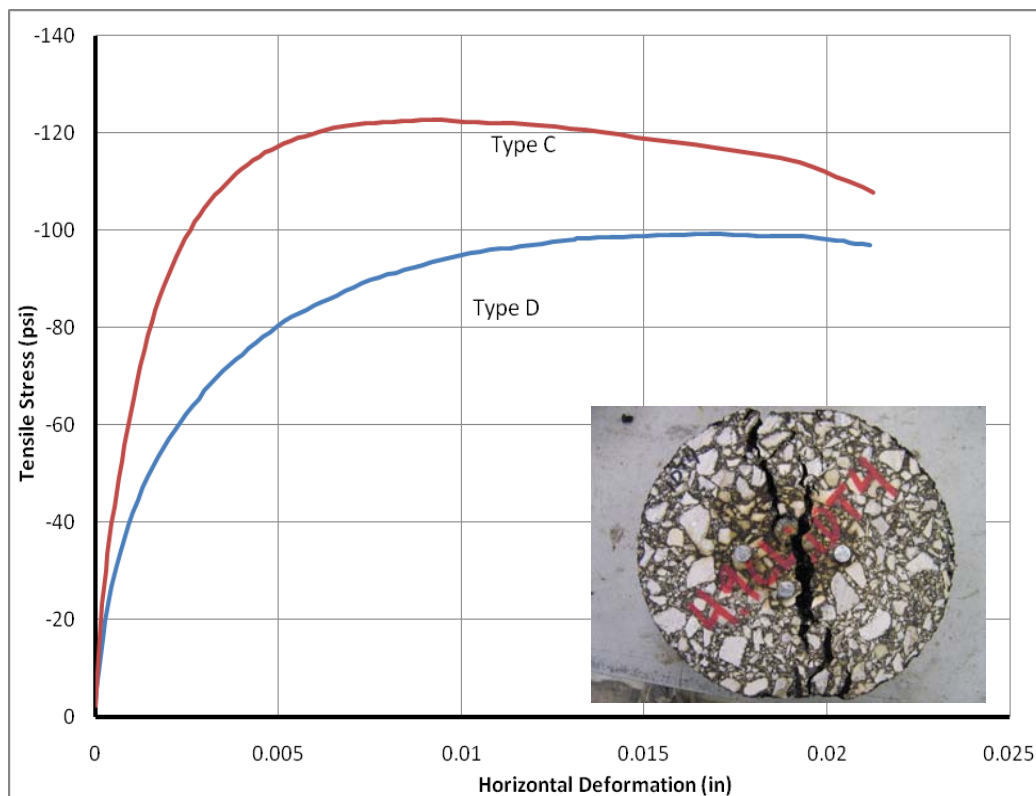
$D$  = specimen diameter, inch (6" in this case).

The strain in the specimen was simplistically defined as the direct measurement of the horizontal deformation in the specimen. IDT test results for mixes Type C and D are summarized in Table 5-4. Detailed IDT test results are included in Appendix C.

**Table 5-4. Average IDT Test Results.**

Mix	Mix-Design	AV (%)	Max Load (lbf)	Max. Tensile Stress (psi)	Hor. Deformation @ Max Load (in)
Type C	4.9% PG 70-22 + Limestone	7.2 (COV=4.9%)	2315 (COV=5.2%)	123 (COV=5.2%)	0.009 (COV=13.3%)
Type D	5.0% PG 70-22 + Limestone	7.2 (COV=5.7%)	1879 (COV=4.8%)	100 (COV=4.8%)	0.017 (COV=20.8%)

Statistical variability in terms of the COV values is acceptable in either mix, i.e., lower than 30 percent. However, the maximum load is achieved at a much higher horizontal deformation in the Type D mix than Type C. The Type D maximum horizontal deformation is almost twice that of the Type C mix. This is indicative that Type D is more ductile and thus better crack-resistant mix than Type C. Based on Figure 5-5, it is apparent that Type C exhibits greater stiffness and that the peak stresses are achieved much quicker relative to the specimen deformation than the Type D mix. Overall and based on simple horizontal deformation analyses, the IDT test ranks mix Type D as a better laboratory crack-resistant mix than Type C.

**Figure 5-5. IDT Stress-Deformation Curves and Typical Crack Failure Mode.**

## MONOTONIC-LOADING SCB TEST RESULTS

The SCB was one of the laboratory test methods that were investigated for characterizing the HMA tensile strength, ductility, and crack-resistance potential based on the tensile stress and displacement/strain measurements. As noted in Table 5-1, the test configuration consists of a three-point compressive loading (monotonic) that induces tension at the bottom zone of a semi-circular shaped specimen. Crack initiation and subsequent propagation was centrally localized through 0.25 inches notching at the base of the specimen.

Due to the complexity nature of the SCB specimen geometry when loaded, horizontal deformations were not measured. For this reason, the vertical ram displacement and stress at maximum load (failure point) were utilized as indicative measures of the HMA ductility, tensile strength, and crack-resistance potential, respectively. From the SCB test data, the stress occurring in a notched specimen was determined as follows (Hofman et al., 2003):

$$S_T = \frac{4.263 \times P}{D \times t} \quad (\text{Equation 5-4})$$

where,

- $S_T$  = tensile stress, MPa,
- $P$  = axial load, N,
- $t$  = specimen thickness, mm, and
- $D$  = specimen diameter, mm.

For convenience and simplicity of interpretation, the stress values were converted into English units (i.e., psi) after computations. The SCB test results for mixes Type C and D are summarized in Table 5-5, and represent an average of at least three replicates specimens. Detailed SCB test results are included in Appendix C.

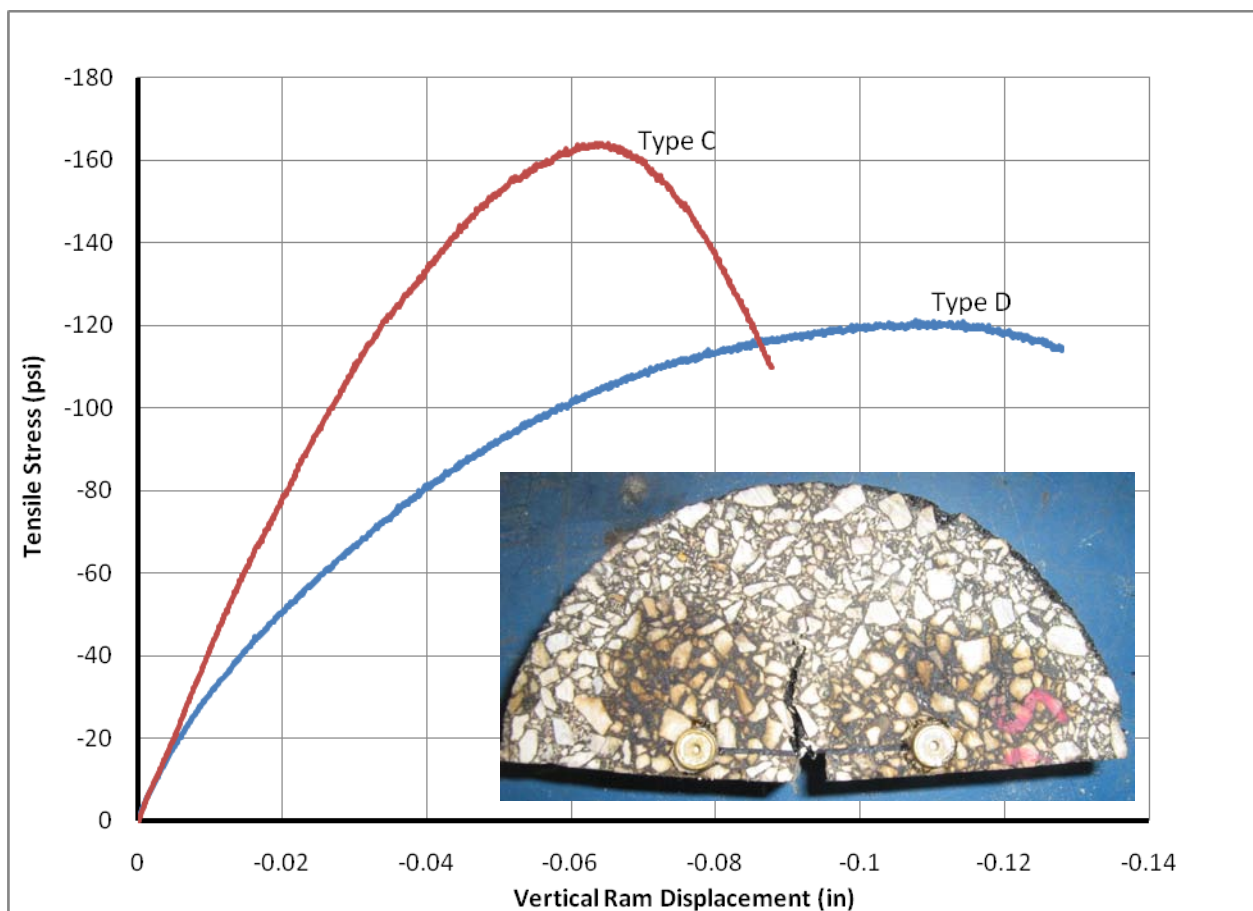
**Table 5-5. Average SCB Test Results.**

Mix	Mix-Design	AV (%)	Max Load (lbf)	Max. Tensile Stress (psi)	Ram Displacement @ Max Load (in)
Type C	4.9% PG 70-22 + Limestone	7.4 (COV=2.6%)	452 (COV=10.6%)	166 (COV=10.8%)	0.070 (COV=6.6%)
Type D	5.0% PG 70-22 + Limestone	7.2 (COV=2.7%)	346 (COV=3.6%)	126 (COV=3.6%)	0.106 (COV=21.8%)



The results in Table 5-5 show reasonable variability for both mixes, i.e., the COV values are less than 30 percent. By contrast, the results indicate that the maximum load is achieved at a much higher ram displacement for the Type D mix than Type C. The average maximum ram displacement for the Type D mix was 1.5 times that of the Type C mix. This is indicative that the Type D mix is more ductile and has more potential to elongate prior to tensile crack failure. Therefore, this mix would be considered to have better laboratory crack-resistance properties than the Type C mix.

The Type C mix on the other hand exhibits considerable stiffness with the peak stress achieved at a much faster rate relative to the specimen deformation. These results are shown graphically in Figure 5-6 together with an illustrative photo of a typical SCB crack failure mode.



**Figure 5-6. SCB Stress-Displacement Curves and Typical Crack Failure Mode.**

## **REPEATED-LOADING IDT (R-IDT) TESTING**

Preliminary repeated IDT loading tests were also conducted to investigate their R-IDT suitability and practicality for characterizing the HMA mix cracking resistance. With the R-IDT test method, the cracking resistance potential of a mix is characterized by the number of IDT load repetitions to crack failure, defined as the ability of a mix to withstand a repeatedly applied constant load. Specimen failure or test termination under this set-up is tentatively considered as full crack propagation through the HMA specimen. However, a threshold number of R-IDT load repetitions will still need to be established to discriminate between good and poor crack-resistant mixes.

Accordingly, the intent of the text below is to describe the process by which the R-IDT testing parameters were chosen and to offer some hypotheses for establishing the R-IDT failure and screening criteria for performance ranking of the mixes in terms of the laboratory cracking resistance.

### **Selection of the R-IDT Input Loads**

Setting up of the R-IDT test was a two-phase process, establishing the input loads via monotonic IDT testing and then using a fractional percentage of the maximum IDT failure load as the R-IDT input load. Only the Type D mix was preliminarily evaluated and the average maximum IDT failure load from monotonic IDT testing was found to be 1,998 lbf at ambient temperature (77 °F). Using this load magnitude of 1,998 lbf, three load levels at 20 (400 lbf), 30 (600 lbf), and 50 (1,000 lbf) percent were arbitrarily selected and utilized as the trial R-IDT input loads.

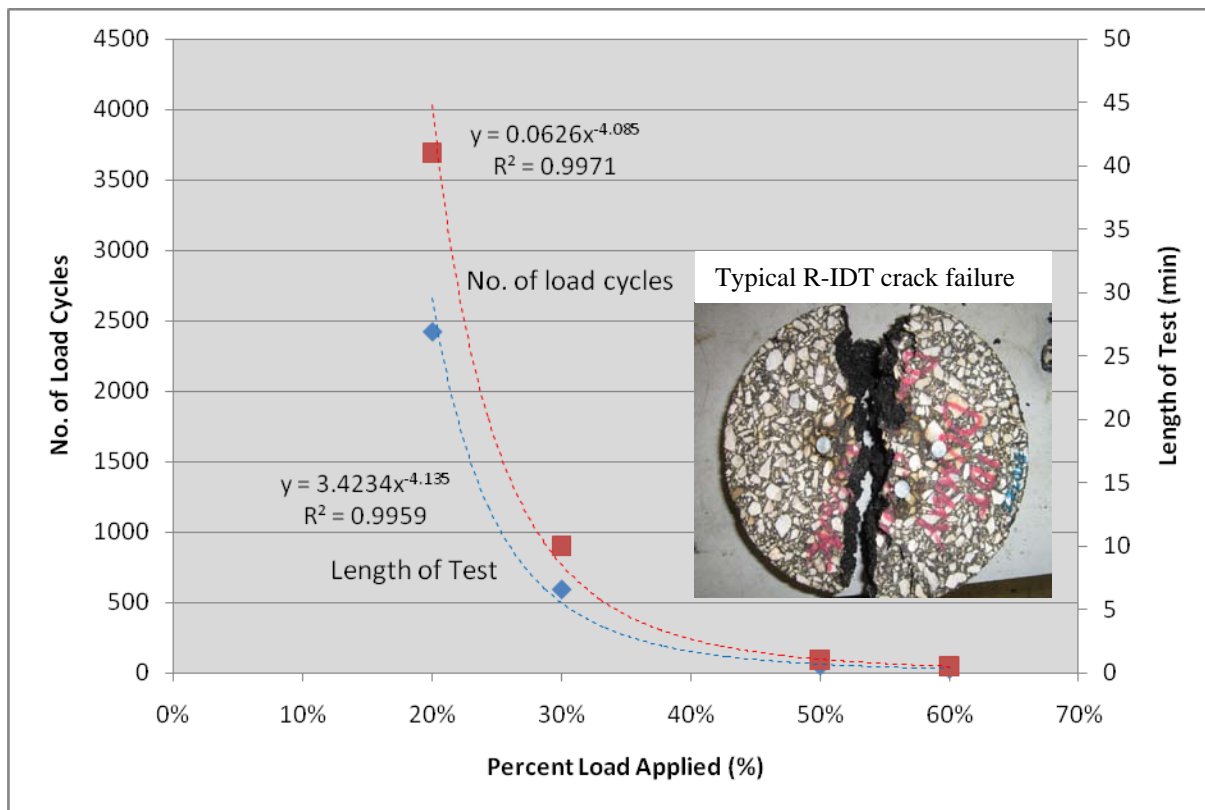
### **Preliminary R-IDT Test Results for Type D Mix**

The R-IDT test was run at 1 Hz without any rest periods till crack failure. Trial testing with a loading frequency of 10 Hz had proved unsuccessful for the IDT test configuration. Preliminary R-IDT results at ambient temperature (77 °F) are shown in Table 5-6 and Figure 5-7, respectively, for the Type D mix.

**Table 5-6. R-IDT Test Results at Various Load Levels for the Type D Mix.**

Test#	% of 1,998 lbf	R-IDT Input Load (lbf)	Time to Crack Failure (min)	IDT Load Repetitions to Crack Failure
1	20%	400	41	2,420
2	30%	600	10	594
3	50%	1,000	1	54

From Table 5-6, one can observe that the 20 percent load level lasted the longest amount of time (41 min) and achieved the largest number of IDT load repetitions to crack failure (2,420) as expected. Figure 5-7 shows a plot of the IDT load repetitions and test time as a function of load level.



**Figure 5-7. Type D R-IDT Percent Load Relationship Curves.**



Based on a second order polynomial fit function and interpolative analysis, 25 percent would be selected as a reasonable R-IDT input load for this mix. The test time would be 30 min with about 2,500 IDT load repetitions prior to crack failure. The plan is to repeat similar tests on other mixes, and then select one load level as the universal R-IDT input load. Thereafter, the number of IDT load repetitions to crack failure would be compared to rank the laboratory cracking resistance of the mixes.

Compared to the IDT, the R-IDT is a good candidate for cracking testing because: 1) it can be more easily compared to the Overlay (although some form of normalization must occur between load cycles to failure or applied load) and 2) the interpretation of the number of load repetitions to crack failure is a much simplicity approach for comparing and ranking the HMA mix cracking resistance. However, establishing an R-IDT crack failure and screening criteria still remains a challenge.

## **REPEATED-LOADING SCB (R-SCB) TESTING**

The hypothesis for setting the R-SCB test is similar to the R-IDT. It is basically a two-phase process involving establishing the input loads via monotonic SCB testing and then using a fractional percentage of the maximum SCB failure load as the R-SCB input load. Like the OT and the proposed R-IDT, the cracking resistance potential of a mix under this test setup is characterized by the number of SCB load repetitions to crack failure, where failure is tentatively considered as full crack propagation through the HMA specimen.

### **Selection of the R-IDT Input Loads**

Only the Type B mix was preliminarily evaluated, and the average maximum SCB failure load from monotonic SCB testing was found to be 484 lbf at ambient temperature (77 °F). Four fractional load levels at 20, 30, 50, and 60 percent were arbitrarily tried as R-SCB input loads.

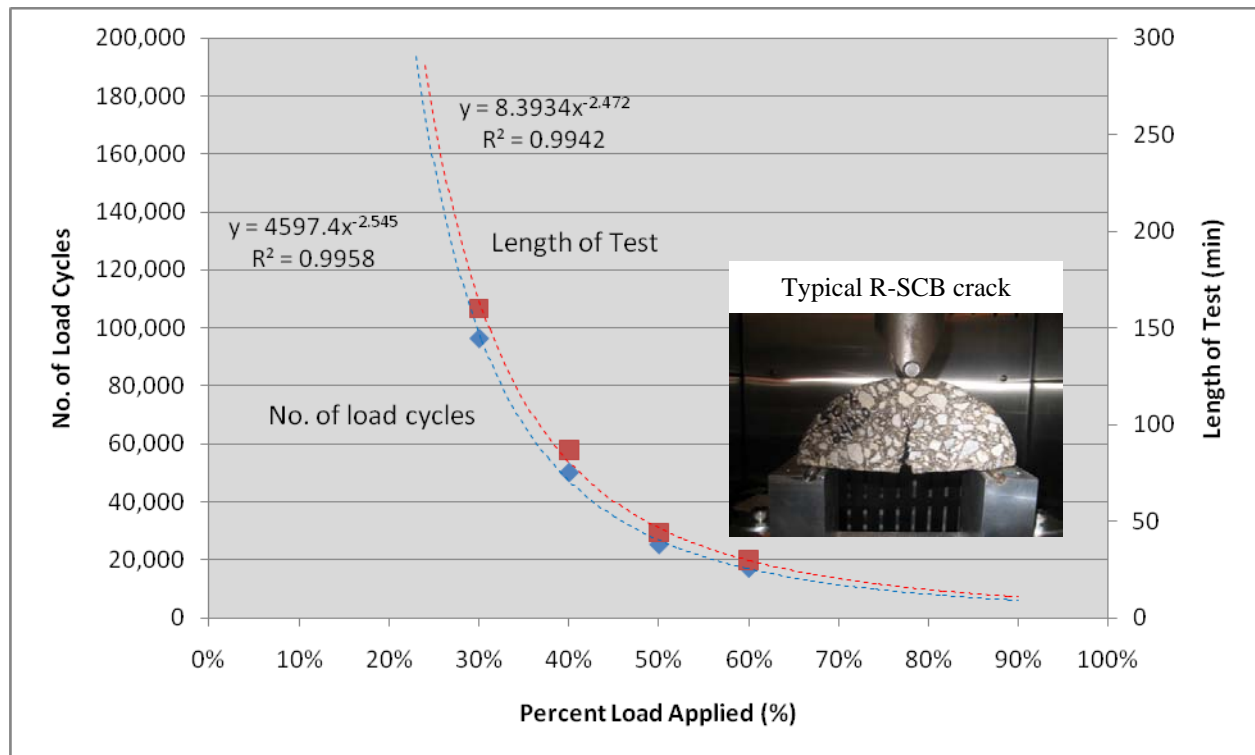
### **Preliminary R-SCB Test Results for Type B Mix**

R-SCB test results at 10 Hz (without any rest period) and ambient temperature (77 °F) are shown in Table 5-7 and Figure 5-8, respectively. For this mix and the loading parameters utilized, 50 percent would be selected as a reasonable R-SCB input load for this mix. The test time would be 44 min with about 25,342 SCB load repetitions prior to crack failure.

The R-SCB is also a good candidate for cracking testing for the same reasons given for the R-IDT. Although the stress distribution in the specimen is more complex, the R-SCB shows greater potential for utility than its monotonic counterpart (SCB) and the R-IDT in characterizing the cracking resistance of HMA mixes. Like for the R-IDT, establishing an R-SCB crack failure and screening criteria is still a challenge. For both the R-IDT and R-SCB, more trial testing with different mixes and test loading parameters will be explored further in the course of this research. For the R-SCB test, a loading frequency of 1 Hz will also be investigated.

**Table 5-7. R-SCB Test Results at Various Load Levels for the Type B Mix.**

Test#	% of 484 lbf	R-SCB Input Load (lbf)	Time to Crack Failure (min)	SCB Load Repetitions to Crack Failure
1	20%	145	160	96,514
2	30%	194	87	50,185
3	50%	242	44	25,342
4	60%	290	30	17,164



**Figure 5-8. Type B R-SCB Percent Load Relationship Curves.**

## **EVALUATION AND COMPARISON OF THE CRACKING TEST METHODS**

Table 5-8 provides a comprehensive summary and comparison of the pertinent characteristics associated with each cracking test method. This table was the basis for the rankings given in Table 5-9 for each mix.

### **MIX AND TEST METHOD RANKING**

The overarching purpose of this task is to choose a possible surrogate crack test that can accurately characterize and predicting mix-cracking resistance with acceptable variability. A pair of cracking ranking systems was chosen that will summarily determine the best possible testing method available in this investigation. For the two mixes evaluated, mix Type D was found from all the laboratory cracking tests conducted to be of superior cracking-resistance properties. Theoretically, mix Type D would thus be expected to perform better than mix Type C if subjected to similar loading and environmental conditions.

While the mix performance is relevant and important, the comparison of test methods is the main objective of this task. Before a more methodical approach to ranking the test methods was developed, a general notion was conceived concerning how the test methods performed and how they would ultimately be utilized after the completion of the project. From the test methods that were comparatively evaluated (as well as Table 5-8), two test methods offer great potential for future work and utility. The 4-inch high DT test had low variability in its results. It is also the most direct method for characterizing the HMA tensile strength and fracture properties including ductility and flexibility potential. The results from the test in this experiment tend to indicate that the method is fairly repeatable. However, sample preparation including parallel cutting and gluing can be a source of impediment to repeatability and a drain on time and resources. Additionally, external LVDTs are required to measure the vertical strain, which can potentially be a problem for daily operations. However, gluing can be a source of impediment to repeatability and a drain on time and resources.

The SCB test is highly repeatable, produces consistent results, and is easy and practical to perform. Based on the two mixes evaluated (Type D and C), both tests (IDT and SCB) are somewhat limited in their ability to distinctively discriminate between a “good” and “bad” mix-design. Table 5-9 summarizes the ability of each test method to discriminate between a mix that performs well and a mix that performs poorly using a ratio of the “good” parameter to the “bad” parameter. Clearly the OT test exhibits the greatest difference between the two extremes.

**Table 5-8. Preliminary Comparison of the Cracking Test Methods.**

<b>Item</b>		<b>OT</b>	<b>DT</b>	<b>IDT</b>	<b>SCB</b>	<b>R-IDT</b>	<b>R-SCB</b>
Test concept	<i>Correlation to field conditions</i>	high	very high	moderate	high	high	high
	<i>Validity of failure criterion</i>	valid	valid	skeptical	valid	valid	valid
	<i>Rationality of failure criterion</i>	yes	yes	skeptical	yes	yes	yes
Test specimens	<i>Shape &amp; size</i>	rectangular, small	cylindrical, medium	disk, small	½-disk, small	disk, small	½-disk, small
	<i>Simplicity of specimen fabrication</i>	simple	average	extremely simple	very simple	extremely simple	very simple
	<i>Specimen weight (lb)*</i>	2	4 - 6	2.25 – 4.5	1 - 2	2.25 – 4.5	1 - 2
	<i>Ease of handling</i>	easy	easy	easy	easy	easy	easy
	<i>Potential to attain AV</i>	moderate	very good	good	moderate	good	moderate
	<i>AV variability</i>	moderate	very low	low	moderate	low	moderate
	<i>Notching required?</i>	no	no	no	yes	no	yes
Test accuracy	<i>Variability</i>	moderate	very low	moderate	low	unknown	unknown
	<i>Repeatability</i>	moderate	moderate	high	high	unknown	unknown
	<i>Correlation with field perf.</i>	very high	high	moderate	high	unknown	unknown
Specimen & test setup	<i>Gluing required?</i>	yes	yes	no	no	no	no
	<i>Curing time</i>	>12 hr	>12 hr	n/a	n/a	n/a	n/a
	<i>Simplicity of test setup</i>	moderately simple	moderate	simple	very simple	simple	simple
	<i>LVDT required?</i>	optional	yes	yes	optional	optional	vptional
Data analysis	<i>Simplicity</i>	very simple	simple	simple	simple	very simple	very simple
	<i>Analysis model required?</i>	no	yes	yes	yes	no	no
Practical application	<i>Routine mix- design &amp; screening</i>	fair	poor	poor	poor	high potential	high potential
	<i>Industry use</i>	fair	poor	fair	fair	high potential	high potential
	<i>Academic research use</i>	fair	good	fair	good	high potential	high potential
Other considerations	<i>Potential to test field cores</i>	high	problematic	very high	very high	very high	very high
	<i>Approx. test time for 1 specimen</i>	< 1 hr	< 5 min	< 5 min	< 5 min	< 1 hr	< 1 hr
	<i>Cost comparison including time and materials</i>	moderate	high	very low	low	moderate	moderate

\*For the ID, DT, SCB, R-IDT, and R-SCB, the specimen weight is dependent on the height (i.e., 4 to 6" or thickness (i.e., 1 to 2") selected.

**Table 5-9. Test Method Discriminatory Ratios.**

<b>Test</b>	<b>Critical Crack Parameter</b>	<b>Good</b>	<b>Bad</b>	<b>Good/Bad Ratio</b>
<b>OT</b>	Cycles to failure ( $N_{OT}$ )	274	38	7.2
<b>4" DT</b>	Average vertical strain ( $\mu\epsilon$ )	2,583	1,529	1.7
<b>6" DT</b>	Average vertical strain ( $\mu\epsilon$ )	5,600	2,908	1.9
<b>IDT</b>	Average horizontal strain (in)	0.106	0.064	1.7
<b>SCB</b>	Vertical ram displacement (in)	0.017	0.009	1.8

In Table 5-9, the low ratios associated with the DT, IDT, and SCB test methods present a situation in which the operator may mistake a bad mix for a good mix because the difference in magnitude between the critical parameters is very small between a poor mix and an adequate crack-resistant mix. However, the R-IDT and R-SCB tests have the highest potential to become surrogate cracking tests based on the logic that a repeated test (such as the OT) will be able to easily distinguish between good and poor mix-designs. Also, these tests do not require gluing, which decreases the test time as well as minimizing operator associated variability. However, further validation on these two tests is definitely needed with known field performance mixes.

Table 5-10 gives a detailed account of the characteristics and their respective effect on the ranking of the test methods. The first column lists the desirable characteristics for a surrogate cracking test. The second column assigns a quantifiable value, in the form of a proportion whose sum total is 100 percent, which weighs the significance of the characteristic relative to the others. Each test method receives a score of up to the specified proportion for that characteristic relative to the other methods. The score can be as low as 0 percent or as high as the specific percentage assigned to that characteristic. The final result is an objective total score based on key performance issues that can be utilized to select the most appropriate surrogate cracking test method. The ranking scores also serve as performance indicators.

It is important to note that “Correlation to field performance” was excluded from Table 5-10 due to a lack of available field data (excluding OT). This characteristic will be more relevant when the mixes are tested from field cores. It is also important to note that variability for the R-IDT and R-SCB test methods could not be quantified as only one specimen was tested at each loading percentage. The scores for R-IDT and R-SCB are normalized by subtracting the “Repeatability and accuracy” and “Variability of test results” from the total attainable score (100 percent) and dividing the sum score by that number. Accordingly, the preliminary results in Table 5-10 show that the R-SCB would be the best surrogate cracking test based on its highest

**Table 5-10. Preliminary Ranking of the Cracking Test Methods.**

<b>Test Characteristic</b>	<b>Importance/Total Attainable Score</b>	<b>OT</b>	<b>4"DT</b>	<b>6"DT</b>	<b>IDT</b>	<b>SCB</b>	<b>R-IDT</b>	<b>R-SCB</b>
Repeatability and accuracy	16%	10%	10%	6%	13%	13%	--	--
Simplicity of specimen fabrication and handling	6%	3%	3%	3%	6%	5%	6%	5%
Potential to attain target AV/ AV variability	3%	2%	3%	3%	3%	2%	3%	2%
Potential to test field cores	7%	6%	3%	2%	7%	7%	7%	7%
Simplicity of test setup	4%	3%	3%	3%	3%	4%	3%	4%
Comparison of test run time	3%	2%	2%	2%	3%	2%	2%	2%
Simplicity of data analysis including raw data reduction	6%	6%	3%	3%	3%	3%	6%	6%
Variability of test results	11%	4%	11%	4%	7%	9%	--	--
Rationality of test concept and failure criterion	18%	11%	15%	15%	7%	11%	11%	15%
Specimen shape and its effects on AV distribution	2%	1%	2%	0%	1%	1%	1%	1%
Applicability of test for daily routine mix-design and screening	21%	20%	4%	4%	8%	8%	17%	21%
Cost comparison (material needed, test equipment, analysis time)	3%	1%	2%	2%	3%	3%	2%	3%
<i>Total:</i>	100%	68%	60%	47%	63%	67%	79% *	88% *

*\*Normalized by excluding "Repeatability and accuracy" and "Variability of test results" from the total.*

score followed by the R-IDT, SCB, OT, IDT, and DT, respectively. A detailed description for the test method evaluation and scoring criteria is included in Appendix C.

## SUMMARY

This section summarizes the preliminary findings based on the results presented in this chapter, including the results of some initial repeated testing. A comparative analysis of the various cracking test methods is also presented. Table 5-11 summarizes the test method utility ranking developed in this chapter, which is based on the potential of each test method to become a surrogate cracking test.

**Table 5-11. Overall Test Method Utility Rank.**

Test Method	Utility Score	Utility Rank
R-SCB	88% *	1
R-IDT	79% *	2
OT	68%	3
SCB	67%	4
IDT	63%	5
4" DT	60%	6
6" DT	47%	7

Based on the two mixes evaluated (Type C and D), the R-SCB was ranked as the most promising surrogate cracking test because the test is a simple and robust method to characterize the tensile properties of a mix and its crack-resistance. This conclusion is based on the research accomplished up to the time of this interim report and is subject to change as more laboratory work is done in the course of this research. The following lists the key findings from this chapter:

- The Type D mix has superior laboratory cracking-resistance properties compared to the Type C mix; it would be theoretically expected to out-perform the Type C mix in the field in terms of cracking resistance.
- The R-SCB test offers the best potential for a surrogate cracking test because its laboratory performance was above average and excelled in all areas that were investigated when compared to other tests.



- The 6-inch high DT test exhibited the worst potential for a surrogate cracking test because it performed below average in all the key areas that were considered in the comparative evaluations.

Overall, the recommendation of this partial experiment would be to select the Type D mix over the Type C mix if choosing between the two mixes for HMA pavement construction. The Type D mix exhibited superior cracking resistance properties and would thus be expected to perform better than the Type C mix when subjected to similar traffic loading and environmental conditions. Furthermore, it is recommended, based on the results presented in this chapter, that the R-SCB test be preliminarily considered as a candidate for a surrogate cracking test because it had superior test characteristics compared to all the other tests that were evaluated. Nonetheless, investigations into the 4-inch high DT, R-IDT, R-SCB, and R-DT will continue. Final results and recommendations will be documented in future reports.



## **CHAPTER 6**

### **OVERLAY ROUND ROBIN TESTING AND VARIABILITY-REPEATABILITY EVALUATION**

As a means to evaluate the variability and repeatability associated with the Overlay cracking test method, a round-robin test was conducted in six independent laboratories, namely:

- four TxDOT labs,
- one private (industry) lab, and
- TTI (academic and research lab).

Concurrently, the round-robin testing program also served as a demonstration forum for the OT test method as well as training of the respective lab technicians. The results of the round-robin testing are presented and analyzed in this chapter. A discussion of the findings and observations made in each respective lab as regards to the OT machine calibration, software, specimen gluing/curing process, and test procedure is also presented. At the end of the chapter, a summary of key findings and recommendations for OT variability/repeatability improvements is made.

#### **THE OT TEST METHOD**

For the round-robin task, the OT testing was conducted in accordance with the Tex-248-F test procedure (TxDOT, 2009). As stated in Chapter 4, the OT is a simple performance test for characterizing the cracking potential of HMA mixes in the laboratory at an ambient (room) temperature of 77 °F. The test loading configuration basically consists of a cyclic triangular displacement-controlled waveform at a maximum horizontal displacement of 0.025-inch and a loading rate of 10 s per cycle (5 s loading and 5 s unloading).

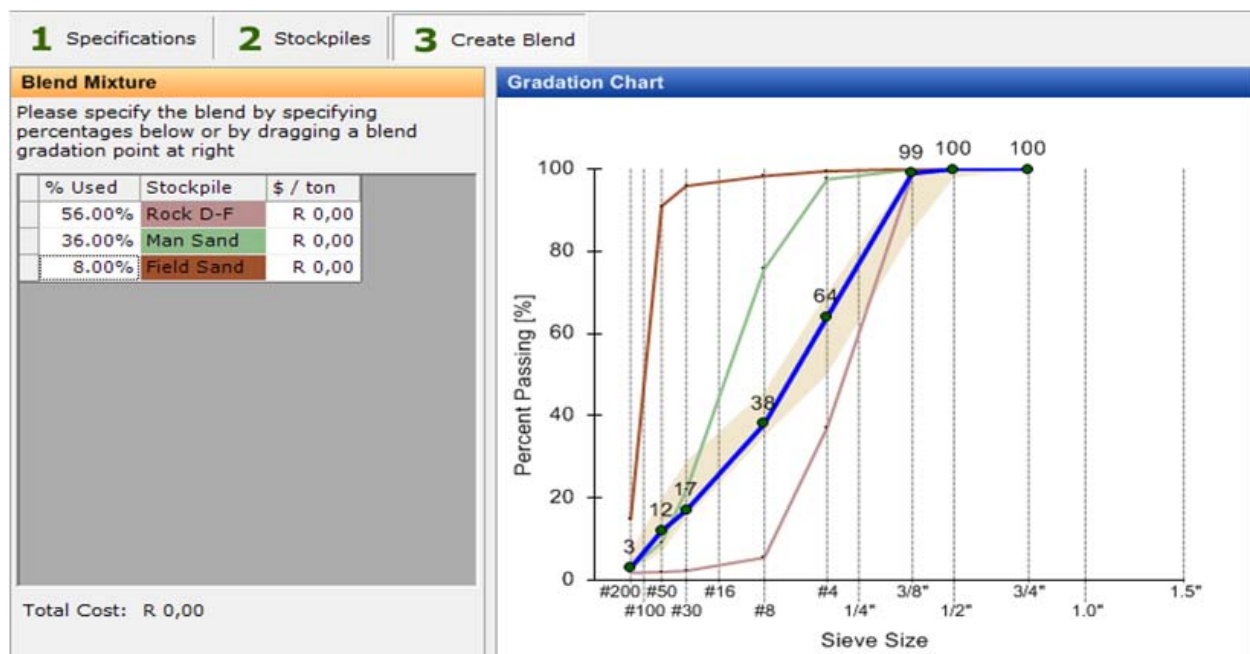
Typical OT test specimens are 6-inch long, 3-inch wide, and 1.5-inch thick that can be conveniently cut by trimming a lab molded (SGC) samples or a 6-inch diameter highway core; refer to Chapters 3 and 4.

## HMA MIX AND SPECIMEN FABRICATION

A dense-graded Type D mix was utilized for this task (round-robin testing) in all the six laboratories. The mix-design characteristics and the aggregate gradation are shown in Table 6-1 and Figure 6-1, respectively; refer also to Chapter 3 for more details.

**Table 6-1. Mix-Design Characteristics for OT Round-Robin Testing.**

Mix type	Asphalt-Binder	Aggregate	Gradation	Aggregate Blend
Type D	5% PG 70-22 (Valero)	Limestone (Chico)	Dense-graded	56% D-F rock + 36% manufactured sand + 8% field sand



**Figure 6-1. Aggregate Gradation for the Type D Mix.**

In line with the test plan discussed in Chapter 3, a minimum of four replicate specimens were tested in each respective lab. For the six labs, this meant a minimum of 24 specimens. To ensure consistent AV and specimen dimensions, all the specimens were gyratory molded and fabricated in the TTI lab. This also discounted for any effects due to potential differences in the batching, mixing, and molding processes among the labs. The molded samples were 6-inch in diameter and 4.5-inch high. The target specimen AV was  $7 \pm 1$  percent.

## OT ROUND-ROBIN TEST PLAN

As mentioned in the introduction, this round-robin testing program also served as a training and demonstration forum for the OT test method. Therefore, meticulous work was a top priority for the TTI researchers. Summarily, the OT round-robin test plan was designed as follows:

- A minimum of four replicate specimens were tested in each of the six labs.
- In each lab, a minimum of two replicate specimens were glued and tested by TTI researchers, and at least, two were glued and tested by the respective lab personnel/technicians. This was necessary to account for the possible influence of the operator effects, since at least two operators were involved in each respective lab.
- For the sake of training and demonstration purposes, the TTI researchers glued and tested their specimens first, and then, the respective lab technicians followed suit.
- To eliminate any possible bias, the specimens were selected randomly and tested randomly.
- Prior to testing, however, the OT machine was first checked for calibration and where necessary, it was adjusted and/or calibrated accordingly. This task was often accomplished via trial testing with dummy specimens. As will be discussed later, there were some discrepancies in the OT software and machine calibration settings.
- With the exception of Austin (TxDOT – Cedar Park), all specimens were fabricated in the TTI lab at an AV content of  $7\pm 1$  percent. For Austin, while the OT samples were molded in the TTI lab, cutting and AV measurements were done at the TxDOT Cedar Park lab. Nonetheless, this did not have any effect on the results.
- Specimens that did not meet the  $7\pm 1$  percent AV content were discarded and not tested.
- To minimize any possible effects of differential oxidative-aging, all the specimens were tested within 4 days after molding (mixing and compaction).
- To account for geometry and density in the subsequent analyses, specimen dimensions such as thickness (i.e.,  $t = 1.5\pm 0.02$  inches) and air voids (i.e.,  $7\pm 1$  percent) were also measured and recorded.

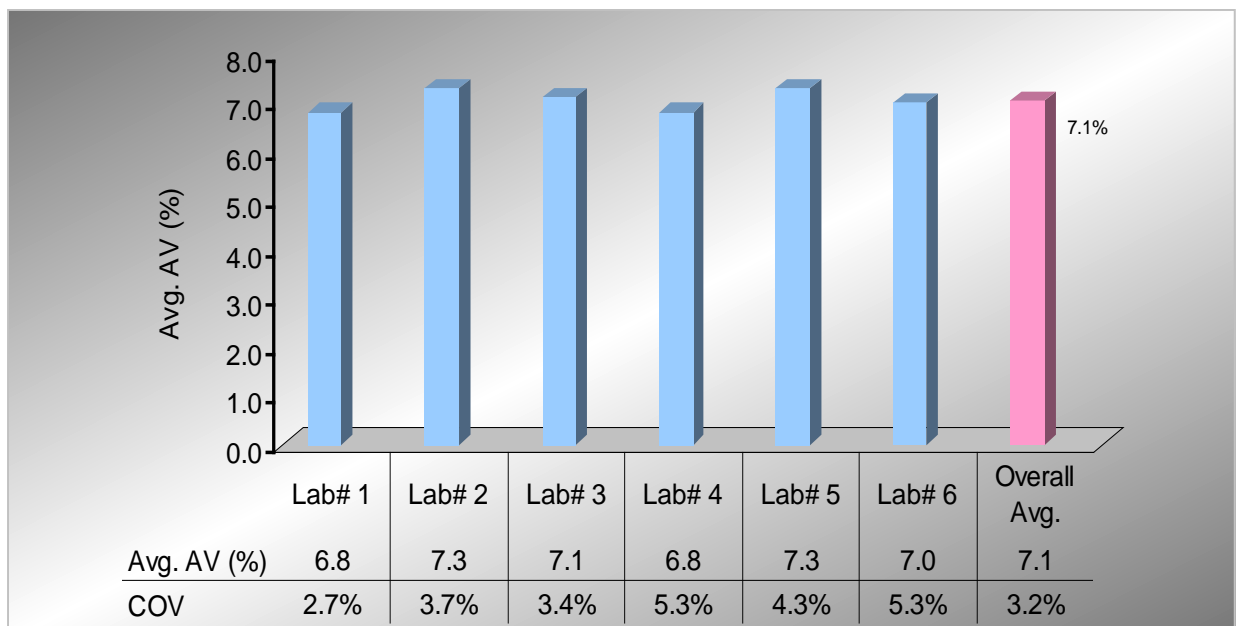
- During data analyses, raw OT data files were also stored and checked to identify any anomalies in the initial loading of the samples (i.e., extremely high start tensile or compressive loads). Ideally, the starting load should be or close to zero.

## OT ROUND-ROBIN TEST RESULTS

Based on the mix (dense-graded Type D) evaluated, the results from the six labs were generally comparable and consistent—an indication that reasonably acceptable variability and repeatability can be obtained with the Overlay tester. These results from round-robin testing are presented and analyzed in this section and includes the AV, initial peak load, and number of OT cycles to failure. Detailed test results are included in Appendix D. For the purposes of statistical analysis for this task, a COV of 30 percent was arbitrarily utilized as the benchmark.

### Specimen Air Voids

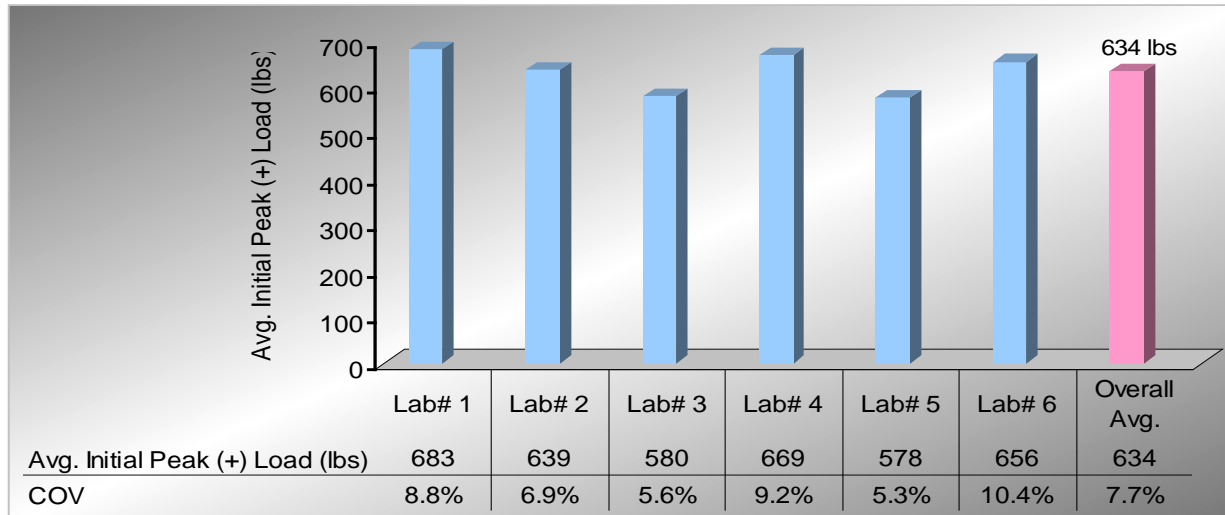
Figure 6-2 shows that the AV for the specimens tested were within the  $7 \pm 1$  percent target limits. The overall average was 7.1 percent with a COV of 3.2 percent and an average range of 6.8 to 7.3 percent. This low COV is an indication of good batching and molding practices in the TTI lab.



**Figure 6-2. Comparison of Air Voids.**

### Initial Tensile Peak Loads

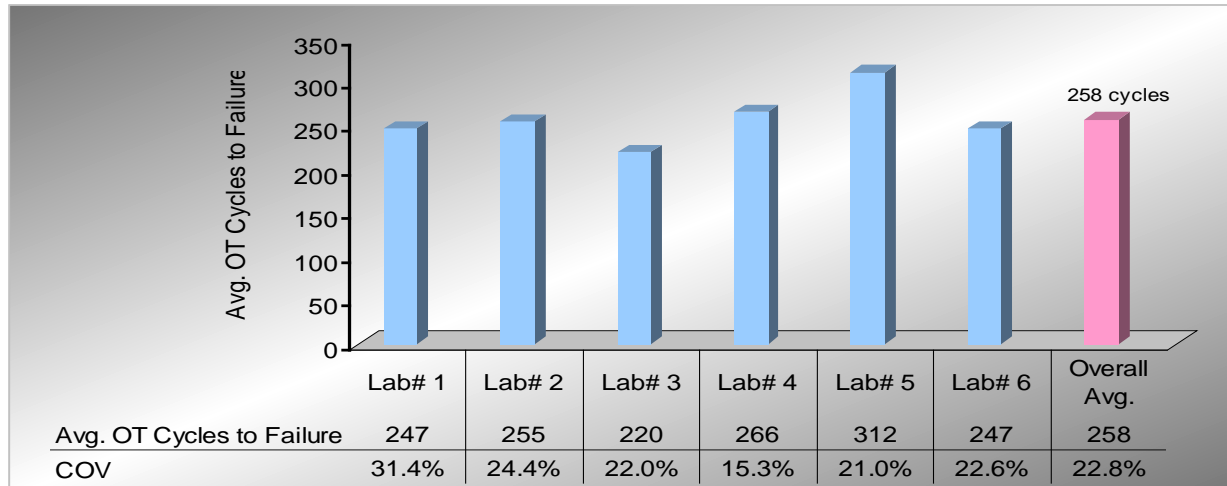
As expected, the initial tensile peaks (+) loads were all comparable, with an average of 634 lb and a COV of 7.7 percent. These results are shown in Figure 6-3.



**Figure 6-3. Comparison of Initial Tensile Peak Loads.**

### Number of OT Cycles to Failure

Considering a maximum horizontal displacement rate of 0.025 inches and single crack failure mode, the average number of OT cycles to failure (considering all the labs) was 258 with a COV of 22.8 percent and an average lab range of 220 to 312 cycles. This level of variability is not unreasonable if a COV threshold of 30 percent is considered and suggests that there is potential for acceptable OT repeatability. These results are shown in Figure 6-4.



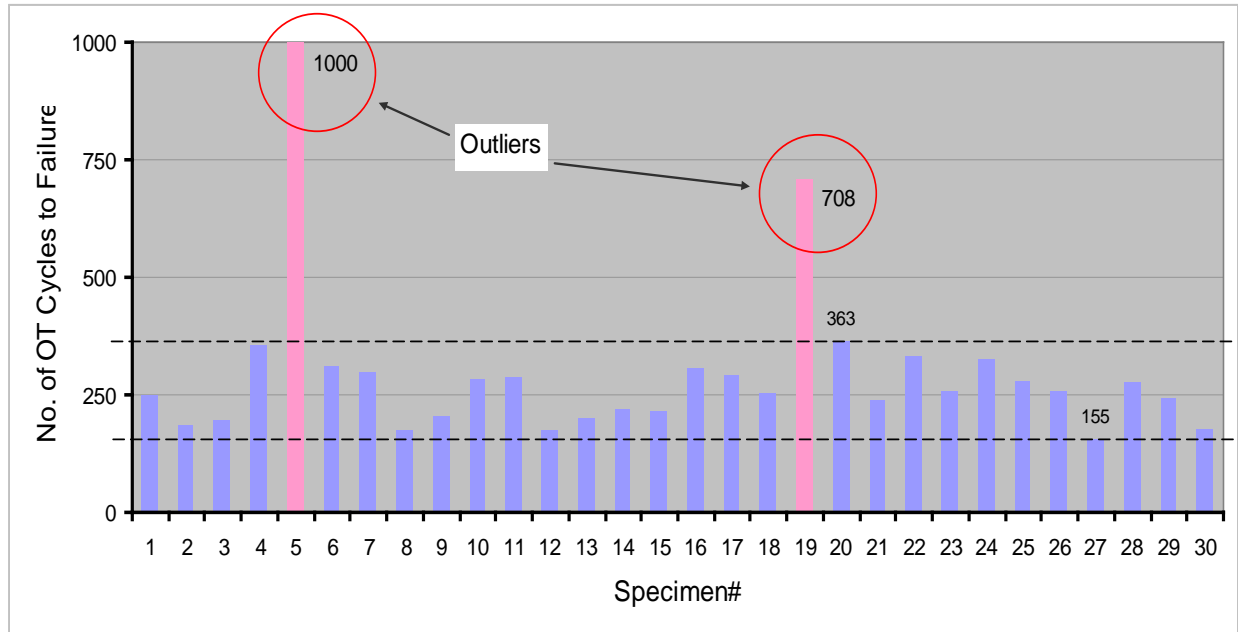
**Figure 6-4. Number of OT Cycles to Failure.**

With the exception of Lab# 1 at 31.4 percent, which is slightly over the 30 percent threshold, the COV values from all the other labs were less than 25 percent. Statistically, the COV values shown in Figure 6-4 for the respective labs are not unreasonable. Conversely, these results are indicative that OT variability can be optimized to acceptable levels if the test specifications and procedures are firmly adhered to.

However, there were some instances of outliers in two labs (namely Lab# 2 and Lab# 5) where two specimens out of the total 30 that were tested had over 500 cycles to failure. One specimen in each of these two labs lasted over 500 cycles, i.e., specimen D1 in Lab# 2 had 1000 cycles while specimen D4 in Lab# 5 had 708 cycles. These results are shown in Figure 6-5. Incorporating these two outliers brings the overage number of OT cycles to failure to 294, with a COV of 56 percent, which is on the higher side (i.e., greater than 30 percent).

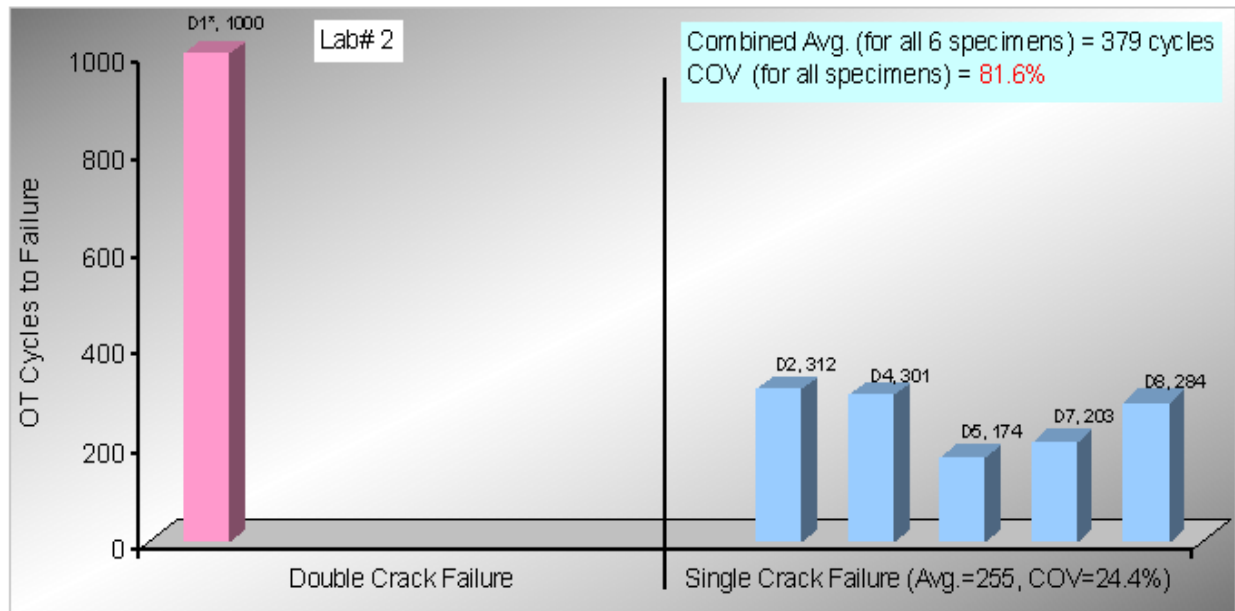
Nonetheless, such outliers are typical expectations of any laboratory test experimentation, to allow a tolerance for unsatisfactory results due to poor specimens, experimental setup, human error, etc. Statistically speaking and from an experimental point of view, the results are not unreasonable especially considering that only two (i.e., 7 percent) out of the total of 30 specimens were way off the range.



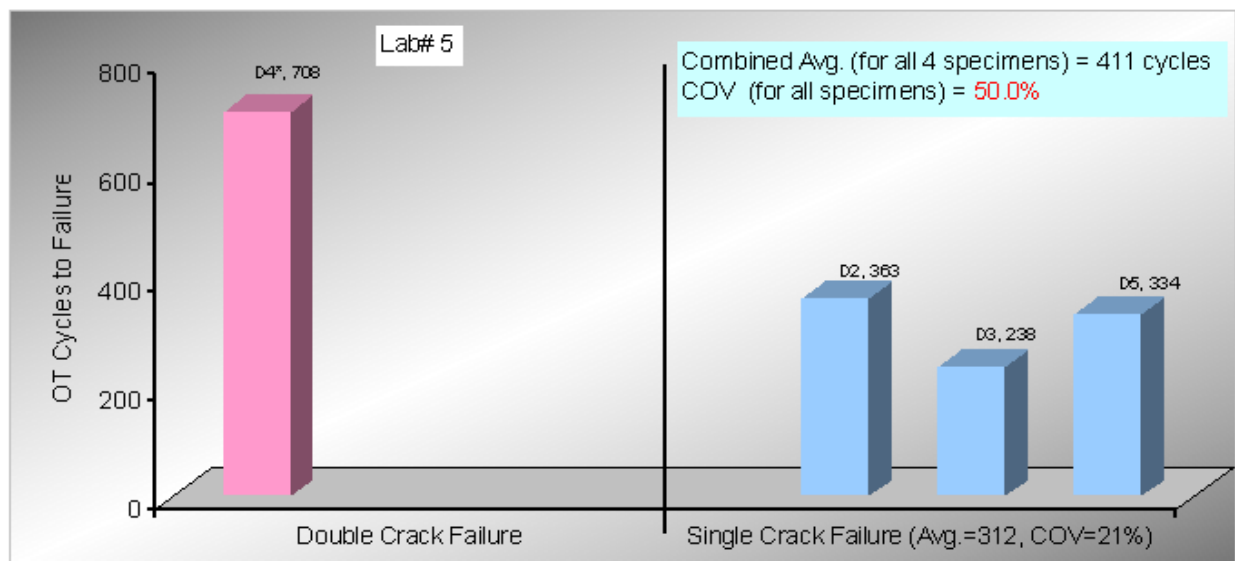


**Figure 6-5. OT Results for All Labs (30 Specimens).**

However, further investigations of the two outliers indicated that the specimen failure mode was double cracking instead of the desired single cracking. As shown in Figures 6-6 and 6-7, incorporating these results in the analysis raises the COV to over 30 percent, indicating an unacceptably high variability. Detailed test results for Figures 6-6 and 6-7 such as the specimen dimensions, AV, and initial peak loads can also be found in Appendix D.

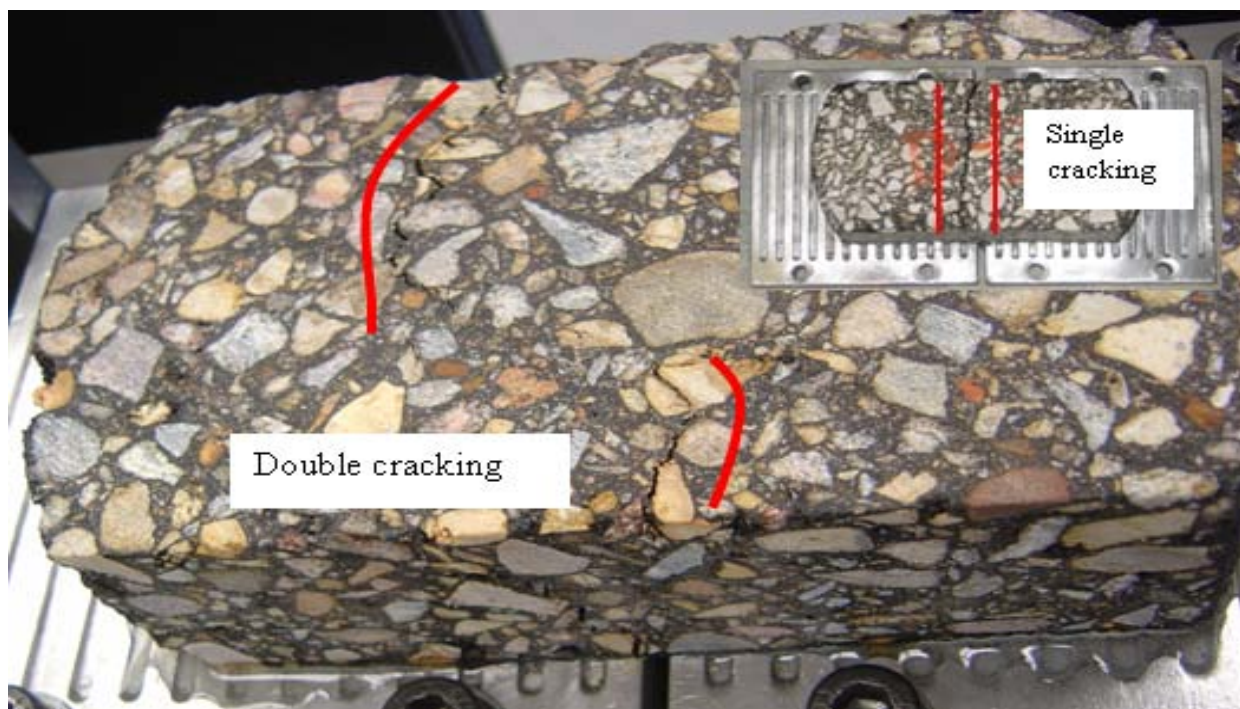


**Figure 6-6. Single versus Double Cracking (Lab# 2, Type D Mix).**



**Figure 6-7. Single versus Double Cracking (Lab# 5, Type D Mix).**

In a non-single crack failure mode, two or more parallel cracks initiate on either side of the specimen, and these, often take longer to connect, thus, the longer number of OT cycles to failure. Figure 6-8 shows an example of double cracking.



**Figure 6-8. Example of Double Cracking in OT Specimen.**

Single cracking is the preferred mode of failure. In the revised Tex-248-F specification, it is proposed that the results for all other crack failure modes should always be noted and recorded as part of the OT testing process for consideration in the subsequent analysis.

Overall, the results obtained from the round-robin testing indicate that OT variability and repeatability can be optimized to reasonably acceptable levels, with careful work (sample preparation, etc.) and adherence to the test specification and procedures. Considering that at least two operators participated in each independent lab, these results are potentially promising and provide a sound platform for continued work toward addressing the OT variability and repeatability issues.

However, just like any other test method, it can not be over emphasized here that the occurrence of outliers cannot be ignored. Furthermore, this round-robin testing was limited only to one mix type. As such, similar future studies should focus on other mix types including those with very poor cracking performance (i.e., less than 100 cycles), coarse-graded mixes (e.g., Type B and C mixes), plant-mixes, and field cores.

## **GENERAL OBSERVATIONS AND DISCREPANCIES**

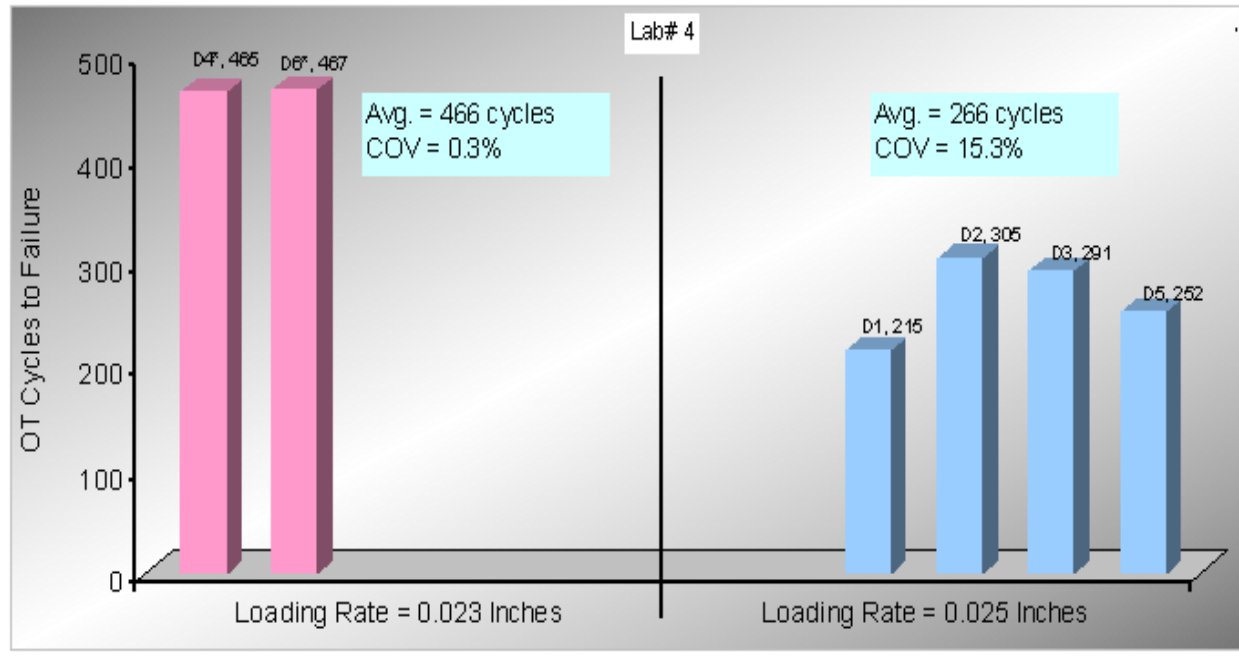
In general, some differences and discrepancies were observed in the various labs. These differences/discrepancies included the OT software, machine calibration, gluing/curing weights, specimen and test set-up, etc. These aspects are discussed in the subsequent text.

### **OT Software**

There is an inconsistency in the software version among the labs; some were old while others were new, with different calibration settings. As such, there were some difficulties in calibrating the machines properly and/or to provide a general solution to software related problems. For consistency and in order to minimize any software related issues, a universal updated version should be installed in all the labs, if at all possible.

### **OT Machine Calibration and Load Rate**

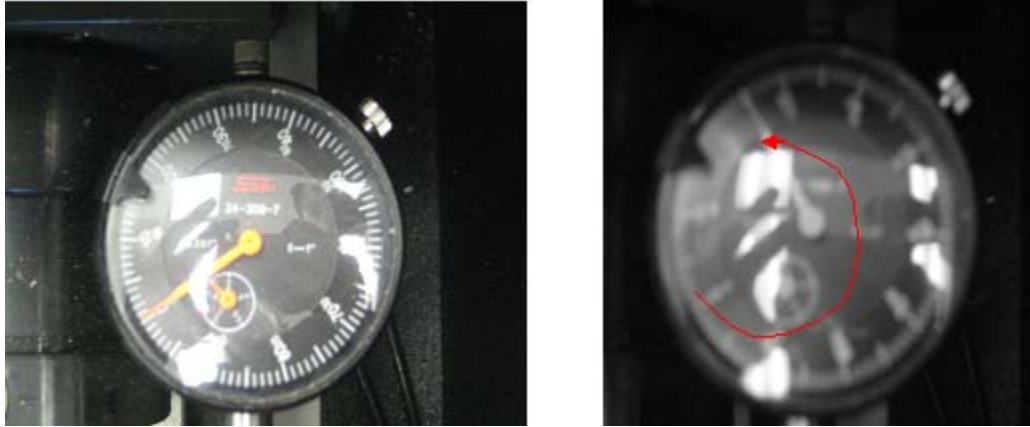
On some OT machines, the maximum horizontal displacement rate was found not be 0.025 inches. Examples are labs designated as Lab# 1 and Lab# 4, where calibrations had to be done to adjust the displacement rate from 0.023 to 0.025 inches. The difference in the loading rate is a critical factor in the repeatability potential of the Overlay Tester. Additionally, the difference in the displacement loading-rate has a significant effect on the cracking performance of the mixes in terms of laboratory OT cycles to failure. Because the test is run in a repeated cyclic mode, a difference of  $\pm 0.002$  inches has a very significant impact on the number of OT cycles to failure, it could actually decrease or increase the number of OT cycles over two folds. Figure 6-9 shows the number of OT cycles obtained when the loading rates were different for the same Type D mix. Detailed results for this figure can also be found in Appendix D.



**Figure 6-9. Effects of Different Displacement Loading Rates (Lab# 4, Type D Mix).**

As shown in Figure 6-9, an average of 466 OT cycles were obtained in Lab# 4 prior to adjusting the machine, with a horizontal displacement rate of 0.023-inch. An average of 266 OT cycles was subsequently obtained in the same lab after adjusting the displacement rate to 0.025-inch. These results emphasize the need to periodically check the OT machine calibration and displacement rate; and adjust accordingly where necessary. In both cases, however, variability measured in terms of the COV is still less than 30 percent.

Based on these observations, it is recommended that the OT machines should be calibrated and checked for the displacement loading-rate regularly, preferably with trial dummy testing. Checking for the displacement loading-rate can easily be achieved by observing the radial movement recorded by an in-built dial gauge in the OT machine. This should read 0.025-inch (i.e., 5 divisional counts on the dial gauge). Figure 6-10 shows an in-built dial gauge in the OT, corresponding to 0.000- and 0.025-inch readings, respectively.

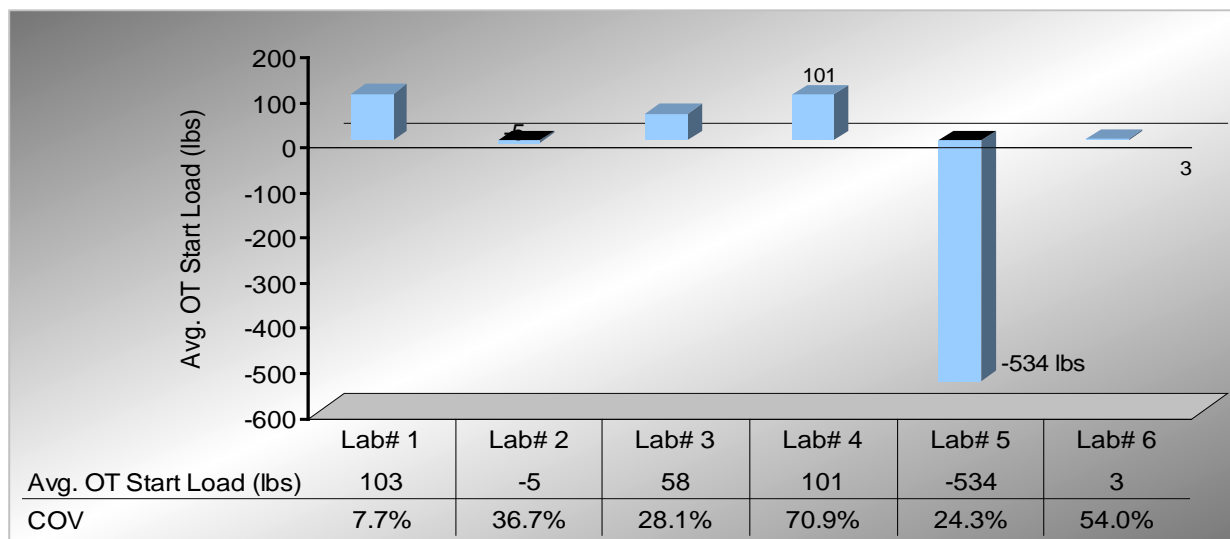


**Figure 6-10. OT In-Built Dial Gauge.**

Alternatively, the actual gap displacement can be manually measured using any appropriate measuring device such as a feeder gauge. If the readings are incorrect, changing the input displacement rate through trial and error should be done until the actual displacement rate is 0.025-inch. In the event that 0.025-inch is not achieved, a full calibration with a calibration kit maybe warranted.

### **Initial Start Loads**

There was an observation that some OT machines started in compressive loading mode, with compressive load magnitudes of up to 500 lb. Figure 6-11 shows a comparative plot of the OT starting loads for all the six labs involved in the round-robin test program.



**Figure 6-11. Comparison of OT Start Loads.**

In Figure 6-11, one lab (Lab# 5) shows an average compressive starting load of 534 lbs while another lab (Lab# 6) shows an average positive starting load of 3 lb. Although this difference in the initial starting loads did not negatively impact the round-robin test results, the starting load should ideally be or close to zero, as was the case for Lab# 2 and Lab# 6. Thus, it is advisable to check the OT machine and load settings, regularly.

### **Sample Drying and Gluing**

Variations were noted in both the specimen drying and gluing procedures amongst the labs. For instance, the glue type, the glue amount per specimen, and the application method were all different. These procedures need to be harmonized in all the labs. In particular, the glue amount per specimen needs to be well quantified. Accordingly, TTI have addressed these issues in the revised Tex-248-F specification, which has been submitted to TxDOT for review and subsequent approval.

Furthermore, when gluing, the smoother cut surface of the specimen should always be glued to the plates. Rough surfaces may often occur due to the warbling effects of the saw blade.

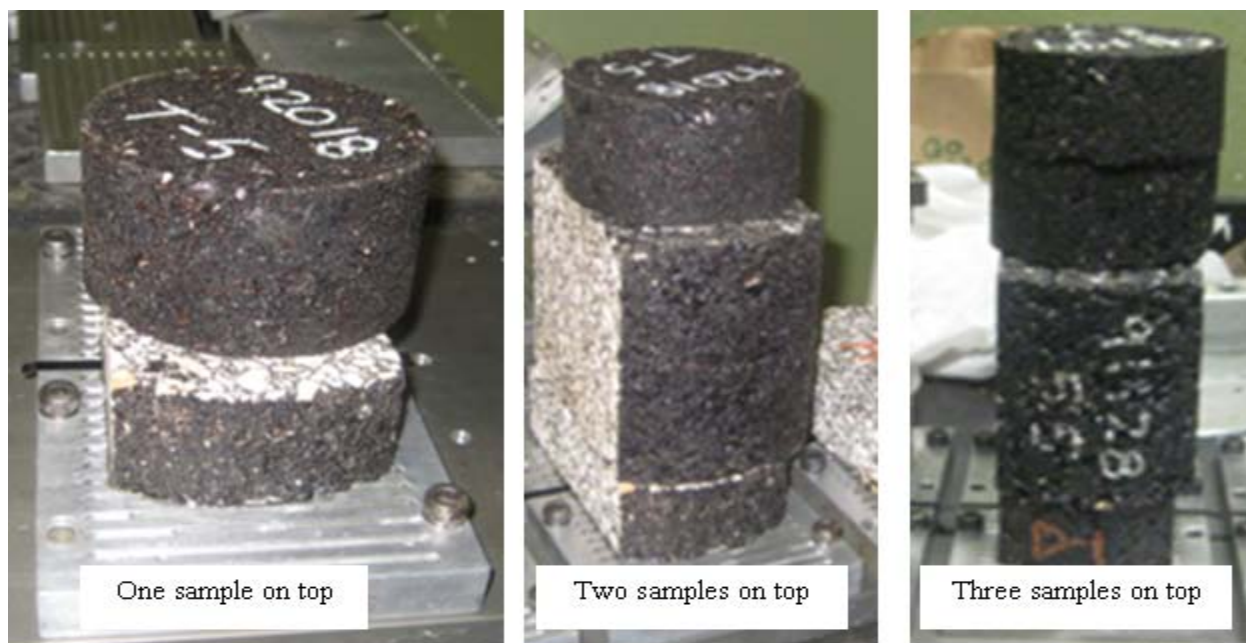
### **Specimen Geometry**

For consistent results, it is imperative that the specimen dimensions, particularly the thickness, be consistent, i.e.,  $t = 1.5 \pm 0.02$ -inch. For the OT test, the specimen thickness has a significant effect on the crack propagation and consequently, on the cracking performance of the specimen in terms of the number of cycles to failure. On this basis, it is recommended that the specimen dimensions particularly the thickness be measured and recorded for use in the subsequent data analysis.

### **Glue Curing and Weights**

Ten lb is the recommended curing and hold-down weight. However, this was not the case in some labs, where other HMA specimens with varying weights were in fact used as curing weights. The curing weight and its consistency have a significant impact on the glue film thickness, which in turn affects the specimen performance. Figure 6-12 shows different curing weights as observed in one of the labs during the round-robin testing.





**Figure 6-12. Example of Inconsistent Curing Weights.**

Without doubt, these inconsistent curing and hold-down weights definitely influence the glue film thickness and the final OT results including variability. To address this issue, TTI has undertaken to supply each of the six labs with a minimum of three 10 lb weights each.

### **Sample Test Setup**

Once glued to the base plate, the specimen should be loaded automatically in the OT machine. In addition, when in load mode, the machine is expected to change automatically to displacement mode once it has started. As noted in some labs, forcing the specimen in the machine or manually changing from load to displacement mode may significantly pre-load the specimen. This is undesired and may negatively impact the results.

### **RECOMMENDATIONS**

Based on the round-robin testing, the following recommendations, as related to improvement of the OT variability and repeatability, are made:

- 1) If possible, check and update the software on all the OT machines. This task should preferably be coordinated with the developers and manufacturers of the OT machine.



- 2) Check and re-calibrate all the OT machines including conducting some trial runs with dummy specimens. This should be done regularly where applicable.
- 3) Harmonize the OT test procedure including sample preparation, gluing, curing, and test set-up. In this regard, TTI have made substantial modifications and revisions to the OT test specification Tex-248-F including video recording of the sample preparation and the OT testing procedure. Both the modified specification and video demo have been submitted to TxDOT for review and subsequent approval.
- 4) Consolidate the revised Tex-248-F test specification and the accompanying video demo for ready availability to all the TxDOT districts, preferably via online access.
- 5) If possible and after the Tex-248-F modification and provision of a video demo, repeat the round-robin test with poor crack-resistant mixes (i.e., with less than 100 OT cycles) or a coarser mix such as Type B and C, respectively. The repeat round-robin test plan should also incorporate plant mixes and field cores.
- 6) To minimize variability and in order to optimize repeatability, it is imperative that the OT test specification is adhered to including the sample preparation process (i.e., batching, mixing, compaction, cutting, etc.).
- 7) OT input fields: prior to OT testing, all the data input fields such as density, specimen dimensions, etc. should be completed.
- 8) Data analysis: results for specimens with more than single cracking should be discarded. In addition, periodically check the raw data files to identify any anomalies in the initial loading of the samples.

## **SUMMARY**

Based on the Type D mix that was evaluated, the major findings from the Round-robin testing are summarized as follows:

- Considering a loading rate of 0.025-inch horizontal displacement and single crack failure mode, the results obtained were potentially promising—an average of 258 cycles with an overall COV of 22.8 percent and an average range of 247 to 312 cycles. Measured in terms of the COV, the level of variability and repeatability among the six labs were fairly reasonable, i.e., the overall COV was less than 30 percent. However, this is not to

discount the occurrence of outliers with COV values greater than 30 percent and the fact that one lab had a COV of 31 percent; i.e., higher than the 30 percent limit.

- With careful work (i.e., sample preparation, set-up, etc.) and adherence to the Tex-248-F test specification and procedures, OT variability and repeatability can be optimized to reasonably acceptable levels.
- Based on observations from the Round-robin testing, modifications have been made to the Tex-248-F specification including provision of a professional video demo. S
- A repeat Round-robin tests with poor crack-resistant mixes (i.e., with less than 50 OT cycles) or coarser mixes such as Type B and C, respectively, is strongly recommended. The repeat round-robin test plan should also incorporate plant mixes and field cores.

# **CHAPTER 7**

## **DEVELOPMENT OF WORKABILITY AND COMPACTABILITY INDICATORS FOR HMA**

The objective of this chapter is to document the progress of Task 4 entitled “Development of workability and compactability index for next generation HMA.” The purpose of this task is to make use of the current gyratory compaction procedure as part of the Superpave mix design to develop performance indices that can relate to the stability of HMA in the field. The gyratory compactor was available in each central and field lab to fabricate asphalt specimen. This task was conducted at University of Texas at San Antonio, in the Superpave facility laboratory.

### **INTRODUCTION**

In this study, the gyratory compactor was used to evaluate the mix compactability, workability, and resistance to cracking and rutting. Concerns have been raised about mixes that are drier and more difficult to compact. The primary objective of this chapter is to develop a parameter from the compaction curve that could be used as part of the design procedure to eliminate mixes that will be too difficult to compact in the field. Pavement compaction is a major task in lay down operations during HMA placement. If not done properly, early failure could occur. Stiff mixes have experienced difficulty in compaction resulting in cracking and debonding at the interfaces. Workability of HMA decreases substantially at a given temperature since the modifiers tend to increase the viscosity of binders.

In general, mixes that experience difficulty in lab compaction will experience the same problems in the field. This chapter also presents detailed analysis of the HMA compaction using the Pine gyratory compactor. An index termed the “Contact Energy Index” is developed to measure the stability of mixes. The contact energy index (CEI) is used to analyze mixes with different constituents such as percent of binder, percent of natural sand, type of aggregate, gradation, and nominal maximum aggregate size.

If performance parameters can be extracted during the already existing compaction process, field and lab engineers can identify early enough the mix long-term performance before lay down operation starts. The organization of this chapter includes the literature review on the current energy indices determined from the compaction curve characteristics, identified parameter to study in mixes stability, preliminary testing on current TxDOT mixes, and future plans.

## **LITERATURE REVIEW**

### **Energy Indices Parameters**

The gyratory compactor actuators exert forces on the specimen during compaction in order to apply the vertical pressure and angle of gyration. The response of the mix to these forces can be monitored and used to evaluate the mix stability. Two main approaches can be identified in the literature in order to achieve this objective. The first approach is analyzing the compaction curve characteristics, and relating them to mix stability. The second approach relies on developing experimental tools and analysis methods to measure the shear stress during compaction and relating them to stability. The following sections discuss these two approaches.

### **Compaction Curve Characteristics**

An experiment conducted under SHRP contract A-001 evaluated the ability of the SGC to discern changes in key mix properties, (SHRP 1994). Results of height measurements taken during the compaction process were used to calculate changes in specimen density expressed as a percent of the maximum specific gravity  $G_{mm}$  percent. A plot was made of the percent maximum specific gravity versus the log of the number of gyrations. This compaction or densification curve is characterized by three parameters.  $C_{10}$  is the percent maximum specific gravity after 10 gyrations, and  $C_{230}$  is the percent maximum specific gravity after 230 gyrations. The slope of the densification curve,  $K$ , is calculated from the best-fit line for all data points assuming that the curve is approximately linear.

A comparison of  $C_{10}$ ,  $C_{230}$ , and  $K$  found that they were sensitive to changes in asphalt content, gradation, or aggregate type. Based on the results of this experiment, it was found that the slope of the compaction curve,  $K$ , was affected by asphalt content and the aggregate percent passing the 75  $\mu\text{m}$  sieve.

The position of the curve however, varied as the experiment variables changed. Other studies have also related K to mix performance; Rand (1997) for example, showed that K is strongly related to the amount of asphalt and coarse aggregates in the mix. A study in France compared the K values for two mixes with known permanent deformation in the field, (Moutier 1997). This study illustrated that higher K values were associated with better performance in the field.

It is noted that most of the studies on the SGC used the average slope of the compaction curve. However, one of the unique features of the Superpave volumetric mixture design procedure developed by SHRP (AASHTO MP2 1996) is the use of the gyratory densification curves to account for the two phases of compaction in situ:

- (a) compaction during construction using rollers at high temperatures, and
- (b) densification under traffic at ambient temperatures.

It is well recognized that a good mixture should be easy to compact during construction, but should show adequate resistance to permanent deformation under traffic. Therefore, in order to be able to effectively evaluate permanent deformation potential, compaction properties should be evaluated relative to these distinct phases. The compaction curve characteristics should be analyzed to identify mixes that:

- (a) can be successfully compacted during construction, but
- (b) can resist traffic induced densification and alternate plastic flow.

### **Shear Stress Measurements**

Other measurements that might be derived from the gyratory compaction are based on the resistance to deformation and the amount of energy required to compact the mix. Compaction in the gyratory compactor occurs due to two mechanisms: vertical pressure at the top of the specimen and shear displacement induced by the gyratory movement.

McRea (1965) proposed a formula to determine the shear stress in the asphalt mixture during compaction in the GTM, the formula is based on a simplicity equilibrium analysis of the mix and the mold by taking the moment about the lower center of the mix (0) (Figure 7-1).

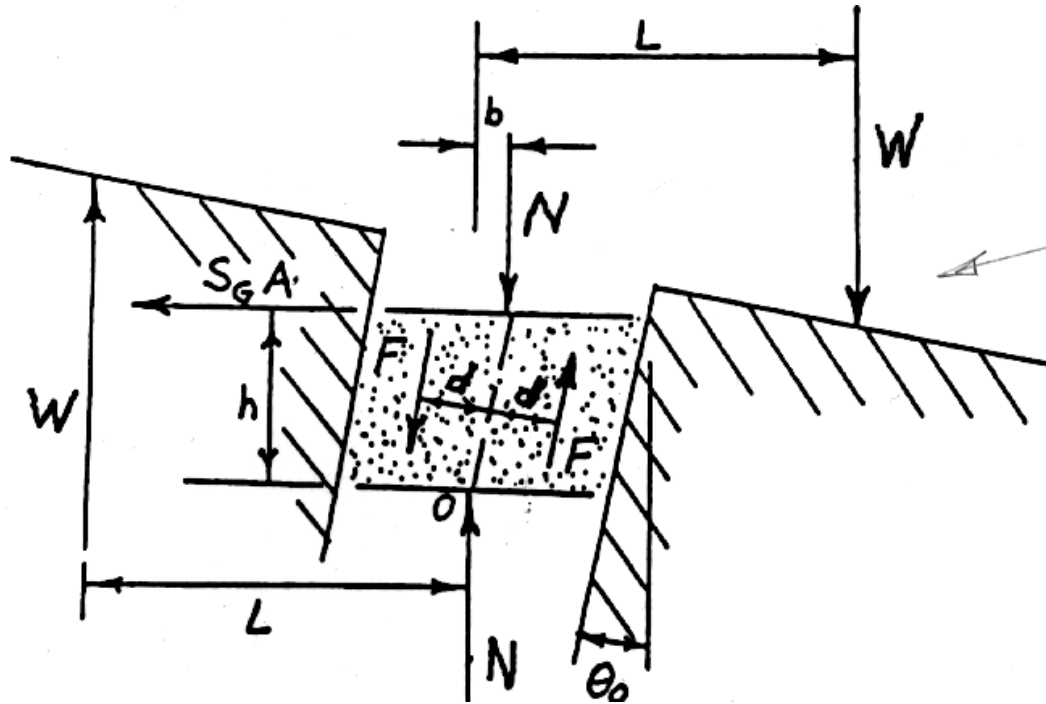


Figure 7-1. Parameters used for Calculating the Shear Stress (McRea 1965).

$$S = \frac{2(W * L - F * d) + (N * b)}{A * h} \quad (\text{Equation 7-1})$$

where,

- S = the shear stress,
- F = the friction force between the aggregate particles,
- d = the distance of the resultant friction from the center,
- N = the applied vertical pressure,
- A = the sectional area and the height, respectively,
- h = the sectional area and the height, respectively,
- W = the applied forced to proceed the angle, and
- L = the moment arm to point (0).

Mc Rea (1965) neglected the distance b—arguing that it is too small—and the friction force F, then he obtained the following equation:

$$S = \frac{2 * W * L}{A * h} \quad (\text{Equation 7-2})$$

It is noted that the free body diagram in Figure 7-1 includes external and internal forces, which is incorrect. Also, the derivation neglects the friction between the mold and the mix. These assumptions are believed to affect the validity of Equation 7-2, and limit its applicability.

A study by *Kumar and Goetz (1974)* was performed to evaluate:

- the GTM design method,
- the relationship between densification and the mixture properties, and
- the job mix formula tolerance limits.

They noted that the gyratory shear results (i.e., Equation 7-2) on gravel mixtures indicated in general that coarse gradation and low percent asphalt combinations were different as compared with fine gradation and high percent asphalt combinations. Kumar and Goetz (1974) showed that the difference in gyratory shear values was insignificant with respect to variations in percent asphalt content. They also indicated that the GTM was sensitive to study the changes in mixture properties caused by small variations in gradation and asphalt content.

*Sigurjonsson and Ruth (1990)* conducted a study to evaluate the sensitivity of the GTM to minor changes in asphalt content and aggregate gradation. They showed that the combined effect of aggregate particle shape, surface texture, and gradation of the aggregate blend could be evaluated for level of attainable shear strength (Equation 7-2) and for sensitivity to slight changes in mix proportions. Also, a minimum S value of 54 psi (372 kPa) should be required for any mixture densified for 200 revolutions. They estimated that a dense-grade structural mix should have a minimum shear stress value of 56 psi (386 kPa) when the pavement lift thickness is greater than 50 mm. They also showed that the GTM densification testing procedure provides information on the shear resistance of the mix regardless of the factors influencing its behavior (e.g., air void content, aggregate characteristics, asphalt content, and VMA).

A study by Ruth et al. (1991) used the GTM air roller testing procedure to evaluate asphalt mixtures and to identify undesirable mixtures which would be susceptible to excess permanent deformation. Regression analyses were used to show the relationships between the

gyratory shear (S) value and physical properties of the mixture. Ruth et al. (1991) used two different sources of aggregate, different aggregate blends, and asphalt AC-30. These mixes conformed to Florida DOT specifications. They concluded that the GTM compaction and densification testing procedure provided rapid assessment of a mixture's shear resistance as related to change in asphalt content, aggregate gradation, percent of natural sand and density. Figure 7-2 shows the influence of binder content sensitivity on gyratory shear measurements in the GTM, while S of 372 kPa at 200 gyrations was thought by them to be applicable for light to medium traffic conditions.

De Sombre et al. (1998) used a gyratory compactor from Finland to estimate the shear stress and the compaction energy for different asphalt mixes. They stated that energy is transferred to the specimen through the moment needed to apply the gyratory action. A load cell located on the piston of the compactor measures the lateral load needed to create this moment as shown in Figure 7-3. De Sombre et al. (1998) measured this moment and used it in conjunction with the sample geometry to calculate the shear stress in the sample at any point in time. The shear stress was calculated using a similar Equation 7-2.

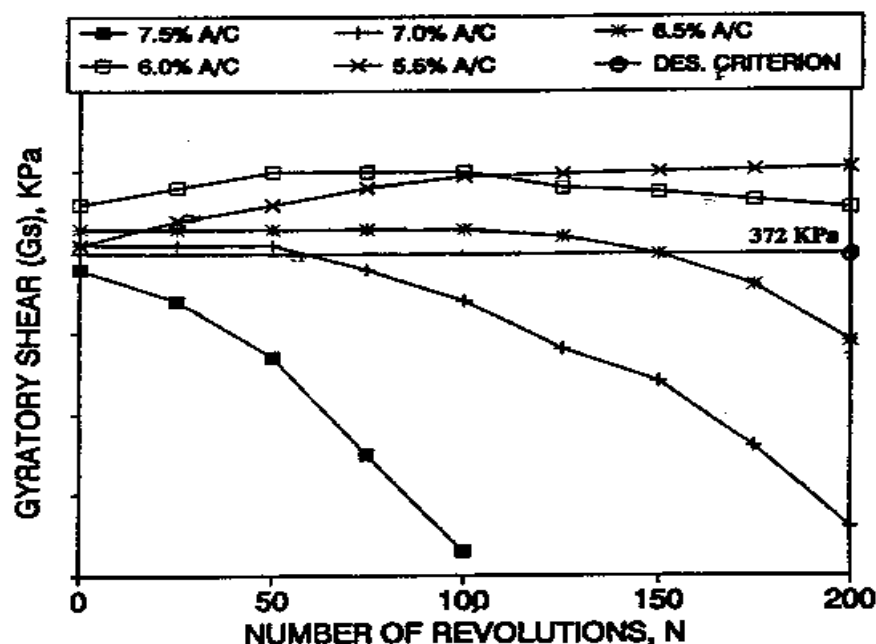
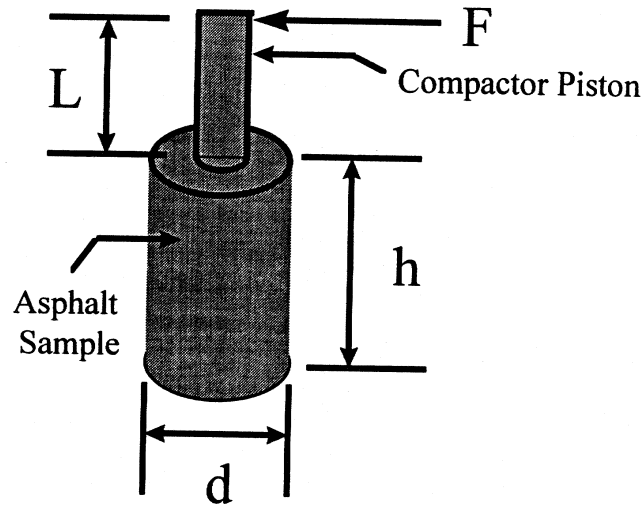


Figure 7-2. Typical GTM Densification Results, (Ruth et al., 1991).





**Figure 7-3. Parameters for the Calculation of Shear Stress (De Sombre et al., 1998).**

De Sombre et al. (1998) argued that the change in height during compaction can be used to calculate the amount of power required during compaction.

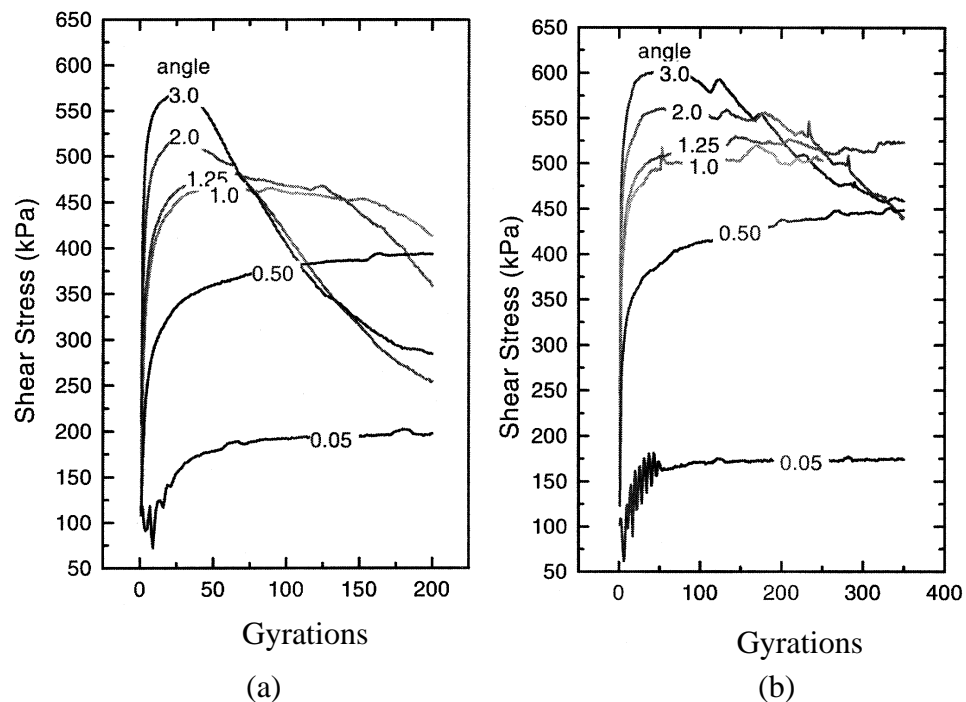
$$\text{power} = \frac{\sum p \cos \alpha \times \Delta h \times r^2 \times \pi}{t} \quad (\text{Equation 7-3})$$

where,

- p = pressure in cylinder,
- $\alpha$  = gyratory angle,
- $\Delta h$  = change in height per cycle,
- r = radius of cylinder and
- t = time.

A study conducted at the Department of Transport in Australia had shown that the shear stress evolution calculated using Equation 7-2 was a function of the applied angle and mix components (Butcher, 1998). At an angle of gyration greater than or equal to  $1.00^\circ$ , the shear stress increased with compaction until a maximum value is reached when it began to decrease with further increase in the compaction level as shown in Figure 7-4. In general, the reduction of shear

stress was shown to be more significant in mixes with softer asphalt (AC14) that were more susceptible to permanent deformation as shown in Table 7-1. This study also used the change in voids at maximum shear stress as a parameter to distinguish among mixes. Figure 7-5 shows that mixes with different asphalt grades experienced distinct changes in percent air voids at maximum shear stress. Other studies have also illustrated the relationship between the change of shear stress with compaction and the change in mix design components (Gauer, 1996. Moutier, 1996).

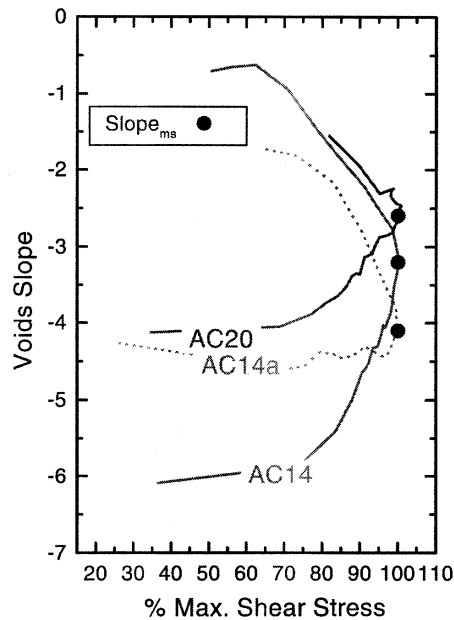


**Figure 7-4. Shear Stress Measurements at Different Compaction Levels: (a) AC14 (Soft Asphalt), (b) AC 20 (Stiff Asphalt) (Butcher, 1998).**

**Table 7-1. Maximum Shear Resistance at Different Angles and Binder Type (Butcher, 1998).**

Angle (Deg.)	Vertical Stress (kPa)	AC14		AC20	
		Max. Shear Stress (kPa)	Voids (%)	Max. Shear Stress (kPa)	Voids (%)
0.05	600	175 (est.)*	-	225 (est.)*	-
0.50		405 (est.)*	-	450 (est.)*	-
1.00		467	5.1	502	4.3
1.25		481	4.4	529	4.0
1.50		-	-	534	4.5
2.00		515	4.4	561	4.9
3.00		571	4.1	601	4.3
2.00	400	365	5.6	398	5.7
2.00	240	231	5.6	250	4.6

\* Maximum shear resistance not achieved and values estimated.

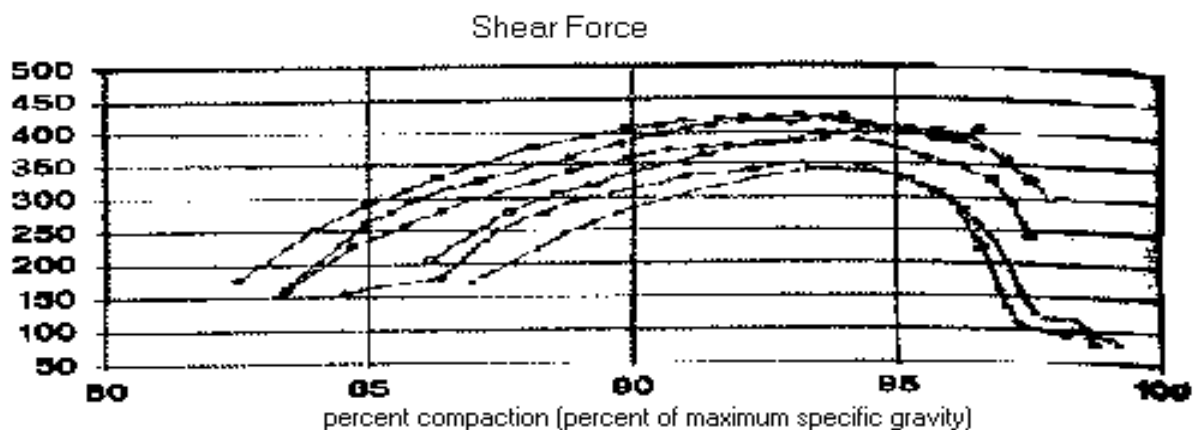


**Figure 7-5. The Change in Percent Air Voids at Maximum Shear Stress (Butcher, 1998).**

Butcher (1998) showed that these results appear to confirm the universal nature of the first stage of shear stress development during compaction. Further confirmation appeared to be in the French work by Moutier (1997) as represented in Figure 7-6. A suggested explanation for the evolution of shear stress as offered by Moutier (1997) was that the shear force increased gradually as the percent compaction increased. The particles tried to interlock to each other with

the assistance of the sufficient binder content. Further compaction may lead the binder to get out between the particles and lead to particles fracture or deformation.

Another study was carried out by Mallick (1999) to develop a method for using the SGC and the GTM compaction data to identify unstable mixes during the construction process by extracting parameters from the compaction curve. Five projects were selected in this study including construction of wearing courses on I-90 in Idaho, I-40 in New Mexico, US-280 and AL-86 in Alabama, and I-385 in South Carolina, knowing the aggregate type and gradation, asphalt binder type and content, and traffic levels of these projects. All of these mixes were compacted with the SGC operated at 600 kPa and a 1.25-degree angle, and all mixes except the I-385 were compacted with the GTM operated at 800 kPa and a 1-degree angle.



**Figure 7-6. French Maximum Shear Stress by Moutier (1997).**

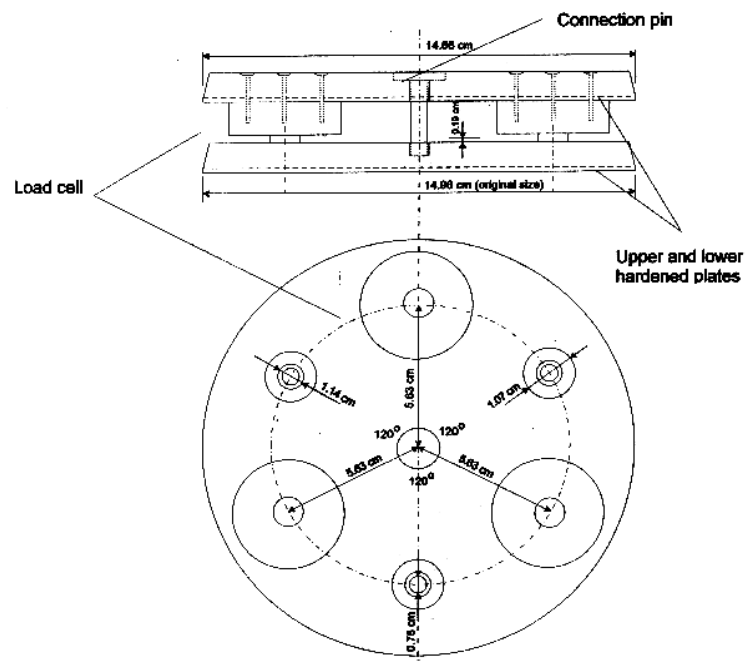
The shear stress measurements in the GTM are shown in Figure 7-7. The results show that the I-90 mix is inferior to the other mixes. In the SGC, Mallick (1991) identified inferior mixes during compaction process by calculating the gyratory ratio between the number of gyrations required by the Superpave gyratory compactor to compact a mix to 98 and 95 percent of theoretical maximum specific gravity. He presented the results in Figure 7-8 to show the relationship between rutting in the field and the gyratory ratio.

A method for using the Superpave Gyratory Compactor (SGC) results to select optimum mixture design was introduced by Bahia et al. (1998). The method divided the measured

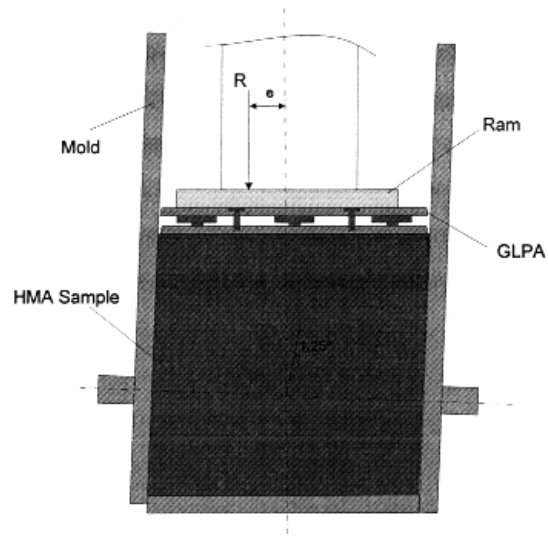
densification curve into two zones. The first zone represents the compaction characteristics related to the construction stage; the second zone represents the densification under traffic.

Bahia et al. (1998) found that the densification curve measured by the SGC could be used to calculate densification indices that represent the performance of mixture during construction and during in-service. They also introduced the Compaction Energy Index and the Traffic Densification Index (TDI) to evaluate the potential performance of mixture during construction and in-service. The values of CEI and TDI for different gradations tested showed that finer gradations, above or passing through the restricted zone, require significantly less energy to compact to 8 percent air voids, also these mixtures offered more resistance to densification between 8 percent and both of 4 percent and 2 percent air voids. This indicated that finer blends could be more favorable for construction and can perform better under traffic densification. They showed the importance of fine aggregate angularity for some mixture and also suggested that blends with high content of rounded sand may offer reasonable performance.

Guler et al. (2000) conducted a study for the purpose of developing a device that can be used in the SGC and allow shear measurements. The device consists of three load cells placed 120° apart on the top plate of the SGC called the Gyrotory Load Cell Plate Assembly (GLPA). Illustration of the GLPA and its components are shown in Figures 7-9.



**Figure 7-7. Gyrotory Load Cell Plate Assembly (Guler et al., 2000).**



**Figure 7-8. Gyratory Load Cell Plate Assembly Placed on the Mold during Gyration Process (Guler et al. 2000).**

They reported that the energy balance for the mixture sample at any gyration cycle could be written using the following equation:

$$W=U \quad \text{(Equation 7-4)}$$

where,

$W$  = work of external forces, and

$U$  = total strain energy of sample.

The above equation was written in the following form:

$$M\theta = S\gamma V \quad \text{(Equation 7-5)}$$

where,

$M$  = applied moment during gyration,

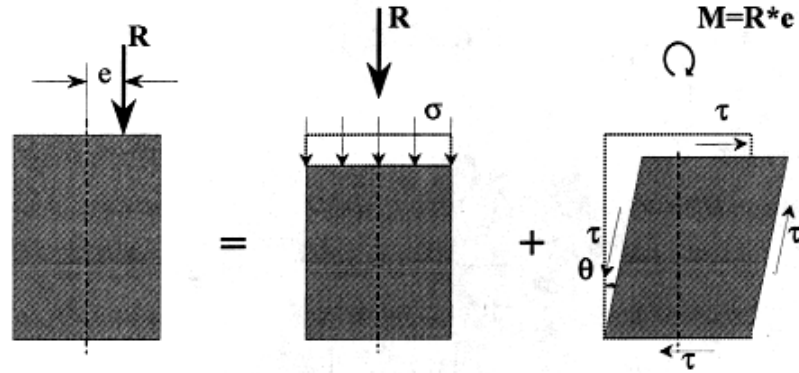
$\theta$  = gyration angle (radians),

$\gamma$  = shear strain,

$S$  = frictional resistance, and

$V$  = sample volume at any cycle.

The forces measured by the GLPA and the top vertical actuator were used to calculate the resultant force (R) and force eccentricity (e).



**Figure 7-9. Applied External Forces and the Stress Distributions Used in Energy Relations (Guler et al., 2000).**

They suggested that two-dimensional distribution of the eccentricity of the resultant load could be used to calculate the effective moment required to overcome the shear resistance of mixture and tilt the mold to the 1.25 degrees. Guler et al. (2000) stated that this effective moment is a direct measure of the resistance of asphalt mixtures to distortion and densification.

As shown in Figure 7-9 the moment M needed to apply the angle can be calculated by multiplying the resultant ram force R, by the average eccentricity, e, for a given gyration cycle. Guler et al. (2000) stated that  $\theta$  and  $\gamma$  in Equation 7.5 are equal, and the shear stress can be calculated as follows:

$$S = \frac{R \cdot e}{A \cdot h} \quad (\text{Equation 7-6})$$

where,

A = sample cross section area, and

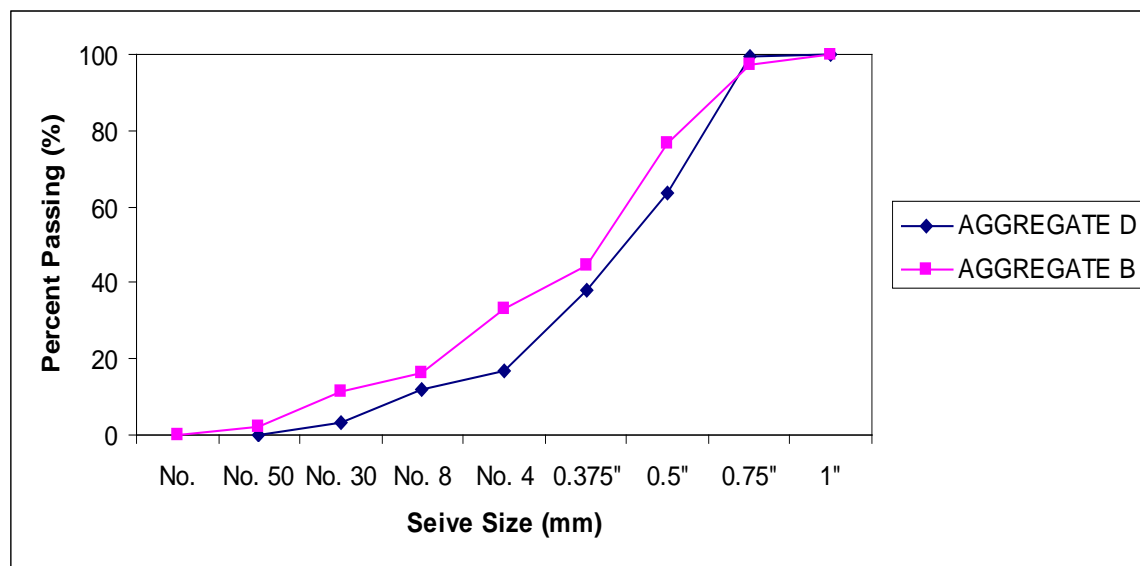
h = sample height at any gyration cycle.

They presented experimental results showing that the derived frictional resistance is sensitive to the asphalt content, aggregate gradation, and fine aggregate angularity. Careful analysis of the derivation provided by Guler et al. (2000) reveals that the shear stress in

Equation 7-6 is actually the frictional stress between the mold and the mix. This equation does not represent the mix shear strength. Also U and W in Equations 7.4 and 7.5 are both calculated from external forces and U does not represent the energy dissipated.

## DESCRIPTION OF SAMPLES

Two mix designs were considered in this task, B-mix and D-mix were used with PG 64-22 and 70-22, respectively. Gradation of the aggregate blend is as shown in Figure 7-10. B-mix “chico source” is a blend of 37 percent B-rocks, 25 percent D-rocks, 28 percent manufactured sand, and 10 percent field sand. D-mix is the combination of 56 percent “D-F” rocks, 36 percent manufactured sand, and 8 percent field sand. Details on the blend percentage and sieve analysis are shown in Appendix D.



**Figure 7-10. Aggregate Gradation for B and D Mixes.**

The binder contents used in the study are the optimum content, optimum +0.5 percent and optimum -0.5 percent. The optimum content for mixes B and D are 4.8 percent and 3.8 percent respectively. The different contents will be used to study the sensitivity of the proposed energy indices. With three replicates at each binder content, a total of 9 mixes were fabricated for each mix. Two gyratory compactors Pine and Servopac were used in the analysis to study the sensitivity of compactor manufacturers. Another set of nine specimens were fabricated for that



purpose. The testing was conducted at the Superpave laboratory at University of Texas at San Antonio with the exception of the Servopac compaction that was conducted at Texas Transportation Institute at College Station.

## Compaction Curve

Table 7-2 lists a number of compaction parameters extracted from the compaction curves (Anderson et al. 2002). Selected parameters calculated based on the reduction of height during the compactions are considered in this study. Compaction energy index (CEI), the construction densification index (CDI), which is the value of the area under the densification curve from  $N_{ini}$  gyrations to of 92 percent Gmm density, represents the work done during the construction period to achieve 8 percent air voids.

The traffic densification index, which is the value of the area under the densification curve from 92 percent density to 98 percent density, represents the work needed to resist traffic loading during pavement service life. Bahia et al. (1998) indicated that that low CEI values are desirable (fewer roller passes will be required) while high TDI values are desirable.

The CEI is calculated as following:

$$CEI_{92} = P * A \sum_{N_{G1}}^{N_{G2}} \Delta h \quad (\text{Equation 7-7})$$

where,

$P$ = vertical pressure (kPa),

$A$ = cross section area ( $\text{mm}^2$ ),

$\Delta h$ = height drops per cycle (mm),

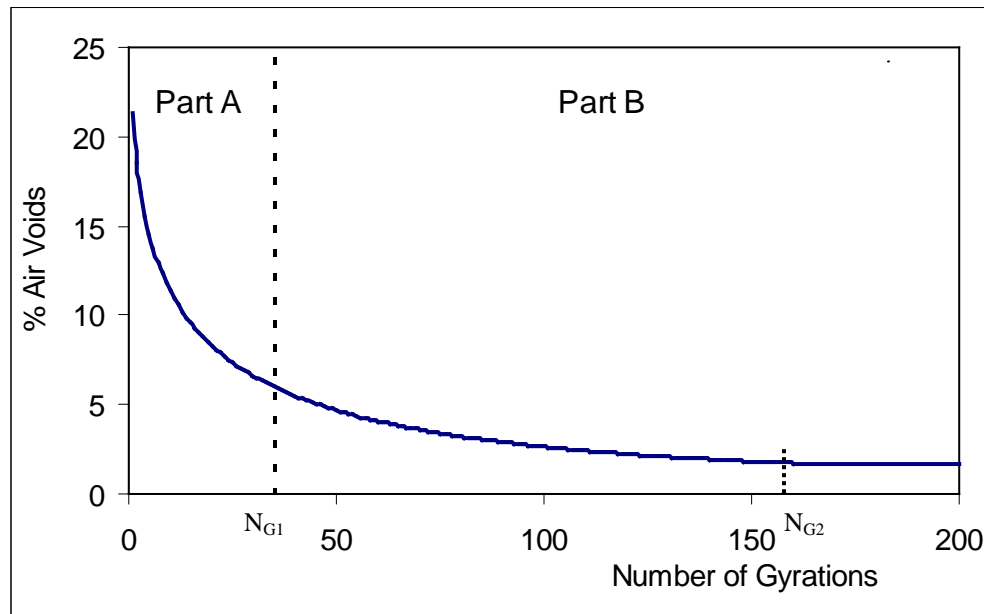
$N_{G1}$ = number of gyrations at beginning of compaction, and

$N_{G2}$ = number of gyrations at 92% density

For other indices the number of gyrations is set at different start and end points according to the corresponding air voids (or Gmm). The compaction parameters were determined for each replicate in the experiment. More focus would be in the last five parameters in Table 7-2.

**Table 7-2. Compaction Parameters Determined from Conventional Compaction Curve (Anderson et al., 2002).**

Parameter	Abbreviation	Description
Compaction slope (Linear)	K	
C <sub>1</sub> Intercept( linear)	C <sub>1</sub>	
Compaction slope (Power Exponent)	B	Power law $Y=aX^b$
C <sub>1</sub> Intercept (Power)	A	Power law $Y=aX^b$
Number of gyrations to 92% Density	N <sub>92</sub>	
Number of gyrations to 95% Density	N <sub>95</sub>	
Number of gyrations to 96% Density	N <sub>96</sub>	
Number of gyrations to 98% Density	N <sub>98</sub>	
Ratio of N <sub>95</sub> to N <sub>92</sub>	N <sub>95</sub> / N <sub>92</sub>	
Ratio of N <sub>98</sub> to N <sub>95</sub>	N <sub>98</sub> / N <sub>95</sub>	
Ratio of N <sub>98</sub> to N <sub>96</sub>	N <sub>98</sub> / N <sub>96</sub>	
Compaction energy index from C <sub>1</sub> to 92%	CEI <sub>92</sub>	
Compaction energy index from N <sub>ini</sub> to 92%	CEI <sub>Nini-92</sub>	
Densification energy index from 92% to 96%	DEI <sub>92-96</sub>	
Terminal Densification index from 96%-98%	TDI <sub>96-98</sub>	
Terminal Densification index from 92%-98%	TDI <sub>92-98</sub>	

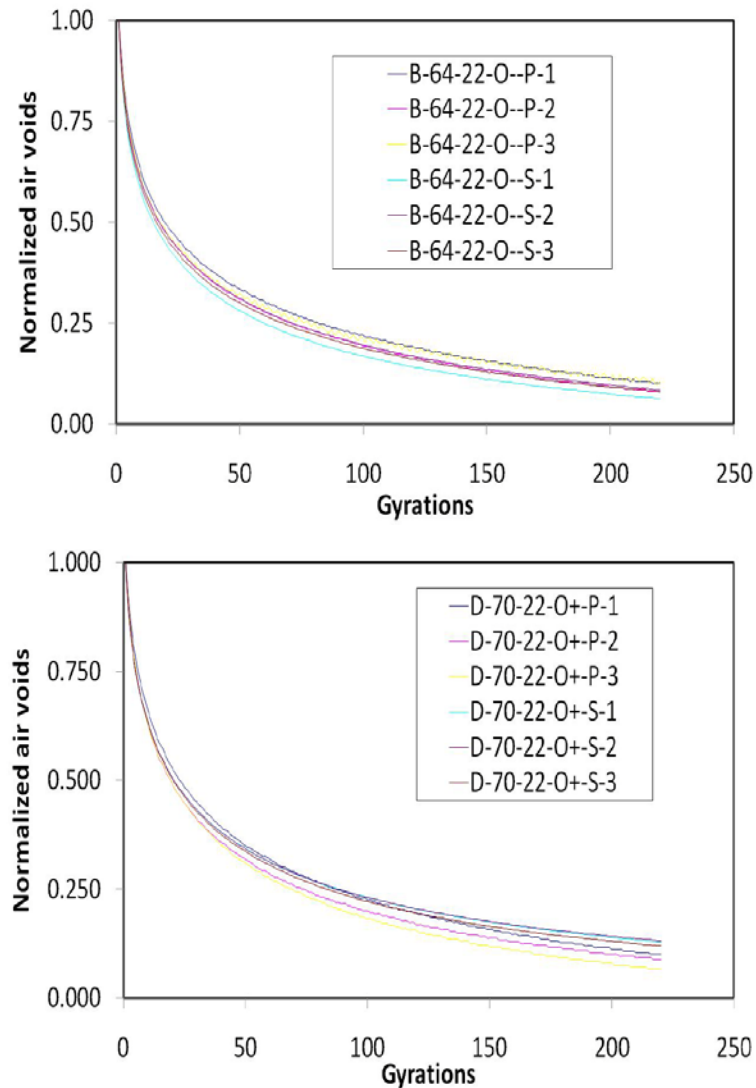


**Figure 7-11. A Schematic Diagram Shows the Two Zones of the Compaction Curve.**

## TESTING RESULTS AND ANALYSIS

### Effect of Apparatus

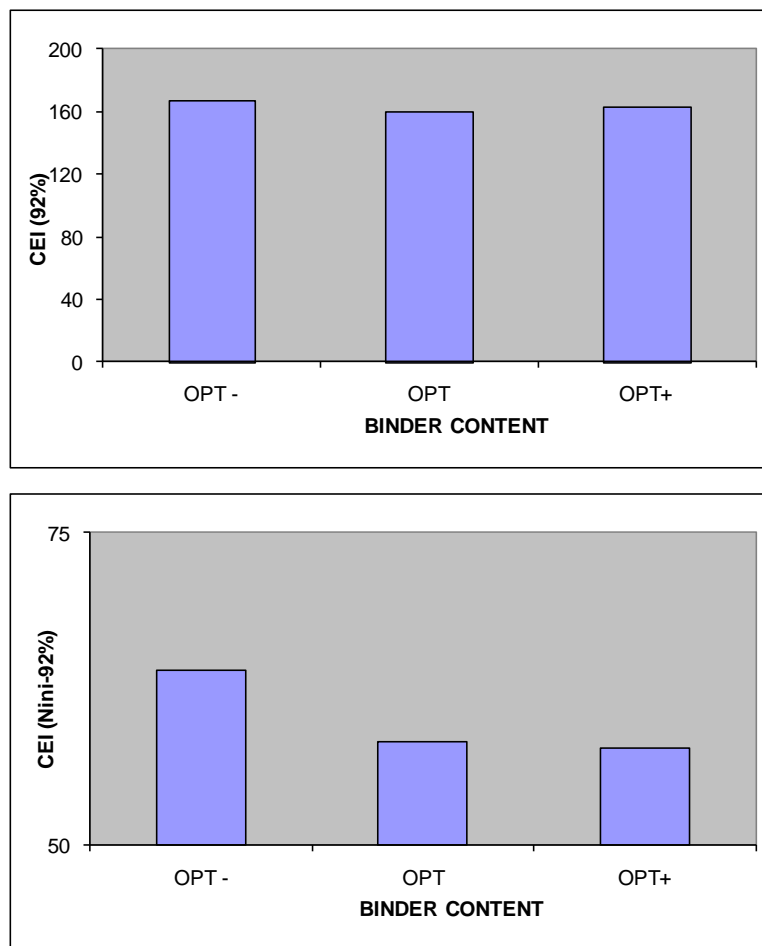
Results indicated that compactor manufacture has negligible effect on the compaction curve. Figure 7-12 illustrates the comparison between compaction of HMA using Pine (P) and Servopac (S) gyratory compactors for B and D mixes. This proves that the compaction mechanism is unique regardless of the source manufacture.



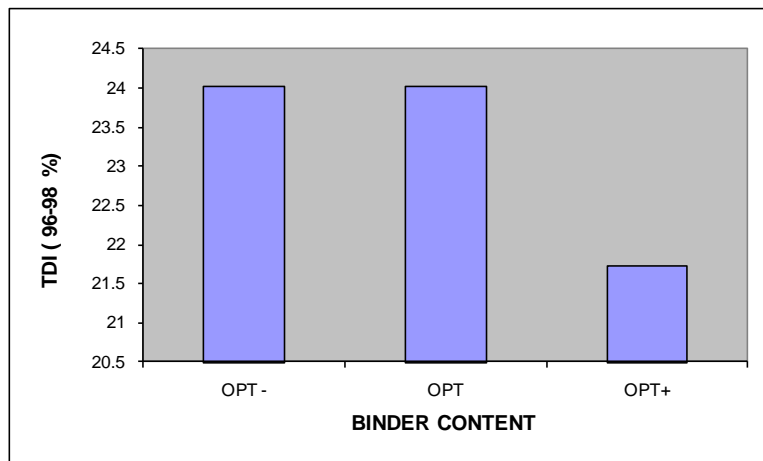
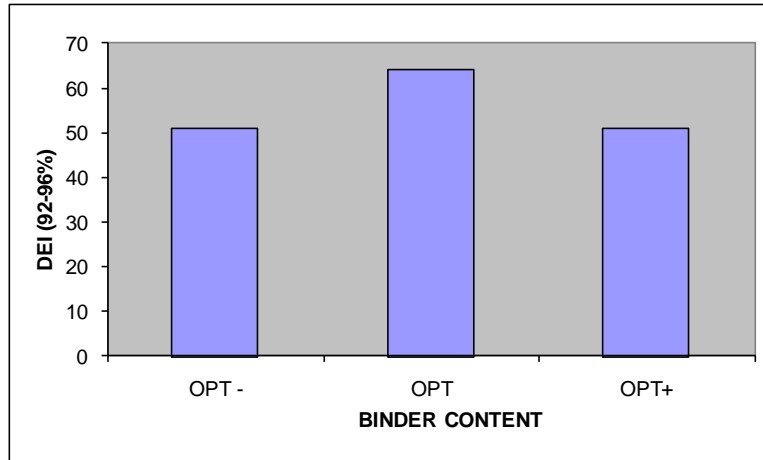
**Figure 7-12. The Effect of Pine and Servopac in B and D Compaction.**

## Effect of Binder Content

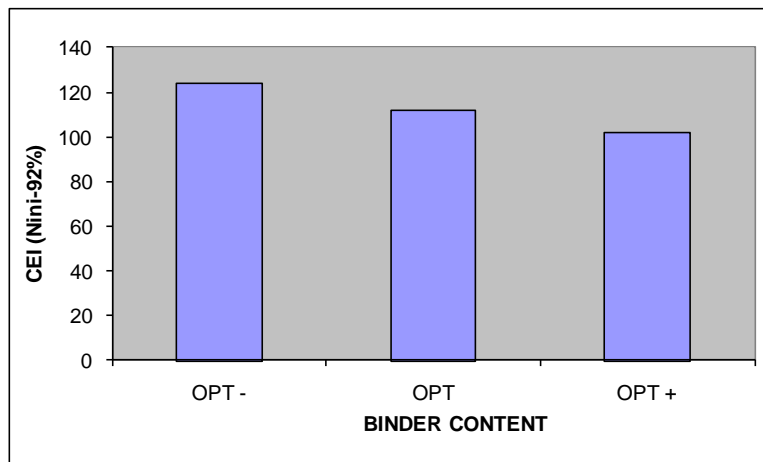
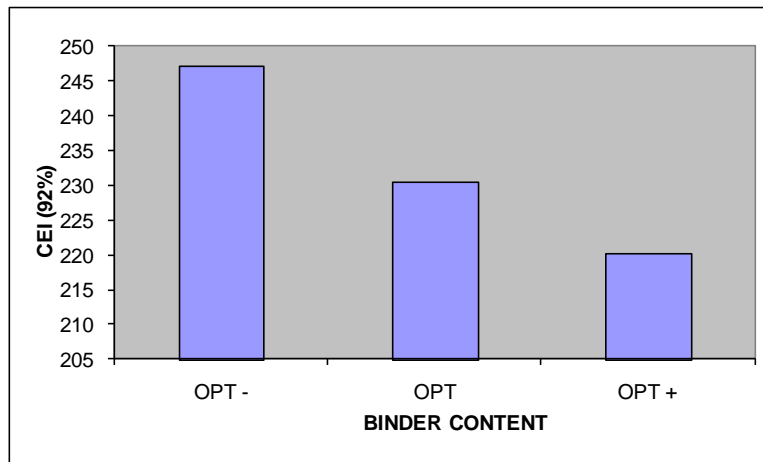
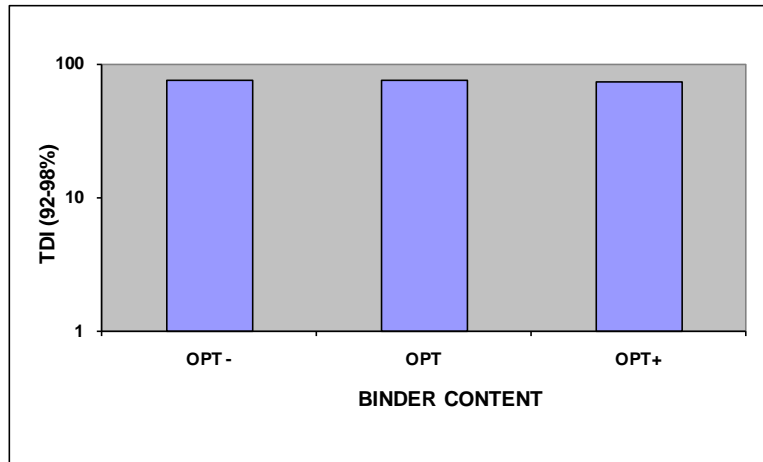
Several studies suggest that a change of 0.50 percent of asphalt content will result in raveling or cracking if it is deficient in asphalt content, or can cause flushing and rutting if it has excessive asphalt content. As used three different binder contents, i.e., optimum plus, optimum, optimum minus, energy indices were varying with the change in binder content. In mix B, as the binder content increased, the energy indices decreased; where as in mix D, as the binder content increased compaction energy indices, i.e., CEI 92 percent and CEI Nini-92 percent were decreased were as DEI, TDI96-98 and TDI 92-98 were increasing (see Figure 7-13 and 7-14).



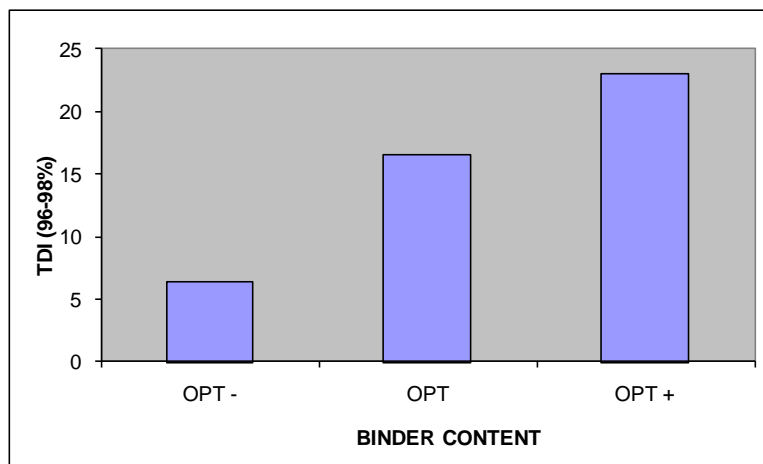
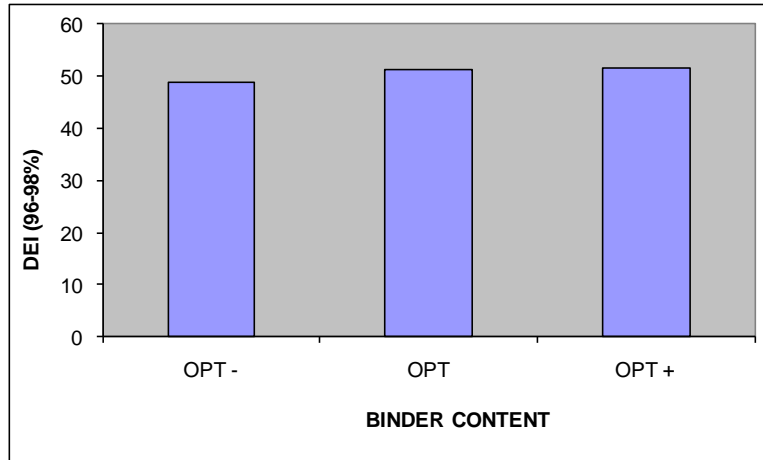
**Figure 7-13. Effect of Binder Content on Compaction Indices of Type B Mix.**



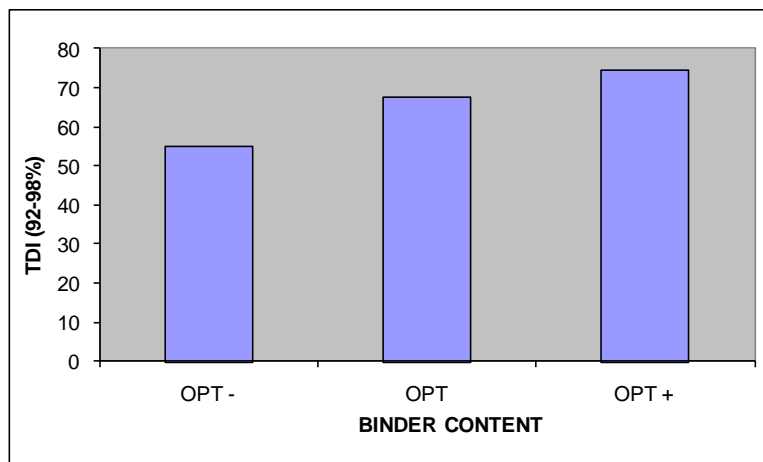
**Figure 7-13. Effect of Binder Content on Compaction Indices of Type B Mix (Continued).**



**Figure 7-13. Effect of Binder Content on Compaction Indices of Type B Mix (Continued).**



**Figure 7-13. Effect of Binder Content on Compaction Indices of Type B Mix (Continued).**

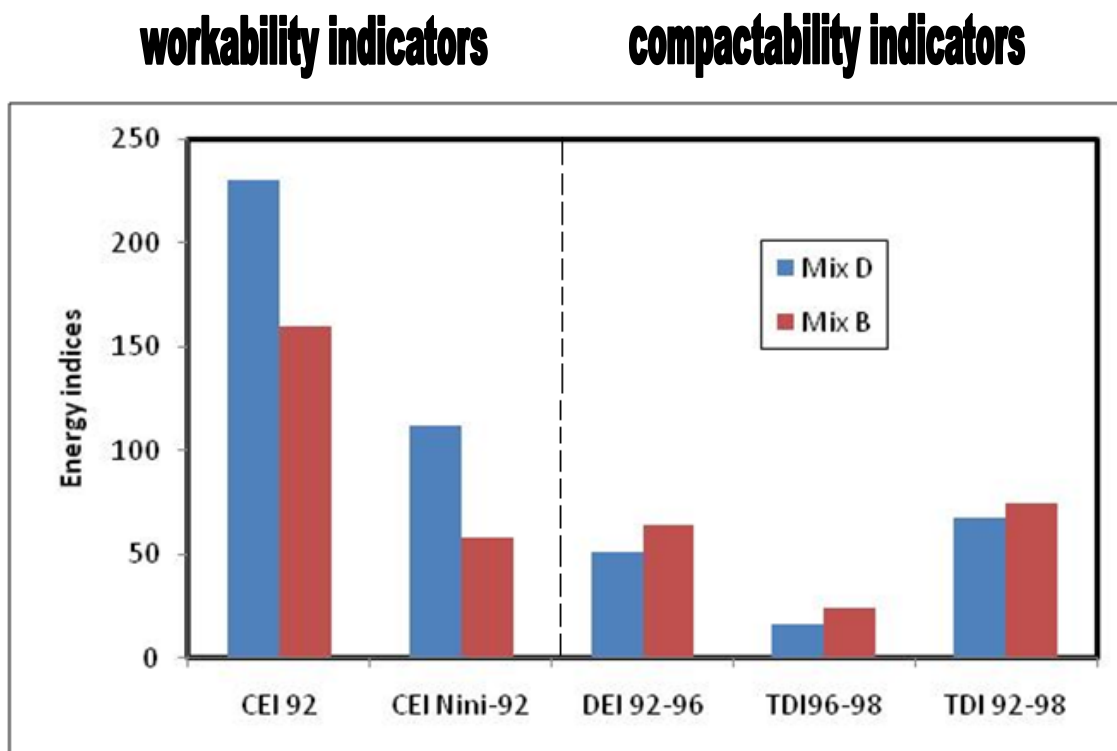


**Figures 7-14. Effect of Binder Content on Compaction Indices of Type D Mix.**

## Effect of Mix Design

The compaction curve produced by the gyratory compactor is divided at 92 percent Gmm. The compactions that occur between Nini and 92 percent Gmm and between 92 percent Gmm and 98 percent Gmm are considered to be representations of the construction compaction and traffic densification, respectively, the construction energy index and the traffic densification index, respectively. The CEI correlates with the construction side of the curve (Nini to 92 percent Gmm), and the TDI correlates with the traffic side of the curve (92 to 98 percent Gmm). The index is thought to represent the energy required for the gyratory to reduce the air voids of the mixture (see Figure 7-15).

The Figure 7-15 shows the difference in different energy indices for two mix types at optimum binder content. Compaction energy index (CEI) is more for both the mixes than other energy indices. Compaction energy index from Nini-92 percent is more in D mix than in B mix while for DEI 92-96, TDI 96-98 percent and TDI 92-98 percent is more for B mix, than D mix.



**Figure 7-15. Preliminary Energy Indices for B and D Mixes.**



## **SUMMARY AND FINDING**

Based on preliminary data the following findings can be drawn:

- Results implied that the energy required to compact B-mix is much less than in D-mix to achieve the 92% density. However, during service life, the energy required to densification D-mix is less than in B-mix.
- D-mix is more sensitive than B-mix for a slight change in binder content.
- The compaction indices have shown sensitivity due to different gradation mix design and binder content. However no change was noticed due to apparatus change.
- Increasing binder content tends to reduce the energy required to compact the mixes.
- The CEI is a suggested potential index to workability measurements of the mix while TDI 92-98 is a suggested potential parameter for compactability measurement.
- Separating the workability and compactability indices can be done by using the compaction curve at a threshold of 92% Gmm or 8% air voids.

These findings are still evaluated under more mixes, C-mix, and Louisiana mix, etc. Changes in the above comments are possible where more mixes are evolved in the study. Also, we will also be looking into more compaction parameters in this study as it progresses.

## **FUTURE WORK**

Below are the ongoing and planned works for the development of workability and compactability indices for HMA mixes:

- Include Type C mixes from different sources in the compactability study.
- Use the plant mixes from the Louisiana Transportation research center to correlate field performance to the compactability indices.
- Evaluate the Oklahoma N8 and N9 plant mixes from NCAT.
- Set a threshold for the allowable minimum and maximum range for workability and compactability indices.
- Investigate the internal microstructure distribution effect in the overall compactability of mixes Type B and D.



## **CHAPTER 8**

### **FIELD EVALUATION OF MIX-DESIGNS AND CONSTRUCTION OF THE APT TEST SECTIONS**

To validate the proposed new mix-design procedures and the associated laboratory test methods, accelerated pavement testing (APT) was incorporated as an integral task of this research study. Primarily, the intent of the APT task is to evaluate and validate the mix-design procedures in terms of their rutting, fatigue cracking, and reflective cracking prediction potential under accelerated traffic loading conditions. Accordingly, the APT field results will then be compared with laboratory predictions.

This chapter starts by providing a description of the mix-design procedures that were evaluated and the HMA mix that was utilized. This is followed by a description of the APT test site and construction details. Quality control/assurance tests conducted during construction of the APT test sections are also discussed in this chapter. A summary is also included at the end of the chapter.

#### **MIX-DESIGN METHODS AND HMA MIX EVALUATED**

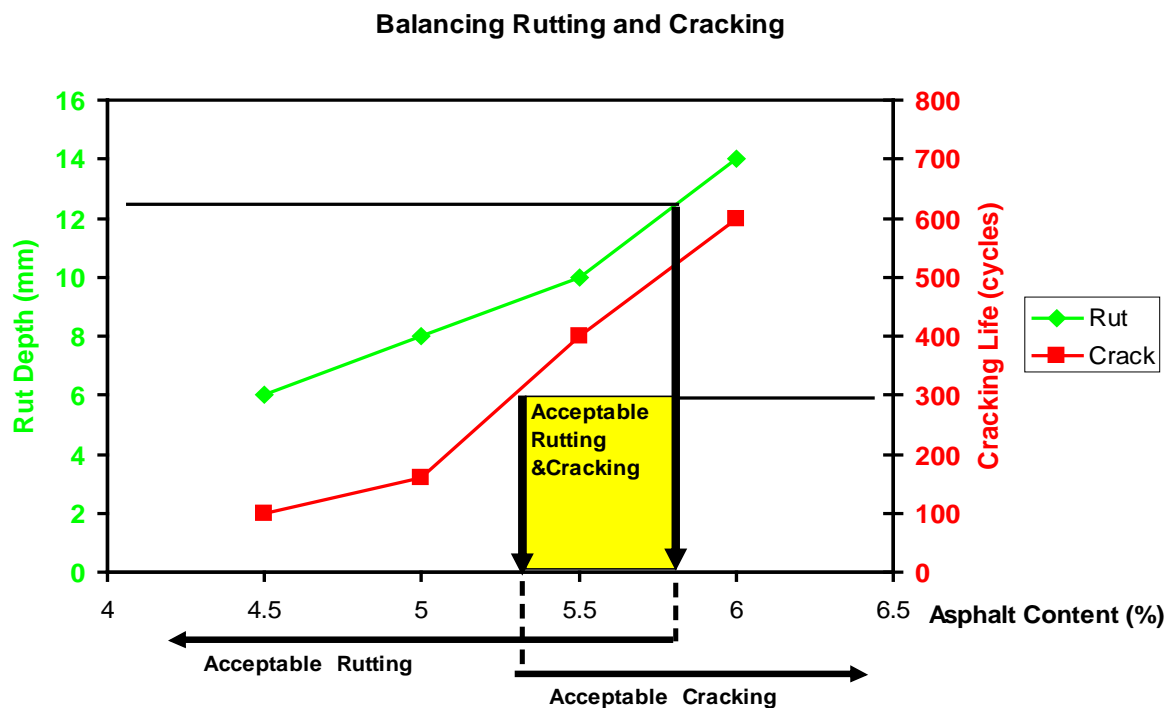
In this interim report, two mix-design methods, namely the Texas gyratory and the balanced mix-design, were evaluated. A typical Texas dense-graded Type C mix was utilized for both laboratory and field (APT) evaluation of the two mix-design methods. These aspects are discussed in the text below.

##### **The Texas Gyratory Mix-Design Method**

The Texas gyratory is the mix-design method traditionally used by TxDOT for designing their mixes (TxDOT, 2009). It is a volumetric-density based method and the OAC is selected based on meeting a prescribed density criterion, i.e., at 96 percent for most dense-graded Texas mixes. Sample molding and compaction at a minimum of three trial asphalt-binder contents is accomplished with the Texas gyratory compactor (TGC). Laboratory mix performance evaluation at OAC is done with the indirect tensile strength and the Hamburg rutting tests. Full details of this mix-design procedure and the TGC can be found in TxDOT test procedures Tex-204-F and Tex-206-F (TxDOT, 2009).

## The Proposed Balanced Mix-Design Method

As discussed in Chapter 1, the concept of the balanced mix-design method is fundamentally centered on ensuring adequate rutting and cracking resistance for the HMA mixes (Zhou et al., 2007). The idea is to design a mix that is at least both rutting-and cracking-resistant. With this concept, the design philosophy is based on designing and selecting an OAC that simultaneously meets certain prescribed laboratory rutting ( $\leq 12.5$  mm) and cracking requirements based on the Hamburg and Overlay tests, respectively. Figure 8-1 shows a graphical illustration of the balanced mix-design concept.



**Figure 8-1. Graphical Illustration of the Balanced Mix-Design Concept.**

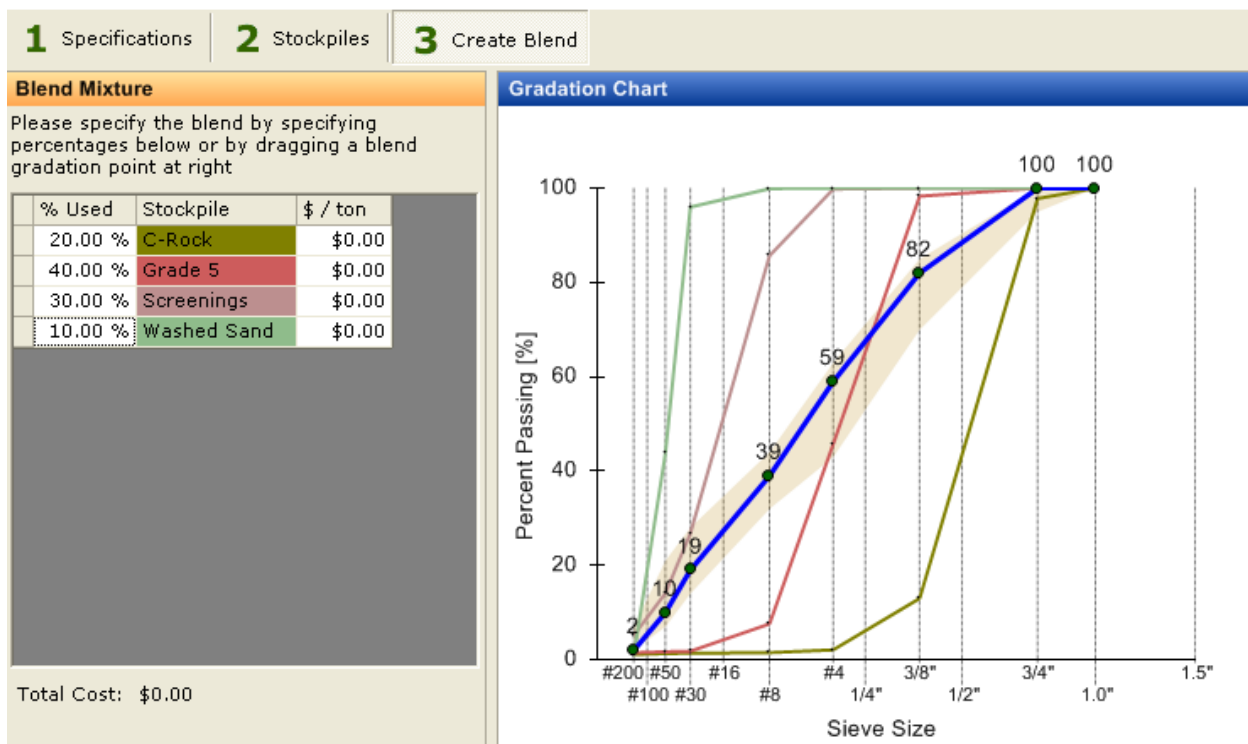
The standard Hamburg rutting criterion is 12.5 mm (i.e.,  $\leq 12.5$  mm rut depth after 10,000, 15,000, and 20,000 HWTT load passes for mixes with PG 64-22, PG 70-22, and PG 76-22 asphalt-binder, respectively). For the Overlay tester, mixes which last over 300 cycles (i.e.,  $\geq 300$ ) prior to crack failure are tentatively considered to have reasonable laboratory cracking resistance. However, 300 cycles is still a subjective OT criterion that has not yet been standardized.

## The HMA Mix Utilized for APT Testing

As discussed in Chapter 3, various mixes were evaluated in the laboratory and the modified Type C (Beaumont) mix was selected for APT testing. The evaluation was based on meeting the balanced mix-design (Hamburg rutting and Overlay cracking) and the Texas gyratory mix-design requirements as described above (Zhou et al., 2007; TxDOT, 2009). Detailed results of the laboratory mix-design evaluations are included in Appendix F. The mix-design details and aggregate gradations for the Type C (Beaumont) mix are shown in Table 8-1 and Figure 8-1, respectively.

**Table 8-1. HMA Mix-Design Details for APT Testing.**

Mix	Materials	Design Method	Mix Designation	OAC	HWTT Rutting	OT Cycles	APT Placement
Type C	PG 76-22 (Valero, TX) +	Texas gyratory	Control	4.3%	4.7 mm	90	Control test sections
Type C	Limestone (Brownwood, TX)	Balanced	Modified	5.2%	7.0 mm	600	All other test sections



**Figure 8-2. Aggregate Gradation for the Type C Mix.**

The Type C mix (both control and modified) described in Table 8-1 and Figure 8-2 is a typical dense-graded Texas mix. Both the asphalt-binder (Valero) and limestone (Brownwood) aggregates were locally sourced in Texas. Note that one of the objectives of APT testing is to compare the balanced mix-design with the traditional Texas gyratory method. Consequently, the design based on the Texas gyratory method (i.e., 4.3 percent OAC) was utilized as the “control mix” for APT testing. As a way of validating the mix-design methods, the APT performance of the 4.3 and 5.2 percent OAC designs compared so as to verify the laboratory predictions shown in Table 8-1.

### **DESCRIPTION OF THE APT FACILITY AND THE ALF MACHINE**

A contractual agreement was developed with the Louisiana Transportation Research Center (LTRC) to test the Texas mixes at their APT facility near Baton Rouge in Louisiana (LA). The climate and environmental conditions in the southern part of LA where the APT facility is located do not differ significantly from that of Texas. Since Texas lacks such an APT facility, it was, therefore, deemed appropriate to do the APT testing at LTRC in LA. LTRC has an established ALF machine shown in Figure 8-3 and have been actively running accelerated load tests for more than 5 years.



**Figure 8-3. LTRC’s ALF Device.**

The ALF device is a 100 ft long and 55 ton accelerated loading device used to simulate truck loading for pavement testing. When running, the weight and traffic movement is simulated repetitively in one direction via a computer-controlled trolley. The LTRC-ALF is a uni-directional APT device with dual wheels that are 9 inches wide, with a 6-inch separation between the tires. The ALF loading is adjustable, ranging from 5 to 10.5 kips per tire, with a maximum operable tire pressure of up to 150 psi. The test area under the ALF is approximately 40-ft long, with tire contact area of 445 inch<sup>2</sup> at 100 psi. The maximum operable ALF speed is 120 mph.

In total, the LTRC facility consists of 12 individual lanes, each 215-ft long and 13-ft wide. The individual lanes are designable to any pavement structure of interest. TTI is utilizing only three lanes; for reflective cracking, rutting, and fatigue crack evaluation of the Type C mix, respectively (see Table 8-1 for the mix-design details).

## **CONSTRUCTION OF THE APT TEST SECTIONS**

Construction of the APT test sections was completed in summer 2009. Two lanes designated as Lanes 2 and 3) with four sections consist of 3-inch thickness of HMA plus 4- to 7-inch thick stone base over a 3- to 6-inch thick cement-treated base (CTB) layer. The third lane (designated as Lane 1) consists of 2-inch thick HMA over 8-inch thick joint concrete pavement (JCP) that is resting on a 7-inch thick CTB layer. A diagrammatical layout of the constructed test sections is shown in Figure 8-4.

### **Subgrade, Subbase, and Base Materials**

The subgrade consists of in-situ natural soil material, i.e., a class A-4 soil material type. On Lane 1, the base is JCP and the subbase is a 5 percent CTB layer. For Lanes 2 and 3, the base and subbase are Kentucky limestone and 10 percent CTB layer, respectively.

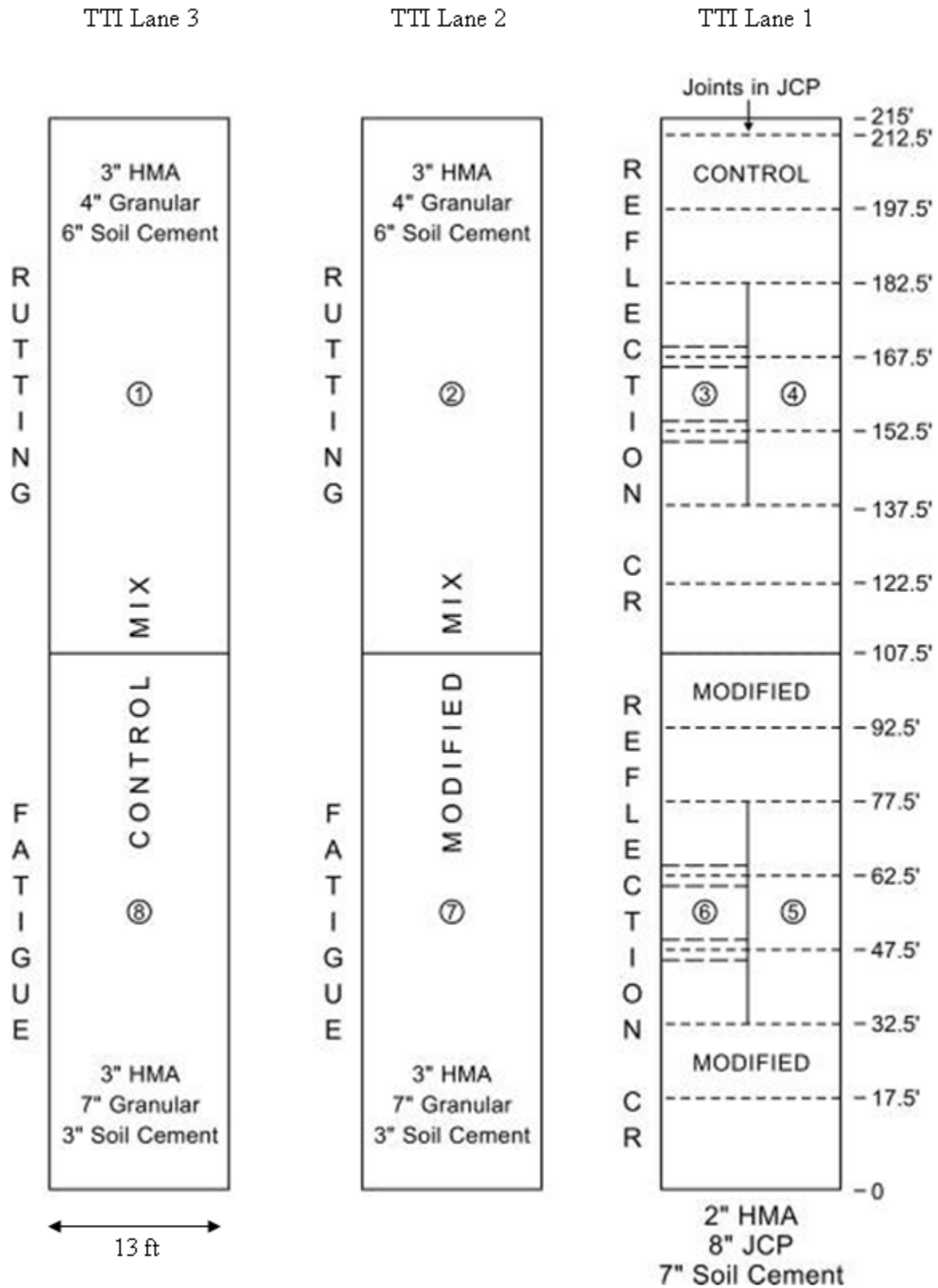
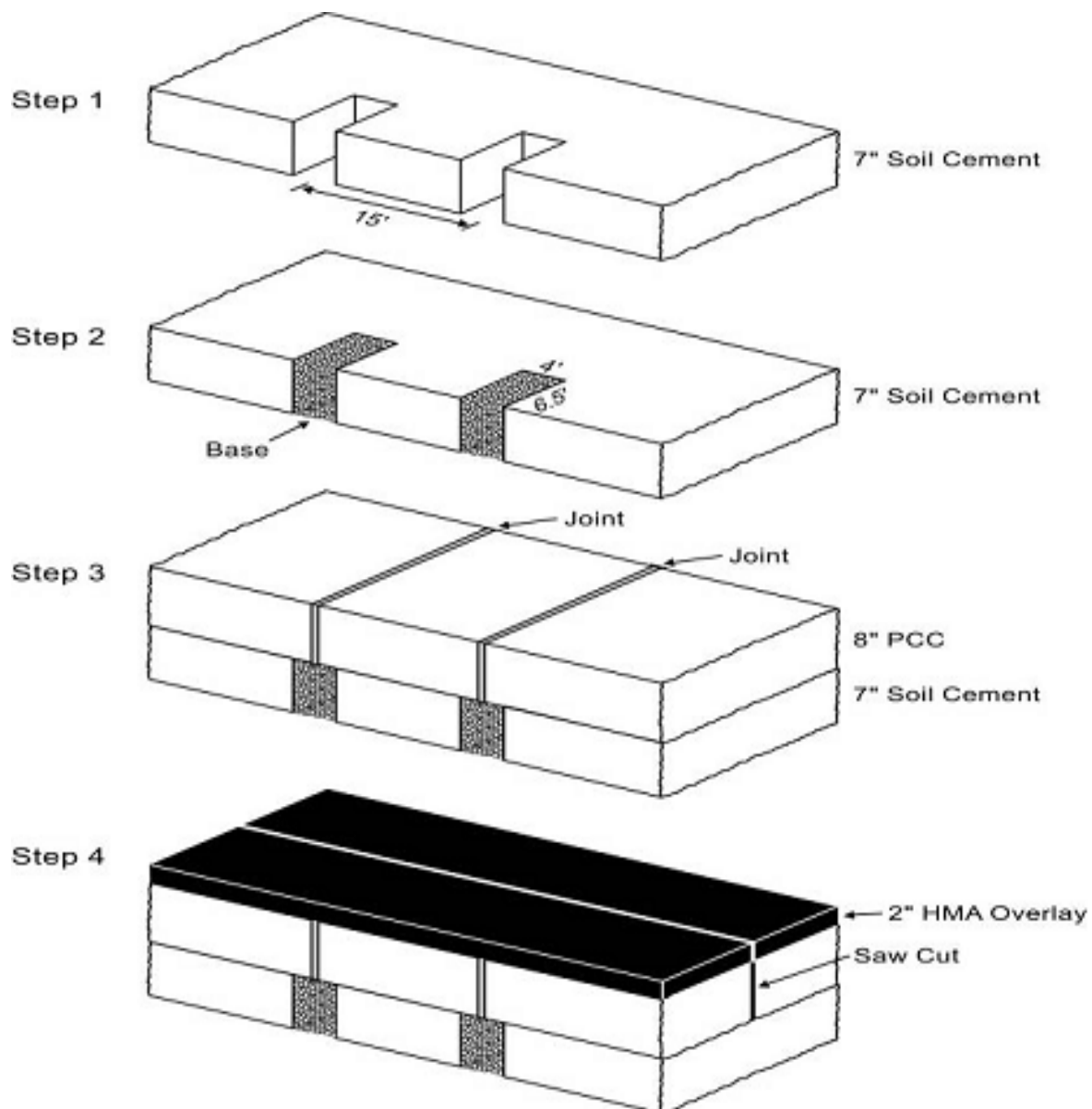


Figure 8-4. LTRC-APT Experimental Test Sections.



### Construction of Joints in the JCP Sections

One innovative feature of this APT test site is that the joints constructed in the experimental JCP sections have poor load transfer efficiency (LTE). The LTE of the control joints is close to 100 percent. However, the LTE was reduced to 50 percent over the other experimental JCP sections. This was necessary to effectively evaluate the reflective cracking potential of the HMA mixes. The joint construction process is illustrated in Figure 8-5.



**Figure 8-5. Construction of the Low LTE Joints at the LTRC-APT Test Site.**

## HMA Placement, Paving, and Compaction Process

HMA placement was consistent with the Texas construction specifications (TxDOT, 2004). No material transfer device was engaged in this construction operation. As shown in Figure 8-6, the trucks dumped the hot-mix directly into the paver.



**Figure 8-6. HMA Placement and Compaction Operations.**

The air and surface temperatures at the time of HMA placement were 82 and 105 °F, respectively, which satisfied the Texas construction specification requirements (TxDOT, 2004). To meet the 143 to 145 pcf density requirements, the compaction rolling pattern consisted of two vibrating passes and two static passes of an 18-ton steel wheel roller; see Figure 8-6. An example of the finished HMA mat at the LTRC-APT test site is shown in Figure 8-7.



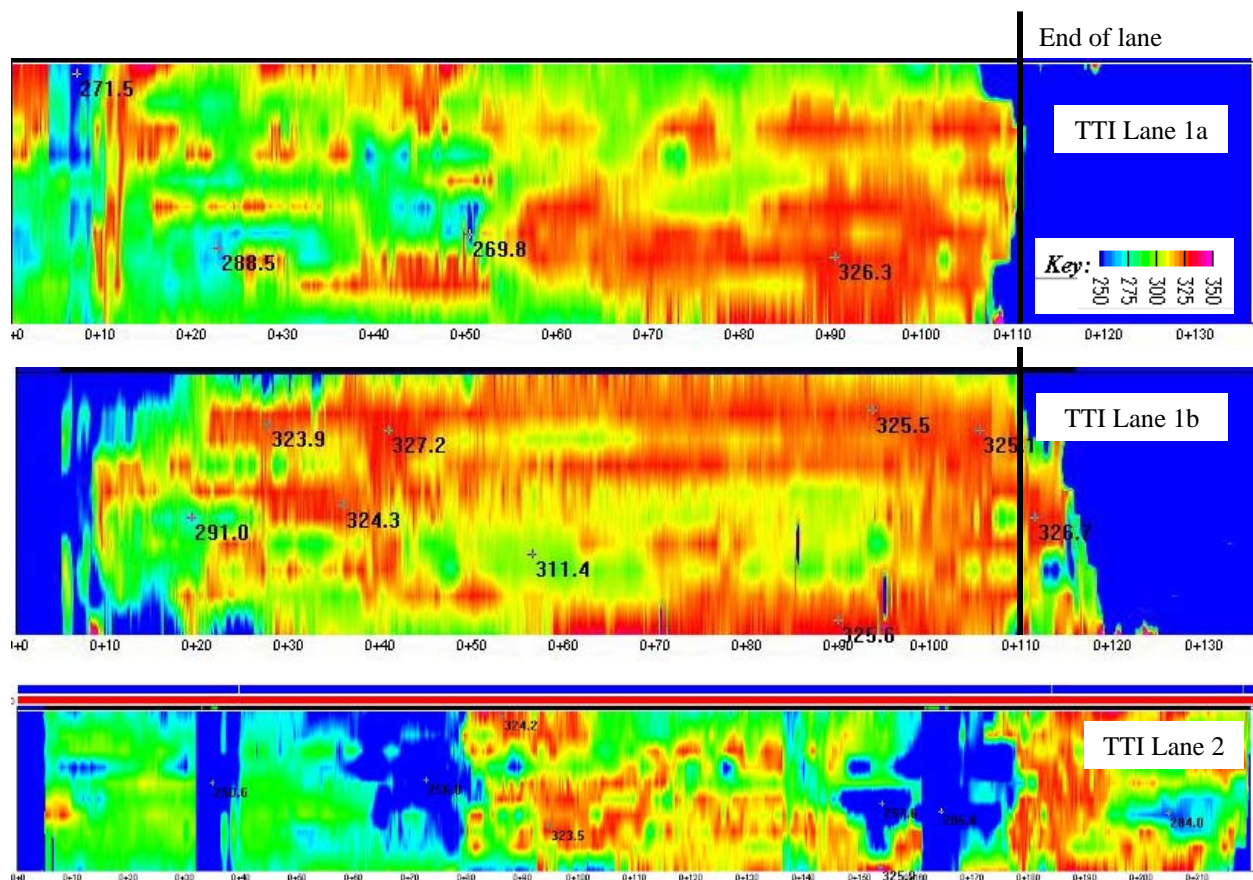
**Figure 8-7. Finished HMA Mat at the LTRC-APT Test Site (August 2009).**

## CONSTRUCTION QUALITY CONTROL-ASSURANCE TESTS

The following QC tests were conducted during construction of the APT test sections and are discussed herein: mat temperatures measurements, density measurements, GPR measurements, and coring.

### IR Thermal Imaging

TTI conducted IR temperature measurements during placement of the HMA mix on all the three lanes at the LTRC-APT test site. The IR thermal imaging of the HMA mat is shown in Figure 8-8.



**Figure 8-8. IR Thermal Imaging of the HMA Mat.**

In Figure 8-8, the red colors represent temperatures around 300 °F, whereas the blue colors are temperatures of around 220 °F. The green colors represent temperatures between 235 and 270 °F. The numbers on the plot are the actual temperatures at that location.

In general, blue is the undesired IR thermal color reading as it often indicates cold spots. For a target HMA mat placement temperature of 300 °F with a tolerance of  $\pm 30$  °F, the green and red IR thermal color readings would be considered as acceptable. As can be seen in Figure 8-8, the mat temperature was not very uniform, with visual evidence of thermal segregation particularly on Lanes 1a and 2. There are some intermittent cold spots (bluish) of thermal segregation in the mat. On Lane 1b, the mat temperatures were fairly uniform, particularly in the middle part of the lane, with an average of about 290 °F.

As will be discussed in the subsequent sections, this thermal segregation did not appear to have significantly affected the uniformity in the compaction operation. The in-situ densities were fairly consistent and within the target range; see Table 8-2.

### Nuclear Density Measurements

With the exception of Test 4 for the control mix, Table 8-2 shows that the HMA mat densities were satisfactorily within the 143 to 145 pcf range. The COV is less 1 percent; which is indicative of uniform compaction and consistent density.

**Table 8-2. QC Nuclear Density Measurements.**

<b>Mix Designation</b>	<b>Test1</b>	<b>Test2</b>	<b>Test3</b>	<b>Test4</b>	<b>Avg.</b>	<b>COV</b>
Control	143.0	144.0	144.6	142.7	143.6	0.6%
Modified	144.3	143.7	143.5	144.5	144.0	0.3%

### QC Asphalt-Binder Tests

As shown in Table 8-3, the QC asphalt-binder contents were slightly less than the design OAC of 4.3 and 5.2 percent, respectively. Nonetheless, the deviations are not more than  $\pm 5$  percent.

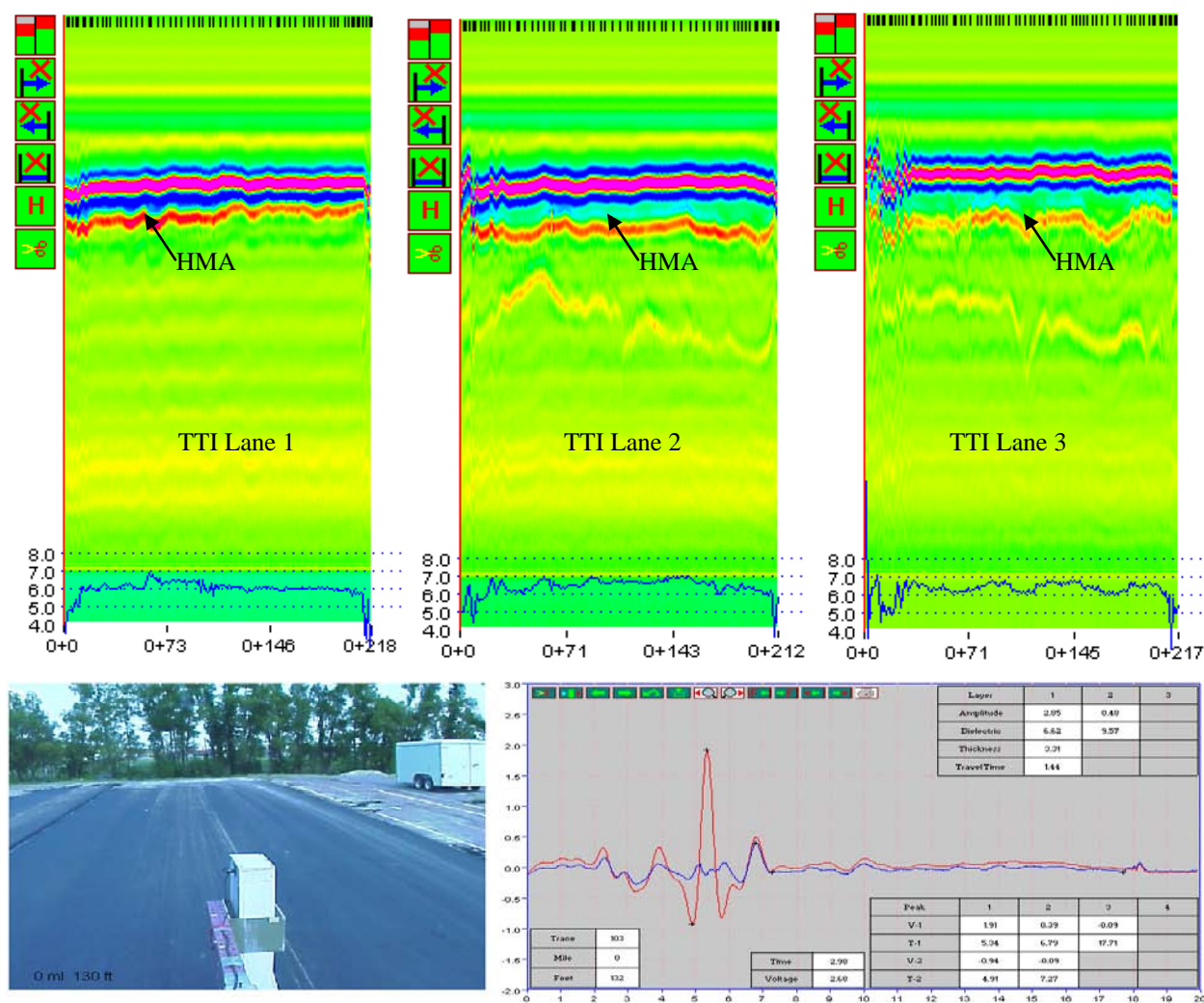
**Table 8-3. QC Asphalt-Binder Content Measurements.**

<b>Mix Designation</b>	<b>Design OAC</b>	<b>QC Asphalt-Binder Content</b>	<b>Remark</b>
Control	4.30%	4.13%	4.0% less
Modified	5.20%	5.10%	1.9% less



## GPR Measurements

Figure 8-9 shows GPR readings taken just after placement of the HMA mat. The GPR readings for Lanes 2 and 3 with some blue coloring suggests density variations within the HMA mat, which may be critical for the rutting performance of the mixes. Cores taken from these locations will serve to verify the in-situ density measurements once laboratory testing is complete.



**Figure 8-9. GPR Measurements.**

From Figure 8-9, both the HMA and the base exhibit inconsistent thickness. This is a construction quality issue that may impact the APT performance of the test sections under ALF loading.

### **Raw Materials, Plant Mixes, and Cores**

Substantial quantities of both the plant-mix and field-extracted cores (both mix designs) were obtained from the APT test site for laboratory testing at the TTI lab. Details of the plant-mix and core extraction points are included in Appendix F. HMA specimens were also molded on site using TTI's mobile lab (see Figure 8-10) and hauled to TTI for subsequent lab testing. Raw materials including asphalt-binder and aggregates were also obtained and are scheduled for testing at the TTI lab. The results of these laboratory tests will be documented in future reports.



**Figure 8-10. TTI's Mobile Lab.**

### **APT TEST PLAN**

Comparative APT testing at LTRC will inevitably allow for a direct comparison of the control and modified Type C mixes (Table 8-1) under the following test conditions:

- Rutting tests over a thin flexible base,
- Reflection cracking test with HMA over a JCP structure, and
- Fatigue cracking test of the HMA over a thick flexible base.

The results for APT comparisons of both mix-designs (control and modified) will in turn allow for validation of the proposed balanced mix-design concept.

The APT testing at the LTRC is a two-phase test plan to be accomplished over a one year period, so that tests can be conducted in both hot and cold weather. The first phase of the ALF

testing involves Sections 1 and 2 (Figure 8-4) in hot weather to measure the rutting potential of both mixes (Table 8-1). Phase two (Sections 3 through 8) is the cold weather testing for crack (fatigue and reflective cracking) evaluation. Detailed ALF test plans including marking of the test sections are included in Appendix F.

## **SUMMARY**

Construction of the APT test sections in Louisiana was completed during this reporting period. Details of the construction process were discussed in this chapter. The list below provides a summation of the key points of this chapter:

- A Type C mix with PG 76-22 asphalt-binder (Valero) and limestone aggregates (Brownwood) was placed as the surfacing HMA layer on the APT test sections.
- Two OAC designs based on the Texas gyratory and balanced mix-design methods, namely the control at 4.13 percent QC asphalt-binder content and the modified at 5.1 percent QC asphalt-binder content were utilized.
- Construction QC tests were conducted and included IR thermal imaging, nuclear density measurements, GPR measurements, and coring for forensic evaluations.
- Planned APT tests for evaluating the mix-design methods and the Type C mix include rutting and cracking (fatigue and reflection).
- The Type C HMA layer thickness for rutting and fatigue crack evaluation is 3 inches while it is 2 inches for the reflective crack evaluation over a JCP.
- On all sections, the subbase consists of a CTB layer, 5 percent for reflective cracking evaluation, and 10 percent for the rutting and fatigue crack evaluations.





## **CHAPTER 9**

### **SUMMARY OF FINDINGS**

This chapter is a summation of this interim report and highlights the major findings from the laboratory work that was done including mix-design evaluations. The laboratory tests conducted include X-ray CT scanning, cracking, Overlay round-robin, and workability. Currently ongoing and future planned works are also discussed in this chapter.

#### **MAJOR FINDINGS TO DATE**

The major findings from this interim report are summarized as follows:

##### **Research Overview and Laboratory Mix-Design Evaluations**

- The current Texas adaption of stiff high PG asphalt-binder grades and the design of rut-resistant mixes have resulted in performance concerns with “drier” mixes that are not only difficult to compact, but are also more susceptible to cracking failures. In fact, most TxDOT districts such as Houston report a lot of cracking problems on their roads as compared to rutting problems. Thus, there is an urgent need to develop new mix-design procedures and methods that incorporate crack evaluation and workability/compactability assessment.
- In this interim report, two mix-design methods (the Texas gyratory and the proposed balanced mix-design) were evaluated in the laboratory. Preliminary findings are that the proposed balanced mix-design method results in a higher OAC asphalt-binder content (about 1 percent) in a mix compared to the traditional Texas gyratory method, and thus, an improvement in cracking resistance performance.
- While the Hamburg rutting performance were insignificantly different in both mix-design methods, the proposed balanced mix-design method yielded far much better laboratory crack-resistant mixes based on the Overlay test compared to the traditional Texas gyratory method. Furthermore, workability in terms of the laboratory compactive effort to achieve the desired density was better with the proposed balanced mix-design method, attributed to the increased OAC with this mix.

- However, both the constructability (workability/compactability) and laboratory performance predictions based on the two mix-design methods are yet to be evaluated and validated in field and APT testing.

### **Literature Review on Cracking Tests**

- Based on the literature reviewed, there is currently no standardized cracking test for routine mix-design and screening purposes. Like most other countries, most states in the USA hardly incorporate crack evaluation in their mix-design procedures; instead focus is on rutting and durability assessment. Texas is however, one of the few states that is striving to incorporate crack evaluation in their mix-design procedures.
- From the literature reviewed, the following cracking tests were selected for evaluation in this study:
  - 1) Uniaxial direct-tension (DT),
  - 2) Indirect-tension (IDT),
  - 3) Semi-circular bending (SCB), and
  - 4) Overlay tester (OT).
- Compared to other tests such as rutting evaluation, it must be emphasized here that HMA cracking tests by nature of their loading configuration are generally associated high variability in the test results and poor repeatability. So, due cognizance of this fact should be taken note of even in this study.
- As reported in the literature, most of the cracking tests such as the flexural and diametral fatigue are associated with high variability in the test results, with a reported coefficient of variation of over 50 percent. In fact, Carl Monismith during the SHRP study, reported a COV of around 100 percent for their bending beam fatigue tests. So, one of the primary objectives in the selected cracking tests in this study will be to optimize variability and repeatability to reasonably acceptable levels as much as it can be achieved.

### **Air Voids and X-Ray CT Scanning Tests**

- Based on the two mixes (Type B and D) evaluated during this reporting period, the X-ray CT results indicated significantly poor AV distribution and higher AV content (i.e., lowest density and weakest area) in the top and bottom 0.8-inch zone of the 6-inch diameter molded samples. Thus, trimming a minimum of 0.8-inch on either side of gyratory molded samples should be given consideration.
- To ensure uniform AV distribution and minimize edge failures in direct-tension testing, transitioning to 4- or 5-inch high by 4-inch diameter DT test specimens as opposed to the current 6-inch high may be warranted. However, caution should be exercised to meet the specimen aspect ratio and NMAS coverage requirements.

### **Cracking Test Evaluations**

- Two mixes, Types C and D, were evaluated in the laboratory using the DT, OT, IDT, and SCB tests. The results from all the tests indicated that the Type D mix had superior laboratory cracking resistance properties. Theoretically, it would therefore be expected to out-perform mix Type C in the field if all other factors are assumed to be equal.
- Based on the two mixes evaluated and the laboratory factors considered, the repeated SCB offers the best promising potential for a surrogate cracking test particularly in terms of variability and repeatability. This is seconded by the repeated IDT test with the OT being ranked third. However, the IDT test excelled in terms of simplicity and potential for practical application.
- However, unlike the OT, both the SCB and IDT are still in their infant stages of development with no established failure criteria or proven correlation with field performance. Also, the requirement for an MTS, particularly for the SCB test, may be a hindrance for industry application. The OT on other hand is a fairly portable stand-alone set-up that does not require an MTS. Likewise, most TxDOT labs and Contractors have (and/or are familiar with) the IDT test protocol, and so, would be easy to implement.
- At the time of this report, only a partial of the crack test evaluation task had been completed. Therefore, the findings reported herein are only preliminary and should not be construed as final recommendations. Research is still ongoing in terms of further developing the test protocols and testing more mixes.

- In particular, significant efforts in the ongoing research work are being directed toward modifying the OT displacement-loading rate, the 4-inch high DT, R-IDT, R-SCB, and R-DT tests. Final results and recommendations will be documented in future reports.

### **Overlay Round-Robin Tests**

A round-robin testing was conducted to evaluate and quantify the variability and repeatability associated with the Overlay Test (Tex Method 248-F). Six different laboratories (four TxDOT labs, one private [industry] lab, and TTI [research lab]) participated. A dense-graded Type D mix (5.0% PG 70-22 [Valero] plus limestone [Chico]) was used. The main findings are:

- Considering a loading rate of 0.025-inch horizontal displacement and single crack failure mode, the average number of cycles to failure was 258 with a coefficient of variation of 23 percent (which based on published literature is very reasonable for a HMA cracking tests; Carl Monismith had reported a COV of around 100 percent in their beam fatigue tests). The average lab range was 220 to 312 cycles. This level of variability is not unreasonable if a COV threshold of 30 percent is considered.
- This level of repeatability is only possible if the Overlay test equipment is properly calibrated and the technicians running the test have been adequately trained. In two cases, OT opening displacements of 0.023-inch were found during calibration instead of the recommended 0.025-inch.
- However, there were also some instances of outliers in two labs where the specimen failure mode was double cracking instead of single cracking. One specimen in each of these two labs had double cracking and lasted over 500 cycles, 1000 cycles in one lab and 708 in another lab. Incorporating these two results in the analysis shoots the COV to over 30 percent. Nonetheless, such outliers are typical expectation of any laboratory tests. Thus, the results were not unreasonable especially considering that only two out of the total of 30 specimens were off the range.
- As noted above, one important finding of this round-robin series was the need to identify double cracks. In the vast majority of cases, a single crack is formed on the top of the sample. In rare cases, two or more independent cracks are formed, which greatly

influences the number of cycles to failure. Recommendations are that such crack failure modes should be noted and reported in the analysis or preferred be excluded.

- Several variances were found in the way the different laboratories run the test. Many of these issues were resolved during the training session conducted by TTI. These variances also required TTI to make recommendations on strengthening the test protocol.
- To facilitate more standardization of the test, a comprehensive video demo has been developed at TTI, which will help in training new lab technicians.
- On problem found in the round-robin sequence is that the different Overlay tester machines are operating different software. This should be standardized before more round-robin exercises are conducted.
- One more series of round-robin tests is proposed where the different labs are supplied samples of a mix with known poor OT performance. In these tests, the labs will be responsible for gluing and testing the samples. To this end, a joint meeting with CST and the participating labs is strongly recommended to discuss the way forward.
- Overall, the results obtained from the round-robin testing indicated that there is potential that the OT variability and repeatability can be optimized to reasonably acceptable levels, with careful work (sample preparation, etc) and adherence to the test specification and procedures.

### **Workability and Compactability Indicator Tests**

- Two mixes, Types B and D, were evaluated for workability and compactability assessment based on the Pine and Servopac gyratory compactors, respectively. At 92 percent target density, the Type B mix required less compaction energy compared to the Type D mix. However, during service life, the Type D mix would require less densification energy compared to the Type B mix. In terms of workability and compactability, the Type D mix exhibited more sensitivity to changes in the asphalt-binder content than the Type B mix.
- For the two mixes evaluated, the compaction indices have exhibited sensitivity to aggregate gradation and asphalt-binder content. However, no changes were noticed due to apparatus change, i.e., both the Pine and Servopac gyratory compactors yielded similar results.

- As theoretically expected, increasing the asphalt-binder content tends to reduce the energy required to compact the mixes, i.e., it makes the mixes more compactable.
- Based on the preliminary evaluation of these two mixes (Types B and D), the compaction energy index is suggested as a potential index for workability measurements of the mixes while the traffic densification index (TDI 92-98) is suggested as a potential parameter for compactability measurements.
- At the time of this report, only two mixes (Types B and D) had been evaluated. Therefore, the findings reported herein are only preliminary and are subject to change as more mixes are evaluated. Additionally, significant efforts will also be directed towards evaluating other compaction parameters. Final results and recommendations will be documented in future reports.

### **Field Mix-Design Evaluations and APT Testing**

- A Type C mix with PG 76-22 asphalt-binder (Valero) and limestone aggregates (Brownwood) was placed as the surfacing HMA layer at the LTRC test site in Louisiana for APT testing. The intent of the APT tests is to evaluate and validate two mix-design methods, namely the Texas gyratory and the proposed balanced mix-design, by way of comparing with laboratory performance predictions (rutting and cracking).
- Two OAC designs based on the Texas gyratory and balanced mix-design methods, namely the “Control” at 4.13 percent QC asphalt-binder content and the “Modified” at 5.1 percent QC asphalt-binder content, were utilized and placed at the APT test sections.
- Construction of the APT test sections was completed during this reporting period. Construction QC tests were conducted and included IR thermal imaging, nuclear density measurements, GPR measurements, and coring for forensic evaluations.
- No significant differences in the constructability characteristics such as workability and compactability were observed between the “Control” (Texas gyratory method) and the “Modified” (proposed balanced mix-design) mixes.
- Planned APT tests for evaluating the mix-design methods and the Type C mix include rutting and cracking (fatigue and reflection). These APT tests are currently ongoing and will be documented in future reports.

## **ONGOING AND FUTURE PLANNED WORKS**

A summary of the ongoing and future planned work is shown in Table 9-1 and includes that the status update of each task as of September 2009.

## **PRODUCT DELIVERABLES**

The required product deliverable from this research project, designated as 0-6132-P1 and entitled “New HMA Mix Design procedure for Texas (Modeling of the HMA in APT Experimentation)” is due to TxDOT on August 31, 2012. However, recommendations for the preliminary procedure will be developed by October 2010. This will continue to be evaluated through out the duration of this study.

**Table 9-1. List of Currently Ongoing and Future Planned Works.**

<b>Task#</b>	<b>Description</b>	<b>%age Done as of 09/09</b>	<b>Actual Work Done as of 09/09</b>	<b>Ongoing and Planned Work</b>
1	Literature search/test protocols	80%	Test protocol development for SCB, IDT, DT, and OT	1) Repeated IDT & SCB tests; 2) Analysis models; 3) Stiffness reduction conception; 4) Other mix-design procedures & test methods
2	Kick-off meeting	100%	Meeting 10/08	None
3a	Cracking testing and evaluation	45%	-OT, DT, IDT, & SCB testing of Type C and D mixes -Repeated IDT & SCB testing of Type B & D mixes -Preliminary evaluation & ranking of the tests	1) Testing of more mixes, namely Type C mixes & plant-mix from the APT site; 2) Conduct repeated DT, IDT, & SCB tests & develop tentative failure criteria; 3) Comparative evaluation & final recommendation of a surrogate cracking test
3b	AV characterization	60%	X-ray CT scanning of Type B and D molded samples	1) Type C molded samples & also to consider different asphalt-binder contents 2) Investigate viability of using 4 inch-high specimens for DT testing
3c	Overlay round-robin testing & revisions to Tex-248-F spec	100%	-Testing Type D mix in 6 different labs -Revising spec -Video shooting of sample prep. & testing procedures	-None, awaiting joint meeting with CST & participating labs on way forward -Recommends another round of round-robin testing with different mix
4	Workability indicator	50%	-Testing & evaluation of Type B & D mixes -Preliminary recommendations on indicators	1) Testing & evaluation of more mixes (Type C) & plant-mixes from the APT site and NCAT; 2) Final development of workability & compactability indices; 3) Investigations of the effects of internal microstructure distribution on mix compactability.
5	Lab test program	45%	Mix-designs & test matrix	1) Completion of Tasks# 3 & 4; 2) Testing of plant-mix from the APT site; 3) Testing raw materials & plant-mixes for materials from Task# 6
6	Eight field test sections in Texas	0%	-	Liaison with Districts to select (and/or construct) field sections; Houston, Childress, & Atlanta are potential candidates
7	APT plan & construction	100%	Design & base construction	None
8	APT test program	20%	Test plan & 1 <sup>st</sup> half of rutting tests	1) Complete rutting & cracking tests; 2) Data analysis
9	Mix-design recommendations	0%	-	Due to TxDOT 08/31/2012
10	TxDOT spec. modifications	0%	-	Due to TxDOT on 08/31/2012
11	Technical & summary reports	25%	Year 1 report	Next report to be submitted after completion of APT testing



## REFERENCES

- Bahia, H., Friemel, T., Peterson, P., and Russell, J., (1998). "Optimization of Constructability and Resistance to Traffic: A New Design Approach for HMA Using the Superpave Compactor." *Journal of the Association of Asphalt Paving Technologists* V.67-98, p.189.
- Butcher, M., (1998). "Determining Gyratory Compaction Characteristics Using Servopac Gyratory Compactor" *Transportation Research Record*, p. 1630.
- Buttlar, William G., Roque, Reynaldo, Kim, Namho, (1996). "Accurate Asphalt Mixture Tensile Strength." *Proceedings of the Materials Engineering Conference*, Vol. 1, 163-172.
- DeSombre, R., Chadbourn, B., Newcomb, D.E., Voller, V., (1998). "Parameters to Define The Laboratory Compaction Temperature Range of Hot-Mix Asphalt." *Journal of the Association of Asphalt Paving Technologists* p. 67.
- Gauer, M. (1996). "Compaction of Asphalt in the Darmstadt Gyratory Compactor." International Workshop on the Use of the Gyratory Shear Compactor, LCPC, Nantes, France.
- Guler, M., Bahia, H. U., Bosscher, P. J., Plesha, M. E., (2000). "Device for Measuring Shear Resistance of Hot-Mix Asphalt in the Gyratory Compactor." *Transportation Research Record*, Journal of the Transportation Research Board 1723, pp. 116-124.
- Hofman, R., Oosterbaan, B., Erkens, S.M.J.G., Van der Kooij, J., (2003). "Semi-Circular Bending Test to Assess the Resistance Against Crack Growth." Paper presented at the proceedings of the 6<sup>th</sup> International Rilem Symposium in Zurich, Switzerland, pp. 257-263.
- Huang, Baoshan, Shu, Xiang, Tang, Yongjing, (2005). "Comparison of Semicircular Bending and Indirect Tensile Strength Tests for HMA Mixtures." *American Society of Civil Engineers Geotechnical Special Publication*, Issue 130-142, pp. 177-188.
- Huang, Likui, Cao, Keming, Zeng, Menglan, (2009) "Evaluation of Semicircular Bending Test for Determining Tensile Strength and Stiffness Modulus of Asphalt Mixtures." *Journal of Testing and Evaluation*, Vol. 37, pp. 122-128.
- Kim, R., Wen, H., (2002). "Fracture Energy from Indirect Tension Testing," *Journal of the Association of Asphalt Paving Technologists*, Vol. 71, pp. 779-793.
- Kumar, A., Goetz W., (1974). "The Gyratory Testing Machine as a Design Tool and Instrument for Bituminous Mixture Evaluation." *Asphalt Paving Technology*, 43, pp. 351-371.

Mallick, R.B., (1999). "Use Of Superpave Gyratory Compactor To Characterize Hot-Mix Asphalt." *Transportation Research Record - Journal of the Transportation Research Board* 1681.

Marasteanu, M.O., Velasquez, R., Herb, W., Tweet, J., Turos, M., Watson, M., Stefan, H.G., (2008). "Determination of Optimum Time for the Application of Surface Treatments to Asphalt Concrete Pavements - Phase II," MnDOT Research Consortium Report, MN/RC 2008-16.

Masad, E., Kassem, E., Chowdhury, A., (2009). "Application of Imaging Technology to Improve the Laboratory and Field Compaction of HMA." Technical Research Report FHWA/TX-09/0-5261-1.

McRea, J. L., (1965). "Gyratory Testing Machine Technical Manual." Engineering Developments Company, Inc. Vicksburg, MS, 2.

Molenaar, A.A.A., Scarpas, A., Liu, X., Erkens, S.M.J.G., (2002). "Semi-Circular Bending Test; Simple but Useful?" *Journal of the Association of Asphalt Paving Technologists*, Vol. 71, pp. 794-815.

Moutier, F., (1997). "Gyratory Compactor (GC or PCG) Justification of its Use in the French Mix Design." Paper presented in the Superpave Asphalt Mixture Expert Task Group.

Rand, D. A., (1997). "Comparative Analysis of Superpave Gyratory Compactors and TxDOT Gyratory Compactors." Master Thesis, University of Texas, Austin, TX.

Ruth, B. E., Shen, X. and Wang, L. H., (1991). "Gyratory Evaluation of Aggregate Blends to Determine Their Effects on Shear Resistance and Sensitivity to Asphalt Content." STP 1147, American Society for Testing Materials.

SHRP (1994), "Level One Mix Design: Material Selection, Compaction, and Conditioning" SHRP-A-408, Strategic Highway Research Program, National Research Council, DC.

Sigurjonsson, S., Ruth, B.E., (1990). "Use of Gyratory Testing Machine To Evaluate Shear Resistance Of Asphalt Paving Mixture." *Transportation Research Record* p. 1259.

Tex-200-F, Sieve Analysis of Fine and Coarse Aggregates, 2004.

Tex-205-F, Laboratory Method of Mixing Bituminous Materials, 2005

Tex-226-F, Indirect Tensile Strength Test, 2004.

Tex-241-F, Superpave Gyratory Compacting of Test Specimens of Bituminous Materials, 2009

Tex-248-F, Overlay Test, 2009.

## APPENDIX A: AGGREGATE GRADATIONS

**Table A-1. Aggregate Gradation for Type D Mix.**

	<b>Sieve Size</b>	<b>TxDOT Specification</b>		<b>Percent passing</b>
	<i>mm</i>	<i>Lower Limit</i>	<i>Upper Limit</i>	
¾"	19	100	100	100
½"	12.5	98	100	100
3/8"	9.5	85	100	99.2
# 4	4.75	50	70	63.8
# 8	2.36	35	46	38.2
# 30	0.6	15	29	16.8
# 50	0.3	7	20	11.7
# 200	0.075	2	7	3.3

**Table A-2. Aggregate Gradation for Type B Mix.**

	<b>Sieve Size</b>	<b>TxDOT Specification</b>		<b>Percent passing</b>
	<i>mm</i>	<i>Lower Limit</i>	<i>Upper Limit</i>	
1-1/2"	37.5	100	100	100
1"	25	98	100	100
¾"	19	84	98	97.3
3/8"	9.5	60	80	76.9
# 4	4.75	40	60	44.6
# 8	2.36	29	43	32.9
# 30	0.6	13	28	16.1
# 50	0.3	6	20	11.3
# 200	0.075	2	7	2.1

## APPENDIX A: AGGREGATE GRADATIONS (CONTINUED)

**Table A-3. Aggregate Gradation for Type C (Hunter) Mix.**

	<b>Sieve Size</b>	<b>TxDOT Specification</b>		<b>Percent passing</b>
	<i>mm</i>	<i>Lower Limit</i>	<i>Upper Limit</i>	
1"	25	100	100	100
3/4"	19	95	100	100
3/8"	9.5	70	85	80.4
# 4	4.75	43	63	52.7
# 8	2.36	32	44	37.3
# 30	0.6	14	28	16.9
# 50	0.3	7	21	11.8
# 200	0.075	2	7	5

**Table A-4. Aggregate Gradation for Type C (Jones) Mix.**

	<b>Sieve Size</b>	<b>TxDOT Specification</b>		<b>Percent passing</b>
	<i>mm</i>	<i>Lower Limit</i>	<i>Upper Limit</i>	
7/8"	22.6	98	100	100
5/8"	16	95	100	98.5
3/8"	9.5	70	85	79.1
# 4	4.75	43	63	54.1
# 10	2	30	40	32.2
# 40	0.42	10	25	13.9
# 80	0.177	3	13	10
# 200	0.075	1	6	5.9

## APPENDIX A: AGGREGATE GRADATIONS (CONTINUED)

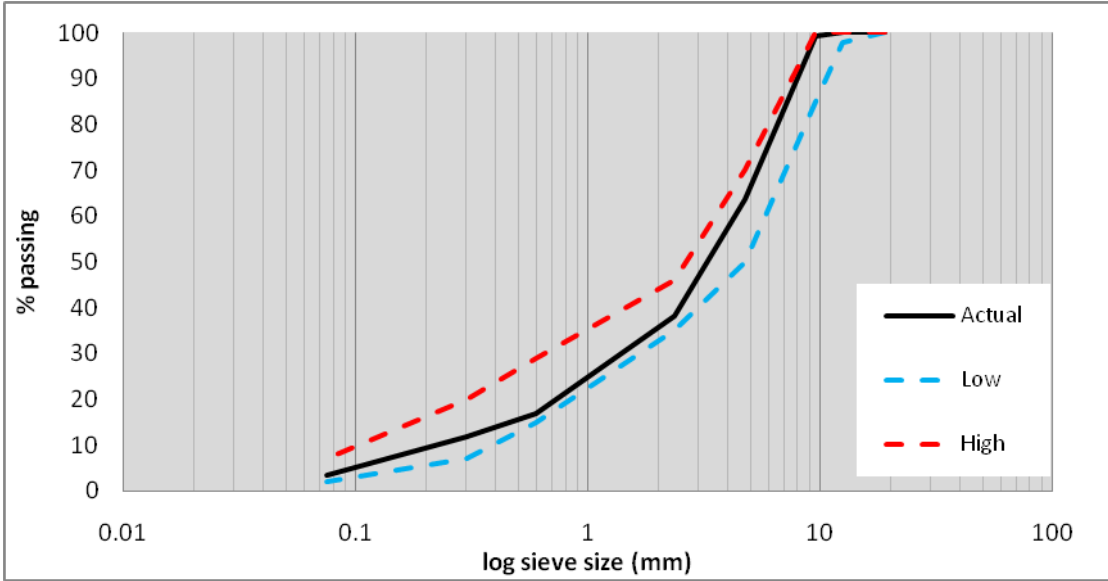
**Table A-5. Aggregate Gradation for Type C (Beaumont-Original) Mix.**

Sieve Size	TxDOT Specification			Percent passing
	<i>mm</i>	<i>Lower Limit</i>	<i>Upper Limit</i>	
1"	25.00	100.0	100.0	100.0
3/4"	19.00	95.0	100.0	99.3
3/8"	9.50	70.0	85.0	79.0
No. 4	4.75	43.0	63.0	51.8
No. 8	2.36	32.0	44.0	36.6
No. 30	0.60	14.0	28.0	23.0
No. 50	0.30	7.0	21.0	12.2
No. 200	0.08	2.0	7.0	2.1

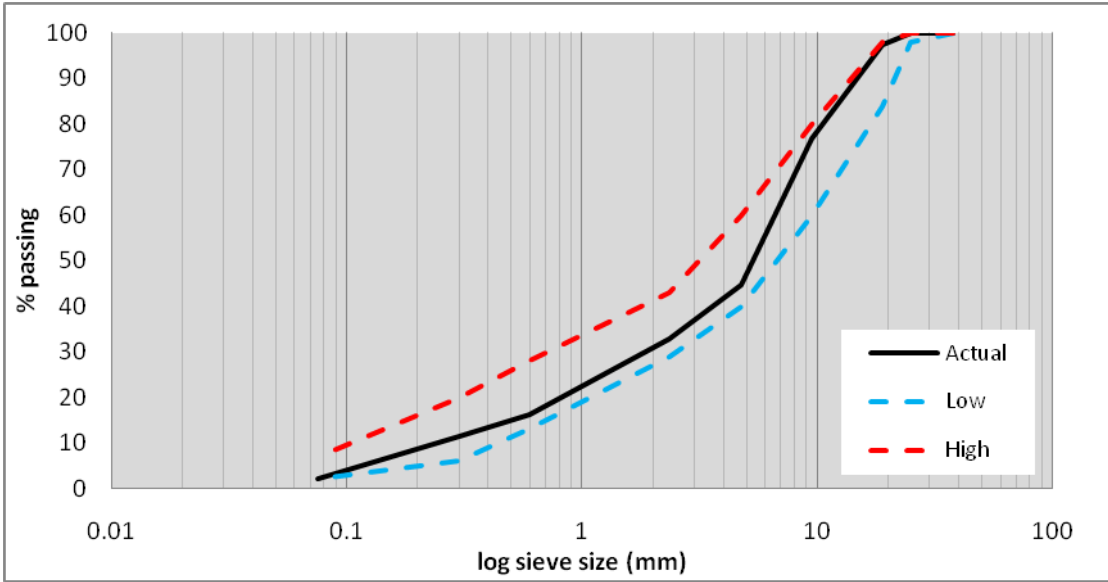
**Table A-6. Aggregate Gradation for Type C (Beaumont-Modified) Mix.**

Sieve Size	TxDOT Specification			Percent passing
	<i>mm</i>	<i>Lower Limit</i>	<i>Upper Limit</i>	
1"	25.00	100.0	100.0	100.0
3/4"	19.00	95.0	100.0	99.6
3/8"	9.50	70.0	85.0	81.9
No. 4	4.75	43.0	63.0	58.7
No. 8	2.36	32.0	44.0	39.0
No. 30	0.60	14.0	28.0	18.6
No. 50	0.30	7.0	21.0	9.6
No. 200	0.08	2.0	7.0	2.5

**APPENDIX A: AGGREGATE GRADATIONS (CONTINUED)**

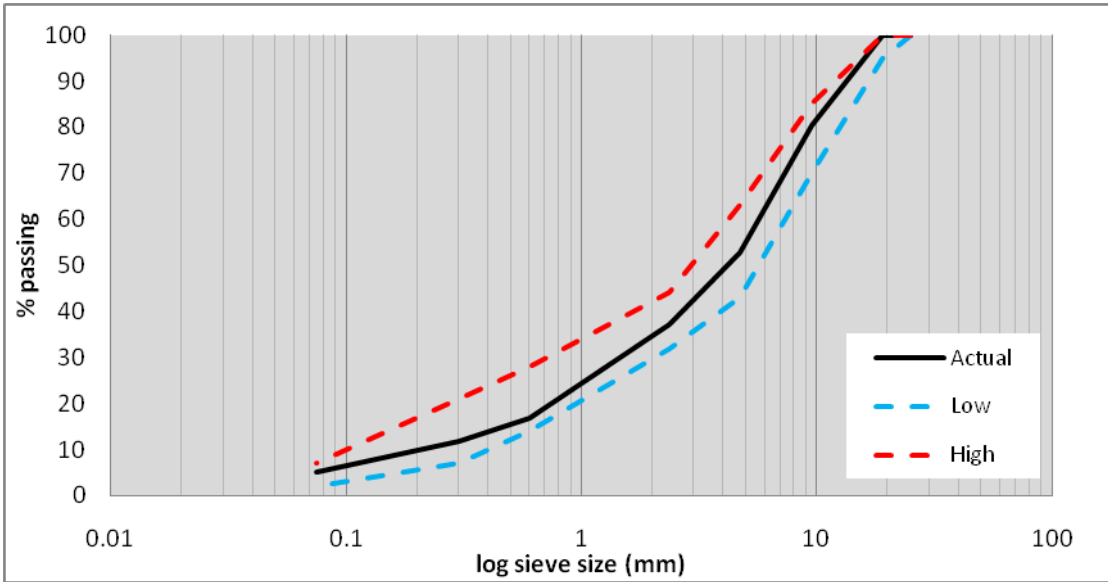


**Figure A-1. Type D Mix Gradation Curve.**

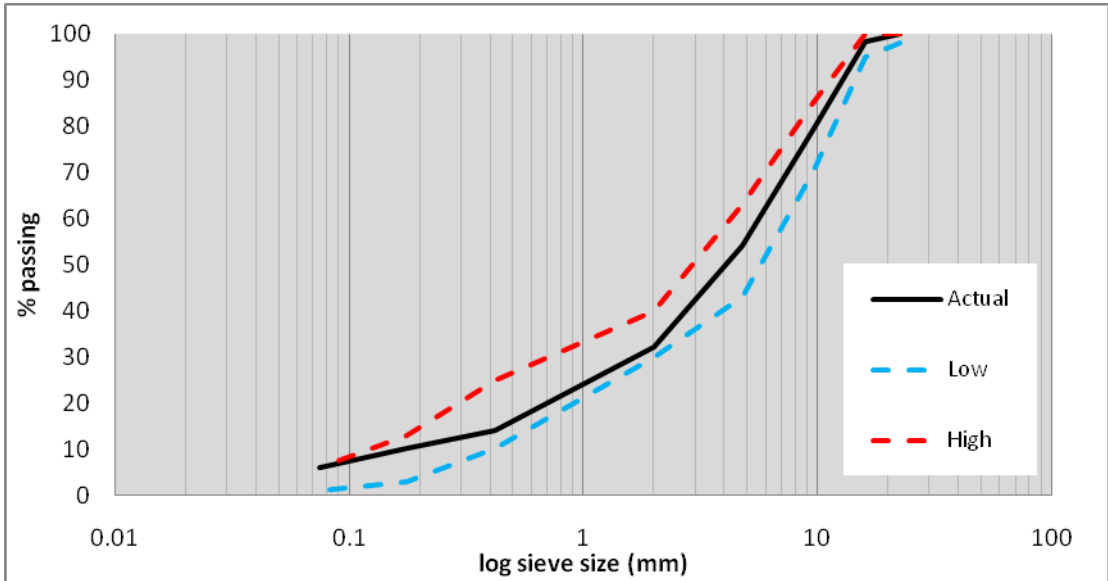


**Figure A-2. Type B Mix Gradation Curve.**

**APPENDIX A: AGGREGATE GRADATIONS (CONTINUED)**

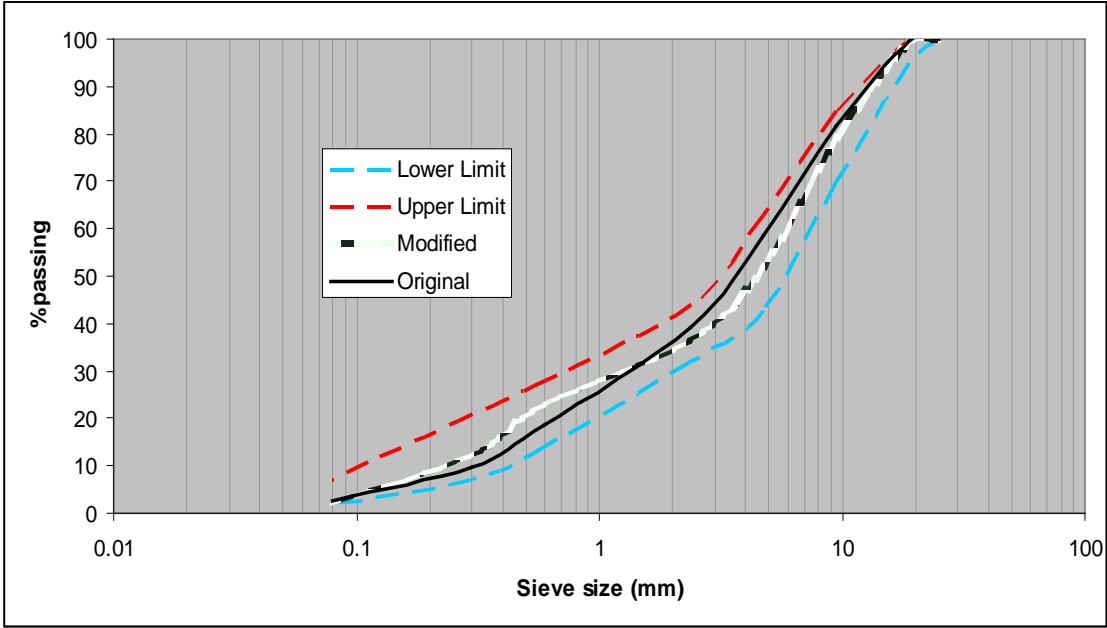


**Figure A-3. Type C (Hunter) Mix Gradation Curve.**



**Figure A-4. Type C (Jones) Mix Gradation Curve.**

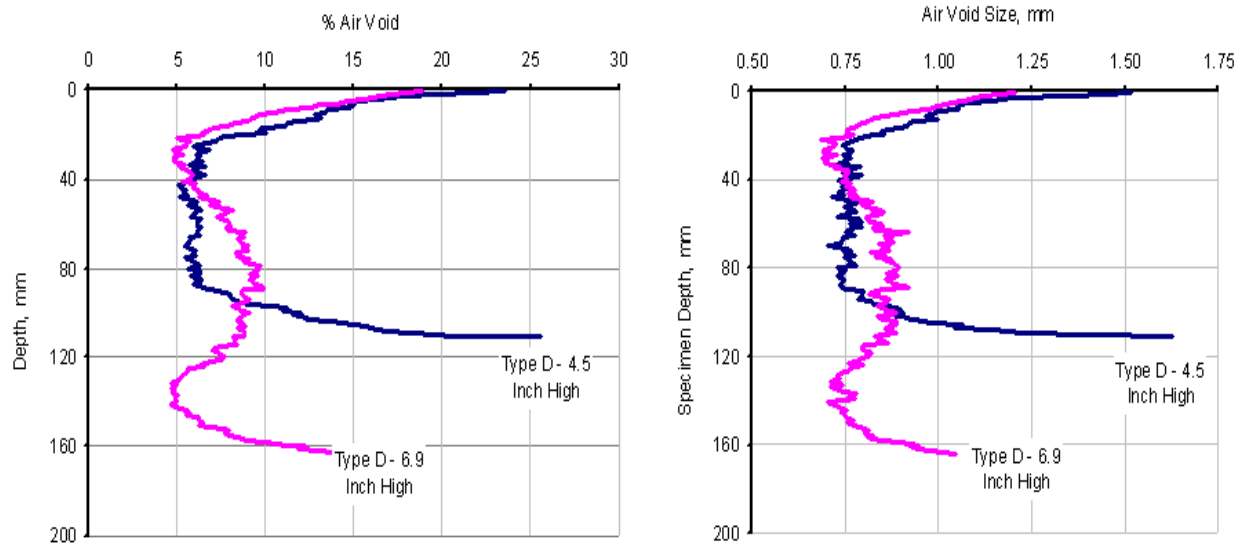
**APPENDIX A: AGGREGATE GRADATIONS (CONTINUED)**



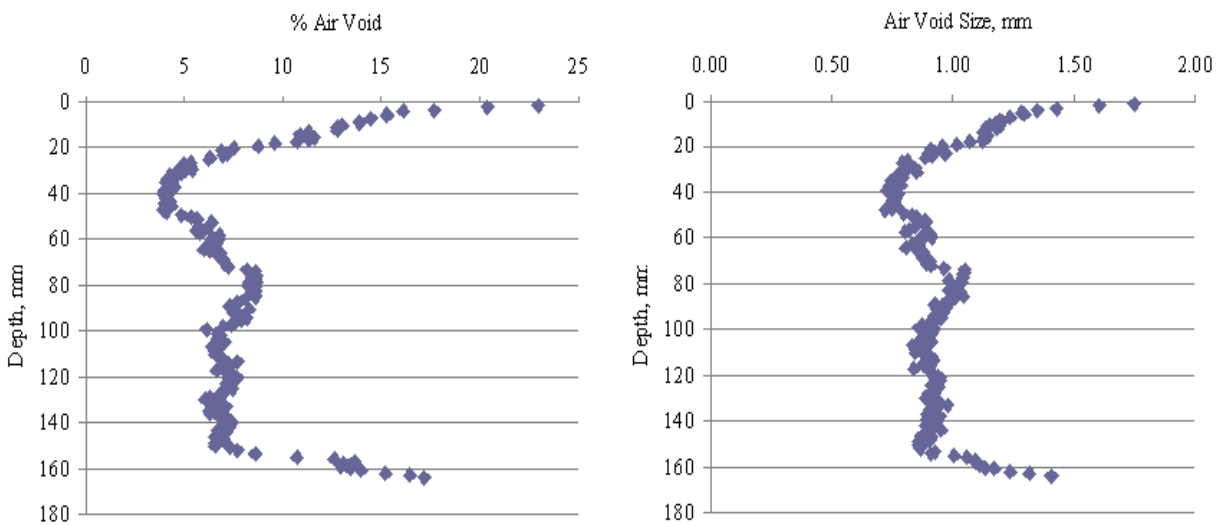
**Figure A-5. Type C (Beaumont) Mix Gradation Curve.**



## APPENDIX B: AIR VOID DISTRIBUTION

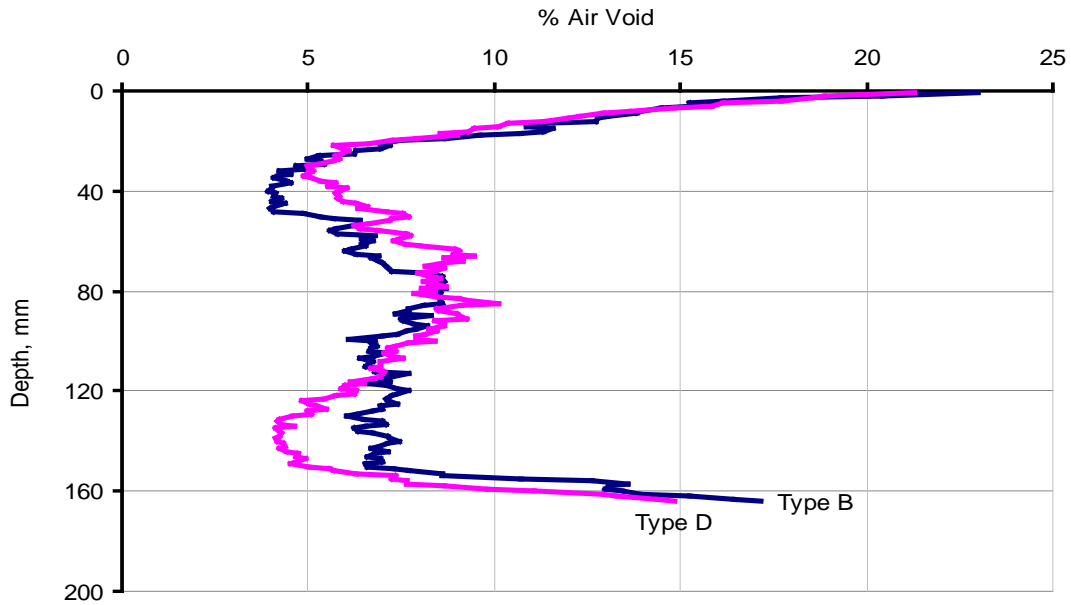


**Figure B-1. Example AV Distribution Comparison for the Type D 4.5- and 6.9-Inch High Molded Samples.**

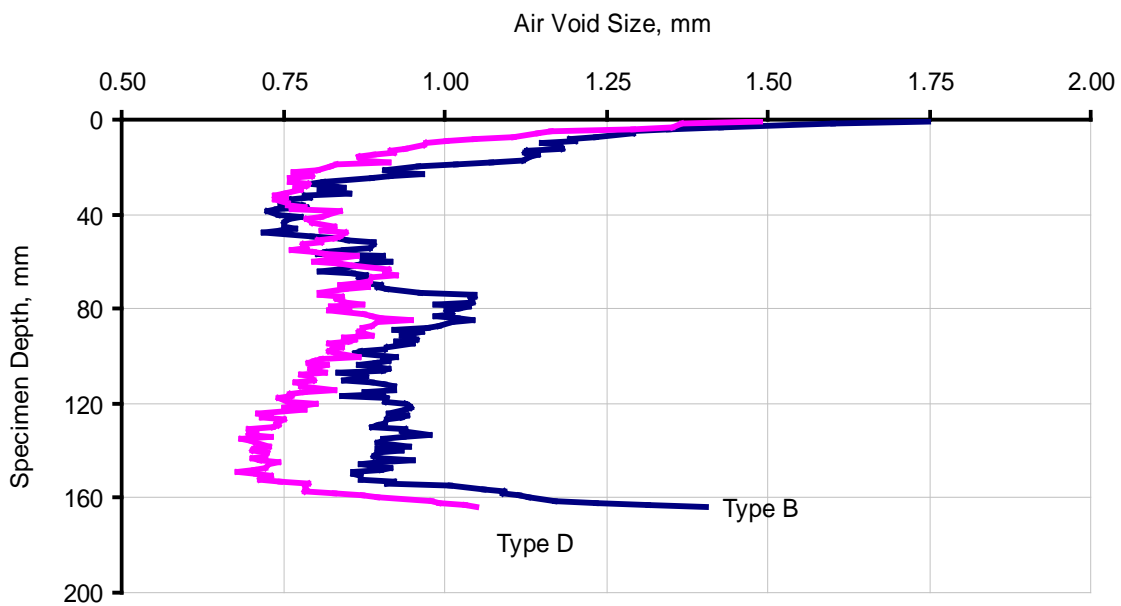


**Figure B-2. Example of Poor AV Distribution in a Type B 6.0-Inch  $\phi$  by 6.9-Inch High Molded Sample (Suggests Vertical Segregation).**

## APPENDIX B: AIR VOID DISTRIBUTION (CONTINUED)

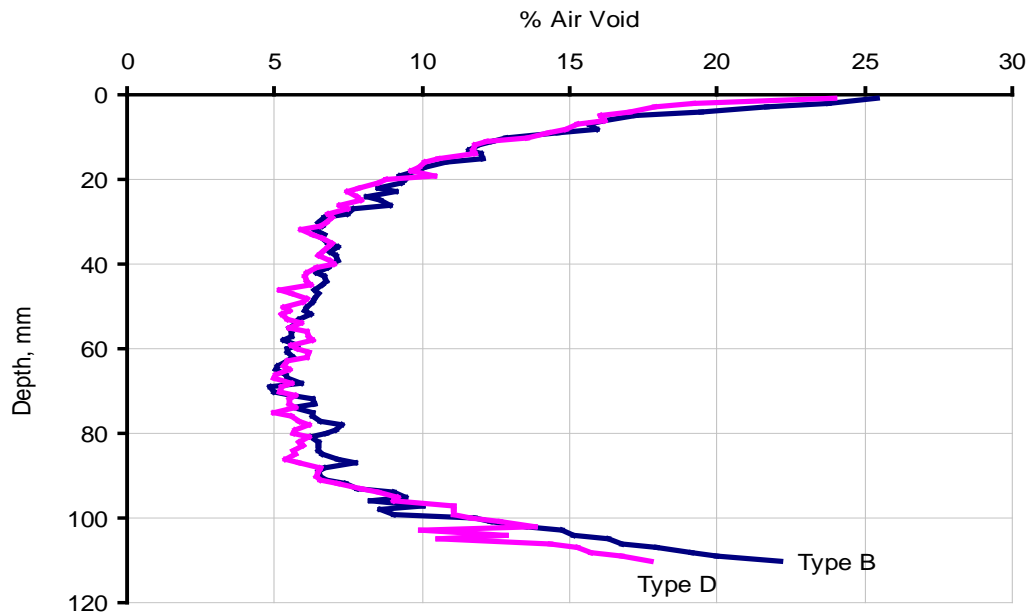


**Figure B-3. Example Percent AV Distribution for 6-Inch  $\phi$  by 6.9-Inch High Molded Samples.**

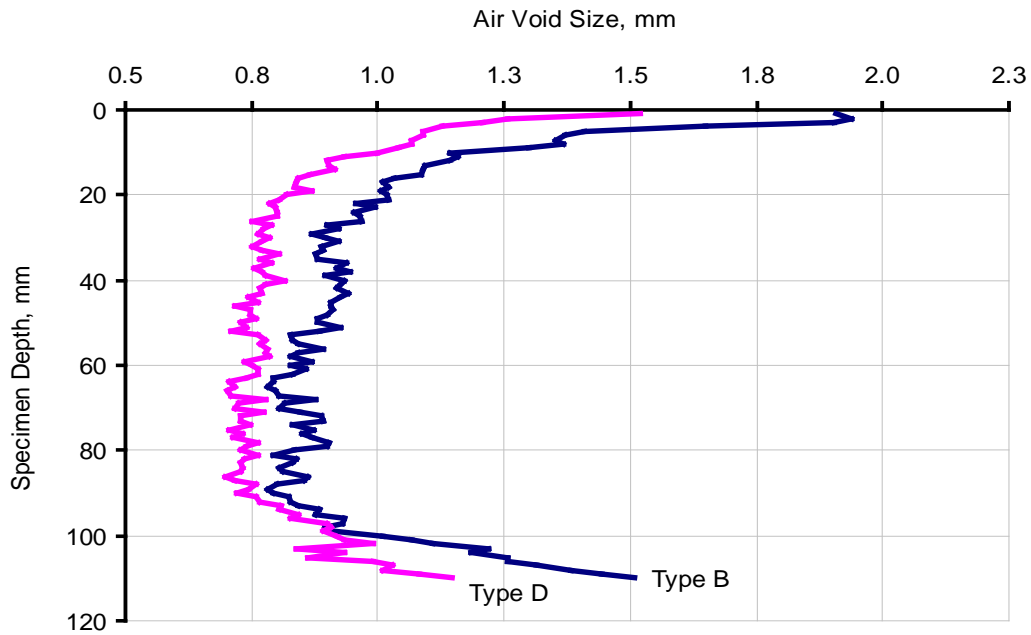


**Figure B-4. Example AV Size Distribution for 6-Inch  $\phi$  by 6.9-Inch High Molded Samples.**

## APPENDIX B: AIR VOID DISTRIBUTION (CONTINUED)



**Figure B-5. Example Percent AV Distribution for 6-Inch  $\phi$  by 4.5-Inch High Molded Samples.**



**Figure B-6. Example AV Size Distribution for 6-Inch  $\phi$  by 4.5-Inch High Molded Samples.**



## APPENDIX C: CRACKING TEST RESULTS

**Table C-1. Type D OT1 Results @ OAC.**

OAC	Sample ID	AV	Initial OT load (lb)	N <sub>f</sub>
5.0%	D3	7.4%	692	259
5.0%	D4	6.9%	657	301
5.0%	D6	7.7%	562	325
5.0%	D7	7.4%	652	203
5.0%	D8	7.1%	601	284
<i>Average:</i>		7.3%	633	274
<i>StDev:</i>		0.3%	51	47
<i>COV:</i>		4.2%	8.1%	17.0%

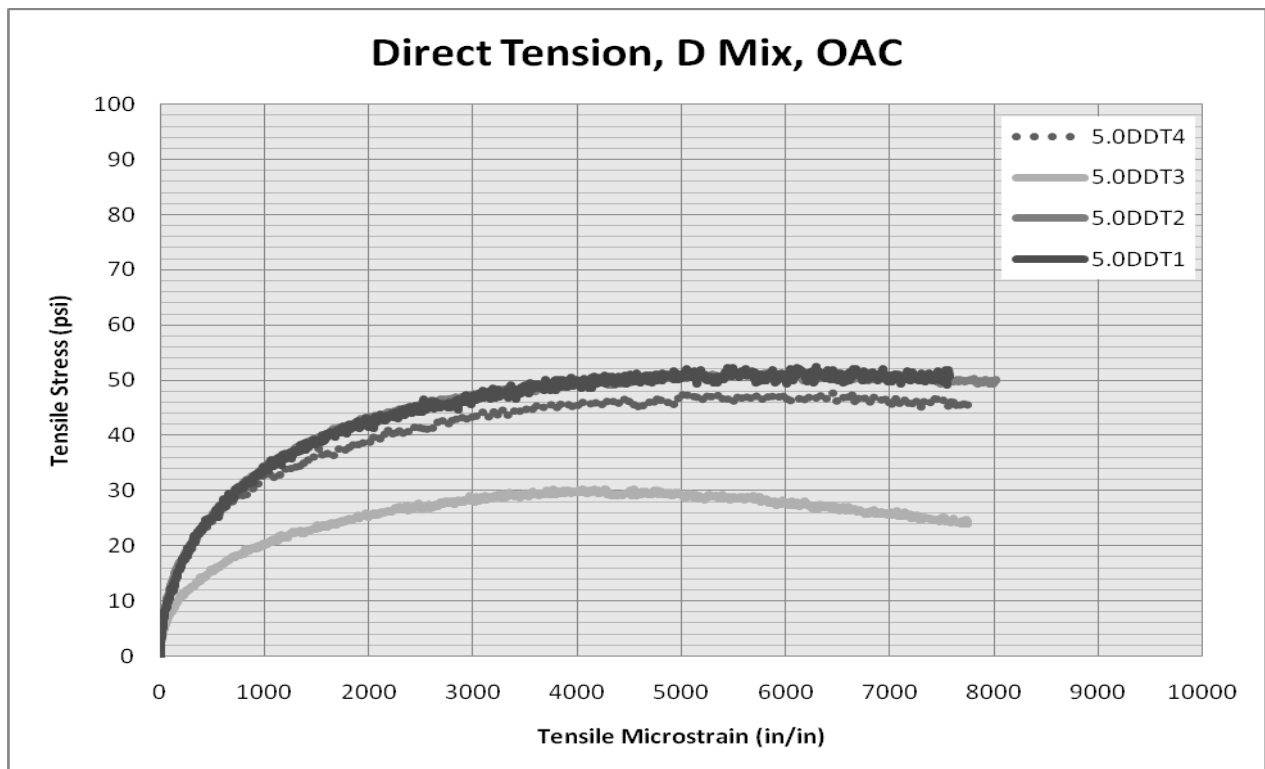
**Table C-2. Type CL OT1 Results @ OAC.**

OAC	Sample ID	AV	Initial OT load (lb)	N <sub>f</sub>
4.9%	C1	6.8%	771	40
4.9%	C2	7.3%	790	30
4.9%	C3	7.0%	705	43
<i>Average:</i>		7.0%	755	38
<i>StDev:</i>		0.3%	45	7
<i>COV:</i>		3.6%	5.9%	18.1%

## APPENDIX C: CRACKING TEST RESULTS (CONTINUED)

**Table C-3. Type D 6-Inch DT Results @ OAC.**

OAC	Sample ID	AV	Max Applied Load (lbf)	Max Tensile Stress (psi)	Microstrain @ Max Load (in/in)	Failure
5.0%	5.0DDT1	6.6%	660	53	6288	Outside LVDTs
5.0%	5.0DDT2	7.0%	646	51	5604	Outside LVDTs
5.0%	5.0DDT3	6.7%	381	30	4056	Middle
5.0%	5.0DDT4	6.7%	601	48	6452	Outside LVDTs
<i>Average:</i>		6.7%	572	46	5600	
<i>StDev:</i>		0.2%	130	10	1093	
<i>COV:</i>		3.00%	22.68%	22.68%	19.51%	

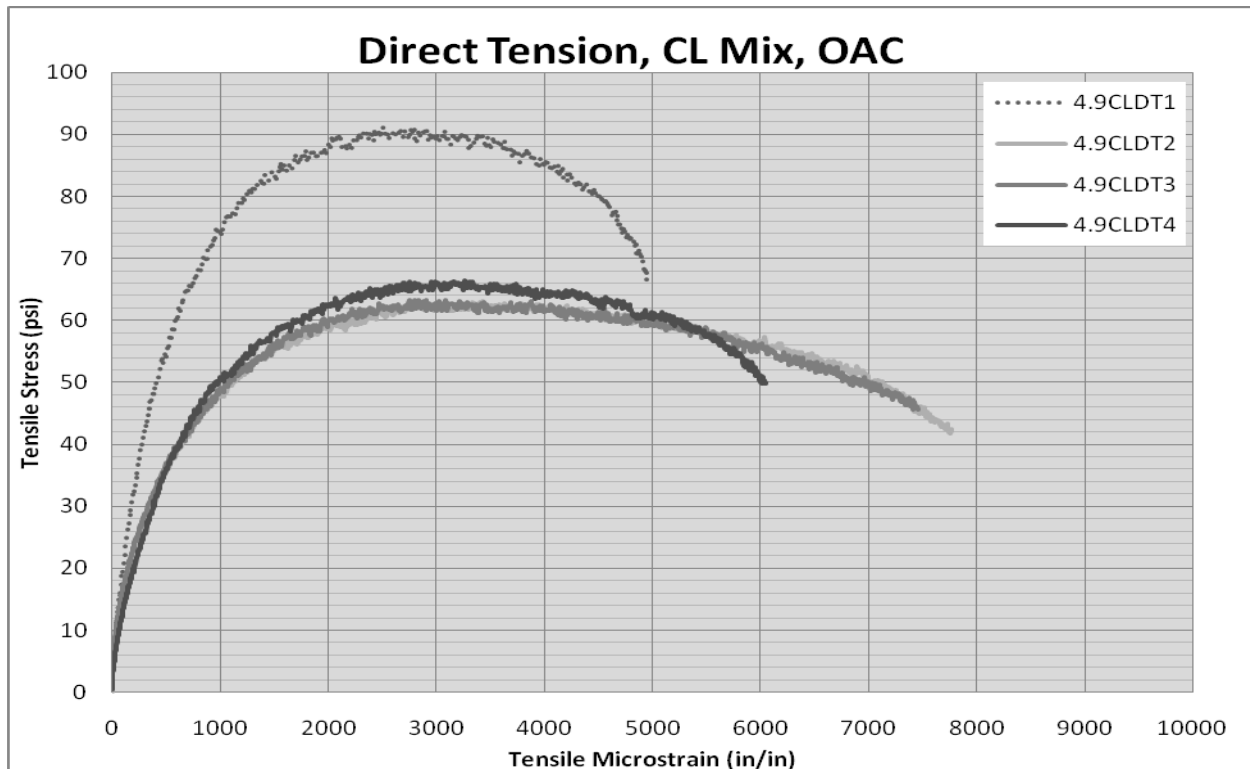


**Figure C-1. Type D 6-Inch DT Stiffness Response @ OAC.**

## APPENDIX C: CRACKING TEST RESULTS (CONTINUED)

**Table C-4. Type CL 6-Inch DT Results @ OAC.**

OAC	Sample ID	AV	Max Applied Load (lbf)	Max Tensile Stress (psi)	Microstrain @ Max Load (in/in)	Failure
4.9%	4.9CLDT1	6.5%	1147	91	2506	Outside LVDTs
4.9%	4.9CLDT2	6.8%	793	63	3024	Outside LVDTs
4.9%	4.9CLDT3	6.7%	796	63	2841	Outside LVDTs
4.9%	4.9CLDT4	6.6%	835	66	3262	Outside LVDTs
<i>Average:</i>		6.7%	893	71	2908	
<i>StDev:</i>		0.1%	171	14	319	
<i>COV:</i>		1.69%	19.14%	19.14%	10.97%	



**Figure C-2. Type CL 6-Inch DT Stiffness Response @ OAC.**

## APPENDIX C: CRACKING TEST RESULTS (CONTINUED)

**Table C-5. Type D 4-Inch DT Results @ OAC.**

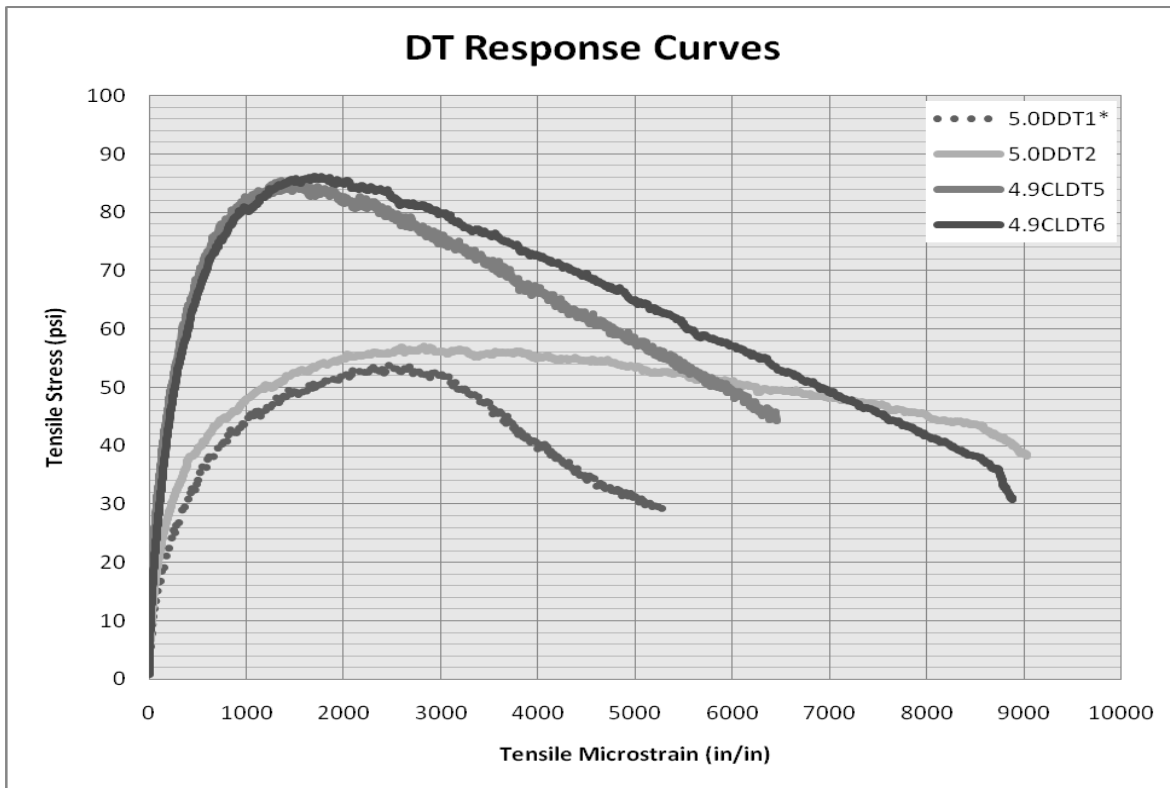
OAC	Sample ID	AV	Max Applied Load (lbf)	Max Tensile Stress (psi)	Microstrain @ Max Load (in/in)	Failure
5.0%	5.0DDT1	6.2%	677	54	2341	Lower end cap
5.0%	5.0DDT2	6.0%	716	57	2826	Inside 2/3 LVDTs
<i>Average:</i>		6.1%	697	55	2583	
<i>StDev:</i>		0.1%	28	2	343	
<i>COV:</i>		1.85%	3.98%	3.98%	13.29%	

**Table C-6. Type CL 4-Inch DT Results @ OAC.**

OAC	Sample ID	AV	Max Applied Load (lbf)	Max Tensile Stress (psi)	Microstrain @ Max Load (in/in)	Failure
4.9%	4.9CLDT5	6.2%	1074	86	1356	Middle
4.9%	4.9CLDT6	6.1%	1083	86	1702	Middle
<i>Average:</i>		6.1%	1078	86	1529	
<i>StDev:</i>		0.1%	6	0	244	
<i>COV:</i>		1.50%	0.56%	0.56%	15.99%	



## APPENDIX C: CRACKING TEST RESULTS (CONTINUED)



**Figure C-3. Type D & CL 4-Inch DT Stiffness Response @ OAC.**

**Table C-7. Type D IDT Results @ OAC.**

OAC	Sample ID	AV	Max Applied Load (lbf)	Max Tensile Stress (psi)	Horizontal Strain @ Max Load (in)
5.0%	5.0DIDT1	7.2%	1783	95	0.021
5.0%	5.0DIDT2	7.4%	1974	105	0.013
5.0%	5.0DIDT3	6.6%	1825	97	0.018
5.0%	5.0DIDT4	7.5%	1935	103	0.015
<i>Average:</i>		7.2%	1879	100	0.017
<i>StDev:</i>		0.4%	90	5	0.004
<i>COV:</i>		5.65%	4.79%	4.79%	20.83%

## APPENDIX C: CRACKING TEST RESULTS (CONTINUED)

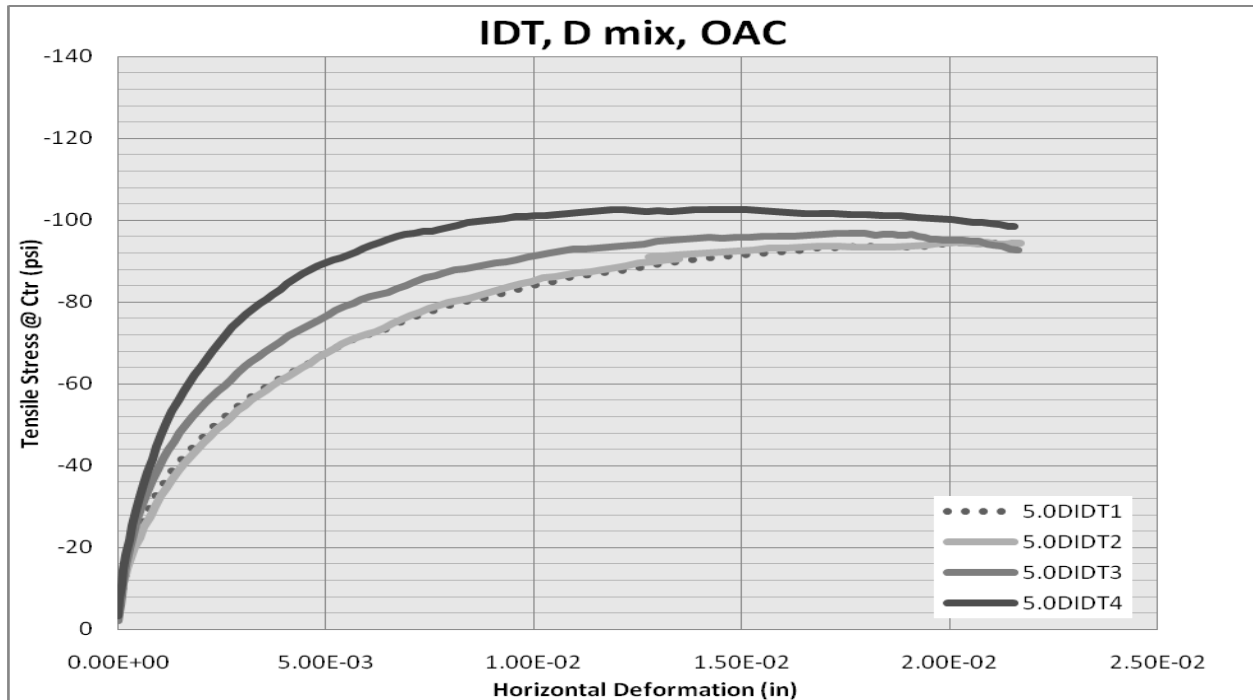
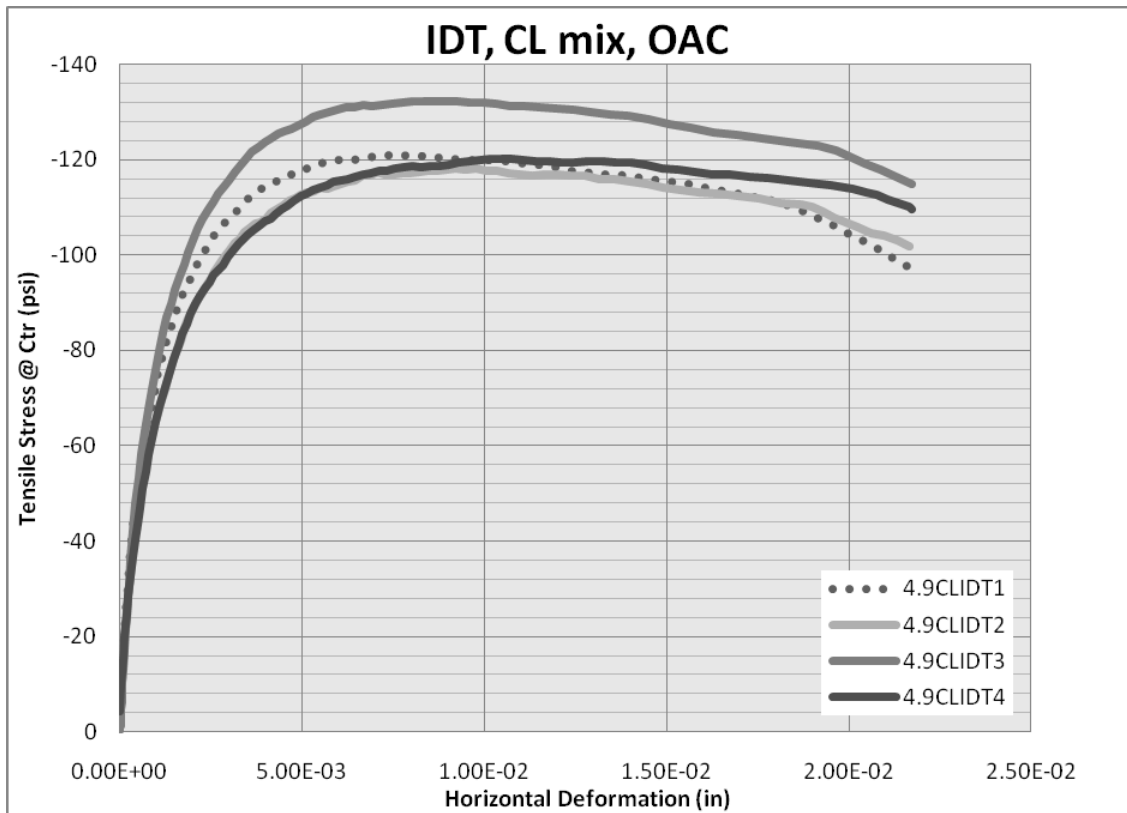


Figure C-4. Type D IDT Stiffness Response @ OAC.

Table C-8. Type CL IDT Results @ OAC.

OAC	Sample ID	AV	Max Applied Load (lbf)	Max Tensile Stress (psi)	Horizontal Strain @ Max Load (in)
4.9%	4.9CLIDT1	7.4%	2278	121	0.008
4.9%	4.9CLIDT2	7.2%	2224	118	0.010
4.9%	4.9CLIDT3	6.7%	2493	132	0.008
4.9%	4.9CLIDT4	7.5%	2265	120	0.010
Average:		7.2%	2315	123	0.009
StDev:		0.4%	121	6	0.001
COV:		4.89%	5.22%	5.22%	13.30%

## APPENDIX C: CRACKING TEST RESULTS (CONTINUED)



**Figure C-5. Type CL IDT Stiffness Response @ OAC.**

**Table C-9. Type D SCB Results @ OAC.**

OAC	Sample ID	AV	Max Applied Load (lbf)	Max Tensile Stress (psi)	Ram Disp @ Max Load (in)
5.0%	5.0DSCB1	7.1%	355	129	0.108
5.0%	5.0DSCB2	7.3%	357	130	0.116
5.0%	5.0DSCB3	7.1%	330	120	0.073
5.0%	5.0DSCB4	7.4%	340	124	0.126
Average:		7.2%	346	126	0.106
StDev:		0.2%	13	4	0.023
COV:		2.68%	3.64%	3.58%	21.76%

## APPENDIX C: CRACKING TEST RESULTS (CONTINUED)

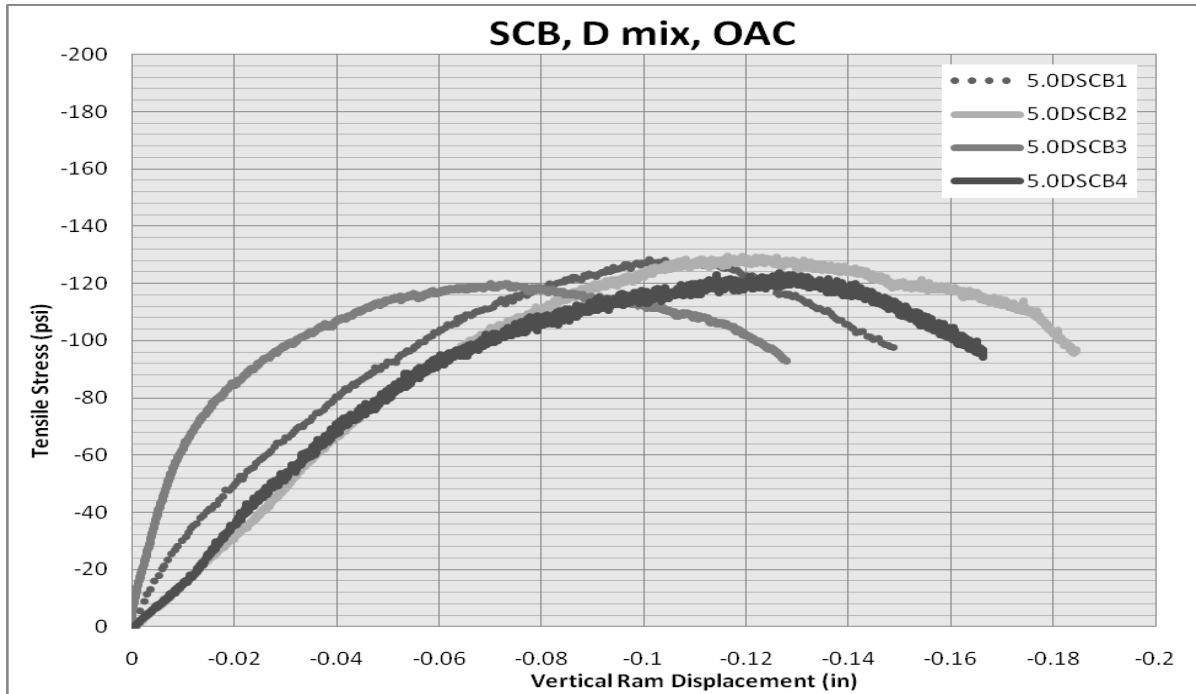
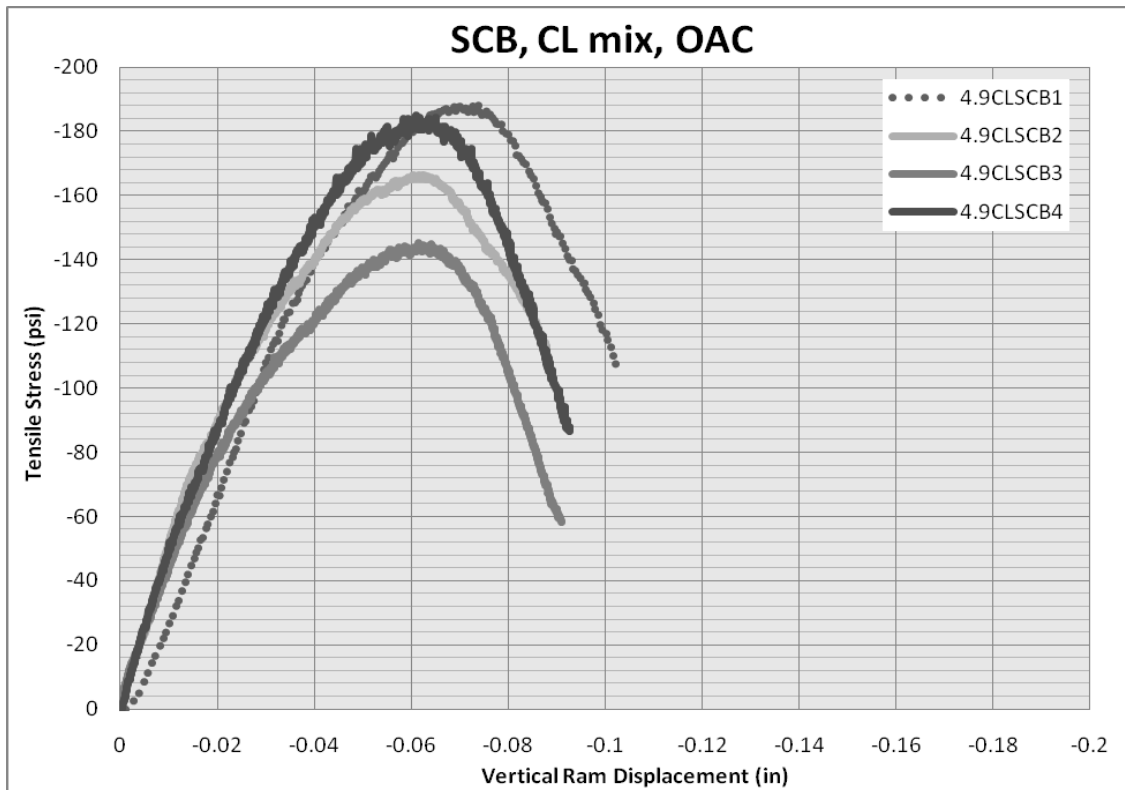


Figure C-6. Type D SCB Stiffness Response @ OAC.

Table C-10. Type CL SCB Results @ OAC.

OAC	Sample ID	AV	Max Applied Load (lbf)	Max Tensile Stress (psi)	Ram Disp @ Max Load (in)
4.9%	4.9CLSCB1	7.1%	513	189	0.070
4.9%	4.9CLSCB2	7.3%	453	167	0.062
4.9%	4.9CLSCB3	7.5%	395	145	0.062
4.9%	4.9CLSCB4	7.5%	447	164	0.061
Average:		7.4%	452	166	0.064
StDev:		0.2%	48	18	0.004
COV:		2.65%	10.63%	10.77%	6.63%

## APPENDIX C: CRACKING TEST RESULTS (CONTINUED)



**Figure C-7. Type CL SCB Stiffness Response @ OAC.**

**Table C-11. Monotonic IDT Test Results.**

OAC	Sample ID	AV	Max Applied Load (lbf)
5.0%	5.0DIDT1	7.1%	2285
5.0%	5.0DIDT2	7.3%	1710
<i>Average:</i>		7.2%	1998
<i>StDev:</i>		0.2%	407
<i>COV:</i>		2.46%	20.35%

## **APPENDIX C: CRACKING TEST RESULTS (CONTINUED)**

### **Test Method Evaluation and Scoring Criteria**

A summary of the mix performance and test method utility rankings can be found in Tables 5-8 and 5-10, respectively. Each test method was evaluated based on its repeatability and time requirements. The 6-inch DT test received the lowest score in this area because the results were more variable than those of the other methods; however, the variability was still acceptable given the tolerance of a maximum COV of 30 percent. The IDT and SCB test methods received the highest score in this aspect because the variability between specimen test results was relatively low, a trait that is desirable for verification of conclusions inferred from test results. The OT, R-IDT, and R-SCB tests received the lowest score in time requirements because, on average, the tests ran 45 minutes (the longest test duration and 40 minutes longer than the run time of the monotonic test methods).

Each of the tests required a certain specimen fabrication procedure. Every method was evaluated based on the ease and repeatability of this process. The 4- and 6-inch DT specimens were the most difficult to prepare for testing. The trimming of the specimen required two machines (a concrete saw and a coring drill) compared with just one machine for the other test specimens. Also, gluing was not easily repeatable and required a minimum of 12 hours for curing before testing could occur.

On the other end of the spectrum, The IDT (R-IDT) specimen scored the highest in specimen fabrication and preparation because the trimming was very easy and repeatable and the preparation required only the gluing of LVDTs to the specimen. Four inch and 6-inch DT specimens had the highest frequency of meeting the target AV after trimming, while the SCB (R-SCB) was problematic in this area. Although the amount of specimens with AV outside the target range was higher than for the other tests, this was acceptable because the SCB (R-SCB) specimens can be fabricated faster than the other specimens.

The IDT (R-IDT) and SCB (R-SCB) tests have the highest potential for field core testing because the specimen geometry closely matches (IDT) or can be trimmed from (SCB) typical cores. In contrast, the 4-inch and 6-inch DT specimens have the lowest potential because typical pavement layers are thinner than the required height for either specimen. Specimen shape, in comparison with the original mold geometry, has a significant influence on the distribution of

AV within the trimmed specimen geometry. As described in detail in Chapter 4, the 4-inch specimen produced a well distributed AV content in the DT specimen. For this reason, the 4-inch DT received the highest score in this area. In contrast to these results, the 6-inch specimen had the largest variation in AV content in the trimmed specimen, thus the 6-inch test was the worst performing in this area. Time and resources cost money; therefore, an assessment of the cost of each test method is pertinent. The OT test proved to be the most draining on time and resources as specimen preparation requires a minimum of 12 hours for gluing and the test run time has the longest duration. The SCB test method was the most efficient because the specimen could be made at least twice as fast as any other specimen and testing preparation required neither plates nor LVDT gluing.

The range of test methods was also subjected to a stringent assessment of the ability of each test to accurately and appropriately characterize the tensile properties of each mix type. All of the monotonic testing analysis models were relatively simple, but the IDT and SCB were the most complicated due mostly to the specimen geometry and/or induced stress concentrations. These analyses could usually be completed in 30 minutes or less; however, the OT (and thus potentially the R-IDT and R-SCB) test was best in this category as the interpretation of the data was extremely simple and could be done within minutes of receiving the number of cycles to failure. Variability of the test results is relatively important because consistent results are necessary for accurate predictions of material properties. The 4-inch DT test gave the least variable results with an average COV of 14.7 percent in the strain and 2.3 percent in the stress (Table 5-3), while the 6 inch test gave the most variable results with an average COV of 15.3 percent for the strain and 20.9 percent for the stress (Table 5-3). However, even the latter COV is below the maximum threshold value for variation. It is also important to note that the OT test did not exhibit the variability issues stated in the literature review.

All the five test methods evaluated thus far have a close correlation to the loading patterns in typical HMA pavements, but the IDT test has the least application to pavement loading because the tensile strength is measured indirectly and stiffness measurements (strain) can be affected greatly by the nominal aggregate size. Both DT test methods are the most appropriate methods for analyzing the tensile properties of a mix if used in a pavement because the specimen is tested in direct tension as opposed to some indirect form. A repeated version of

this test (necessarily a 4-inch height) may prove to be very appropriate as a surrogate in the academic research area.

Also of relative importance is the ease with which the chosen test can be incorporated into daily mix-design processes. Although the OT test is often used in TxDOT designs presently and offers a readily interpretable parameter for crack resistance properties of a mix, the test requires a large amount of precious time for preparation and testing that may be necessary for more pressing matters in field construction. The OT, IDT, and SCB received the same score in this area because the two qualities are somewhat reversed. The IDT and SCB require very little time, relative to the OT test, for specimen fabrication and testing preparation, but the parameter for crack resistance characterization cannot be interpreted as quickly. However, both DT test methods require the same time demand as the OT for test preparation, and the parameters can be interpreted in a similar timeframe to the IDT and SCB tests. This compounding of disadvantageous properties scores both DT tests the lowest in the area of daily mix-design applicability. The introduction of the R-IDT and R-SCB tests allows the incorporation of the good qualities of the SCB and IDT tests with those of the OT test. The R-SCB test has the best potential to become a surrogate test in the area of routine mix-design and screening.



## APPENDIX D: OT ROUND-ROBIN TEST RESULTS

**Table D-1. OT Cracking Test Results for Lab# 1.**

<b>Specimen#</b>	<b>Mix</b>	<b>Specimen Thickness (inches)</b>	<b>AV (%)</b>	<b>Loading Rate (inches)</b>	<b>Initial Peak Load (lb)</b>	<b>OT Cycles to Failure (N<sub>OT</sub>)</b>	<b>Failure Mode</b>	<b>Comment</b>
D1	Type D = 5% PG 70-22 + Limestone	1.50	6.9	0.025	608	250	Single cracking	TTI researchers
D2	Type D = 5% PG 70-22 + Limestone	1.50	6.7	0.025	750	186	Single cracking	TTI researchers
D4	Type D = 5% PG 70-22 + Limestone	1.50	7.0	0.025	705	196	Single cracking	Lab technician
D6	Type D = 5% PG 70-22 + Limestone	1.51	6.6	0.025	669	355	Single cracking	Lab technician
Avg.		1.50	6.8	0.025	683	247		
COV		0.0%	2.7%	0.0%	8.8%	31.4%	COV is slightly greater than 30%	
Range		1.50–1.51	6.6–7.0	0.025–0.025	608–750	186–355		

## APPENDIX D: OT ROUND-ROBIN TEST RESULTS (CONTINUED)

**Table D-2. OT Cracking Test Results for Lab# 2.**

Specimen#	Mix	Specimen Thickness (inches)	AV (%)	Loading Rate (inches)	Initial Peak Load (lb)	OT Cycles to Failure (N <sub>OT</sub> )	Failure Mode	Comment
D1*	Type D = 5% PG 70-22 + Limestone	1.54	8.0	0.025	604	1000	Double cracking	TTI researchers
D2	Type D = 5% PG 70-22 + Limestone	1.53	7.6	0.025	608	312	Single cracking	Lab personnel
D4	Type D = 5% PG 70-22 + Limestone	1.52	6.9	0.025	657	301	Single cracking	TTI researchers
D5	Type D = 5% PG 70-22 + Limestone	1.51	7.3	0.025	713	174	Single cracking	Lab personnel
D7	Type D = 5% PG 70-22 + Limestone	1.50	7.4	0.025	652	203	Single cracking	Lab personnel
D8	Type D = 5% PG 70-22 + Limestone	1.53*	7.1	0.025	601	284	Single cracking	Lab personnel
Avg. (all)		1.52	7.4	0.025	639	379	Avg. OT cycles is 255 if only single cracking is considered	
Avg. (single cracking only)		1.52	7.3	0.025	646	255		
COV (all)		1.0%	5.2%	0.0%	6.9%	81.6%	COV is 24% if only single cracking is considered, which is reasonable (< 25%)	
COV (single cracking only)		0.7%	3.7%	0.0%	7.0%	24.4%		
Range (all)		1.50–1.54	6.9–8.0	0.025–0.025	604–713	174–1000	Range is 174 to 312 OT cycles if only single cracking is considered	
Range (single cracking only)		1.50–1.53	6.9–7.6	0.025–0.025	608–713	174–312		

## APPENDIX D: OT ROUND-ROBIN TEST RESULTS (CONTINUED)

**Table D-3. OT Cracking Test Results for Lab# 3.**

<b>Specimen#</b>	<b>Mix</b>	<b>Specimen Thickness (inches)</b>	<b>AV (%)</b>	<b>Loading Rate (inches)</b>	<b>Initial Peak Load (lb)</b>	<b>OT Cycles to Failure (N<sub>OT</sub>)</b>	<b>Failure Mode</b>	<b>Comment</b>
D1	Type D = 5% PG 70-22 + Limestone	1.51	7.4	0.025	536	287	Single cracking	Lab technician
D3	Type D = 5% PG 70-22 + Limestone	1.50	6.9	0.025	613	173	Single cracking	TTI researchers
D4	Type D = 5% PG 70-22 + Limestone	1.49	7.0	0.025	580	201	Single cracking	TTI researchers
D5	Type D = 5% PG 70-22 + Limestone	1.51	6.9	0.025	592	220	Single cracking	Lab technician
Avg.		1.50	7.1	0.025	580	220		
COV		0.0%	3.4%	0.0%	5.6%	22.0%	COV is reasonable (< 25%)	
Range		1.49–1.51	6.9–7.4	0.025–0.025	536– 592	173– 287		

## APPENDIX D: OT ROUND-ROBIN TEST RESULTS (CONTINUED)

**Table D-4. OT Cracking Test Results for Lab# 4.**

Specimen#	Mix	Specimen Thickness (inches)	AV (%)	Loading Rate (inches)	Initial Peak Load (lb)	OT Cycles to Failure (N <sub>OT</sub> )	Failure Mode	Comment
D4*	Type D = 5% PG 70-22 + Limestone	1.50	7.0	0.023	698	465	Single cracking	TTI researchers
D6*	Type D = 5% PG 70-22 + Limestone	1.51	6.7	0.023	695	467	Single cracking	Lab technician
D1	Type D = 5% PG 70-22 + Limestone	1.50	7.0	0.025	674	215	Single cracking	TTI researchers
D2	Type D = 5% PG 70-22 + Limestone	1.52	6.9	0.025	617	305	Single cracking	Lab technician
D3	Type D = 5% PG 70-22 + Limestone	1.50	7.1	0.025	631	291	Single cracking	TTI researchers
D5	Type D = 5% PG 70-22 + Limestone	1.50	6.3	0.025	754	252	Single cracking	Lab technician
Avg. (for 0.025 inches only)		1.50	6.8	0.025	669	266		
COV (for 0.025 inches only)		0.6%	5.3%	0.0%	9.2%	15.3%	COV is very reasonable (< 25%)	
Range (for 0.025 inches only)		1.5–1.52	6.3–7.1	0.025–0.025	617–754	215–305		

## APPENDIX D: OT ROUND-ROBIN TEST RESULTS (CONTINUED)

**Table D-5. OT Cracking Test Results for Lab# 5.**

Specimen#	Mix	Specimen Thickness (inches)	AV (%)	Loading Rate (inches)	Initial Peak Load (lb)	OT Cycles to Failure (N <sub>OT</sub> )	Failure Mode	Comment
D4*	Type D = 5% PG 70-22 + Limestone	1.50	6.7	0.025	621	708	Double cracking	Lab technician
D2	Type D = 5% PG 70-22 + Limestone	1.51	7.1	0.025	550	363	Single cracking	TTI researchers
D3	Type D = 5% PG 70-22 + Limestone	1.50	7.0	0.025	576	238	Single cracking	TTI researchers
D5	Type D = 5% PG 70-22 + Limestone	1.49	6.7	0.025	566	334	Single cracking	Lab technician
Avg. (all)		1.50	6.9	0.025	578	411	Avg. OT cycles is 312 if only single cracking is considered	
Avg. (single cracking only)		1.50	7.3	0.025	564	312		
COV (all)		0.5%	3.0%	0.0%	5.3%	50.0%	COV is 21% if only single cracking is considered, which is reasonable (< 25%)	
COV (single cracking only)		0.7%	4.3%	0.0%	2.3%	21.0%		
Range (all)		1.49–1.51	6.7–7.1	0.025–0.025	550–621	238–708	Range is 238 to 363 OT cycles if only single cracking is considered	
Range (single cracking only)		1.49–1.51	6.7–7.1	0.025–0.025	550–576	238–363		

## APPENDIX D: OT ROUND-ROBIN TEST RESULTS (CONTINUED)

**Table D-6. OT Cracking Test Results for Lab# 6.**

Specimen#	Mix	Specimen Thickness (inches)	AV (%)	Loading Rate (inches)	Initial Peak Load (lb)	OT Cycles to Failure (N <sub>OT</sub> )	Failure Mode	Comment
D1	Type D = 5% PG 70-22 + Limestone	1.50	7.4	0.025	692	259	Single cracking	TTI researchers
D2	Type D = 5% PG 70-22 + Limestone	1.49	7.7	0.025	562	325	Single cracking	TTI researchers
D3	Type D = 5% PG 70-22 + Limestone	1.51	7.2	0.025	667	281	Single cracking	TTI researchers
D4	Type D = 5% PG 70-22 + Limestone	1.50	6.8	0.025	632	257	Single cracking	TTI researchers
D5	Type D = 5% PG 70-22 + Limestone	1.51	6.7	0.025	726	155	Single cracking	TTI researchers
D6	Type D = 5% PG 70-22 + Limestone	1.51	7.0	0.025	593	277	Single cracking	TTI researchers
D7	Type D = 5% PG 70-22 + Limestone	1.50	6.9	0.025	614	242	Single cracking	TTI researchers
D8	Type D = 5% PG 70-22 + Limestone	1.49	6.6	0.025	760	177	Single cracking	TTI researchers
Avg.		1.50	7.0	0.025	656	247		
COV		0.6%	5.3%	0.0%	10.4%	22.6%	COV is reasonable (< 25%)	
Range		1.49–1.51	6.6–7.7	0.025–0.025	562–760	155–325		

## APPENDIX E: MIX-DESIGN DETAILS FOR WORKABILITY AND COMPACTABILITY INDICATOR TESTS

**Table E-1. Gradation Sheet for B Mix (Chico).**

			Bin No.1	Bin No.2	Bin No.3	Bin No.4
Individual Bin (%):			Bin No.1 = 37%	Bin No.2 = 25%	Bin No.3 = 28%	Bin No.4 = 10%
Aggregate Source:			Hanson p Hill	Hanson p Hill	Hanson p Hill	T.X.I.
Sample ID:			TY "B"	TY "D-F"	MAN-SAND	SAND
INDIVIDUAL	Sieve Size:		Aggregate	Aggregate	Aggregate	Aggregate
	Passing	Retained	Weight	Weight	Weight	Weight
	-	1-1/2"	0.0	0.0	0.0	0.0
	1-1/2"	1"	0.0	0.0	0.0	0.0
	1"	3/4"	123.2	0.0	0.0	0.0
	3/4"	3/8"	877.5	38.3	0.0	0.0
	3/8"	No. 4	561.1	867.4	22.7	0.9
	No. 4	No. 8	81.6	205.9	229.3	9.9
	No. 8	No. 30	6.7	3.4	724.5	23.9
	No. 30	No. 50	0.0	1.1	170.1	43.2
	No. 50	No. 200	1.7	1.1	83.2	328.1
	No. 200	Pan	13.3	7.9	30.2	44.1
Totals			1665.0	1125.0	1260.0	450.0

## APPENDIX E: MIX-DESIGN DETAILS FOR WORKABILITY AND COMPACTABILITY INDICATOR TESTS (CONTINUED)

**Table E-2. Gradation Sheet for D Mix (Chico).**

			Bin No.1	Bin No.2	Bin No.3
Individual Bin (%):			Bin No.1 = 56%	Bin No.2 = 36%	Bin No.3 = 8%
Aggregate Source:			HANSON	HANSON	T.X.I
Aggregate Number:			Type "D-F"	MAN_SAND	SAND
Sample ID:					
<b>INDIVIDUAL</b>	Sieve Size:		Aggregate Weight	Aggregate Weight	Aggregate Weight
	Passing	Retained			
	-	3/4"	0.0	0.0	0.0
	3/4"	1/2"	0.0	0.0	0.0
	1/2"	3/8"	32.8	1.6	0.0
	3/8"	No. 4	1552.3	38.9	1.8
	No. 4	No. 8	796.3	353.2	4.3
	No. 8	No. 30	80.6	871.6	8.6
	No. 30	No. 50	7.6	205.7	17.6
	No. 50	No. 200	5.0	98.8	274.7
	No. 200	Pan	45.4	50.2	52.9
	Totals		2520.0	1620.0	360.0



## APPENDIX F: APT CONSTRUCTION DETAILS

**Table F-1. Laboratory HMA Mix Evaluation.**

#	Mix	Comment	Remark
1	Type C (Hunter-Modified), 4.9% PG 70-22 + Limestone	Unsatisfactory <ul style="list-style-type: none"> <li>• Very low OT cycles (&lt; 50)</li> <li>• Poor quality aggregates; highly absorptive</li> </ul>	X
2	Type D (Chico), 5.0% PG 70-22 + Limestone	Unsatisfactory <ul style="list-style-type: none"> <li>• Trouble with Texas Gyratory</li> </ul>	X
3	Type C (Chico), 6.0% PG 76-22 + Limestone	Unsatisfactory <ul style="list-style-type: none"> <li>• Could not meet the balanced mix-design criteria (more rutting @ higher OAC)</li> </ul>	X
4	Type C (Beaumont-Original), 4.3% PG 64-22 + Limestone	Unsatisfactory <ul style="list-style-type: none"> <li>• Did not pass the Hamburg</li> </ul>	X
5	Type C (Beaumont-Control), 4.3% PG 76-22 + Limestone	<i>Satisfactory – to be used as the control mix for APT testing.</i>	√
6	Type C (Beaumont-Modified), 5.2% PG 76-22 + Limestone	<i>Satisfactory – to be used as the modified mix for APT testing.</i>	√

# APPENDIX F: APT CONSTRUCTION DETAILS (CONTINUED)

## Marking of the Test Sections

During this reporting period, marking had been completed for the rutting sections only. The test area under the ALF is considered to be 40-ft long and the dual wheels are each 9-inch wide, with a 6-inch separation between tires. Based on these considerations, the rutting test sections were thus marked as follows:

- a) Put a paint strip down the center of both sections, the center of the ALF tires will be positioned as close as possible around this line.
- b) Detailed measurements will be made at 5-ft intervals in the center of each ALF tire. Data will be collected 7.5-inch on either side of the paint strip at 5-ft spacing as shown below. It may be useful to place a small paint spot at 7.5-inch offsets on either side of the center paint strip. This will be a total of 18 test points on the pavement ( 0, 5, 10, 15, 20, 25, 30, and 40 ft and  $\pm 7.5$ -inch either side of paint strip).
- c) In addition to the 18 spots discussed above, there will be another 6 spots marked as shown below (Figure F-1). These will be at 15, 20, and 25 ft and another 7.5-inch outside the original spots (these will be 15-inch from the center strip to measure upheaval).
- d) In addition, one randomly selected control spot will be established no where close to the test area. This spot will just be utilized to check the gauge repeatability.

For a total of 26 test spots on each section.

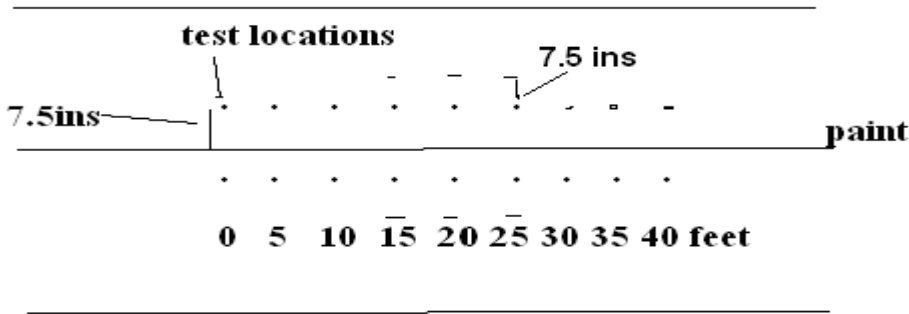


Figure F-1. Test Measurement Spots.

## APPENDIX F: APT CONSTRUCTION DETAILS (CONTINUED)

### **Upfront Testing**

Prior to the start of the ALF testing, it is proposed that the following measurements will be made. Test at all the 26 locations.

- a) FWD deflections at all the 26 locations. Put FWD load plate on each spot, measure deflections at 2 or 3 different FWD loads. Measure temperature of the HMA during all the FWD tests, take readings in the middle of HMA layer at beginning, middle, and end of FWD testing.
- b) Density measurements at all the 26 locations using either a thin life nuclear gauge or a non-nuclear density gauge or both. Note the same gauge(s) with the same settings will be used throughout the test program. This is necessary to determine if either mix is changing substantially.
- c) Measure initial rut profile transversely over the 9 locations (0, 5, 10, 15, 20, 25, 30, 35, 40 ft).

### **ALF Rutting Test Program**

The objective is to test the two rutting sections in hot weather to measure the rut potential of both mixes. The goals of this first round of ALF testing are:

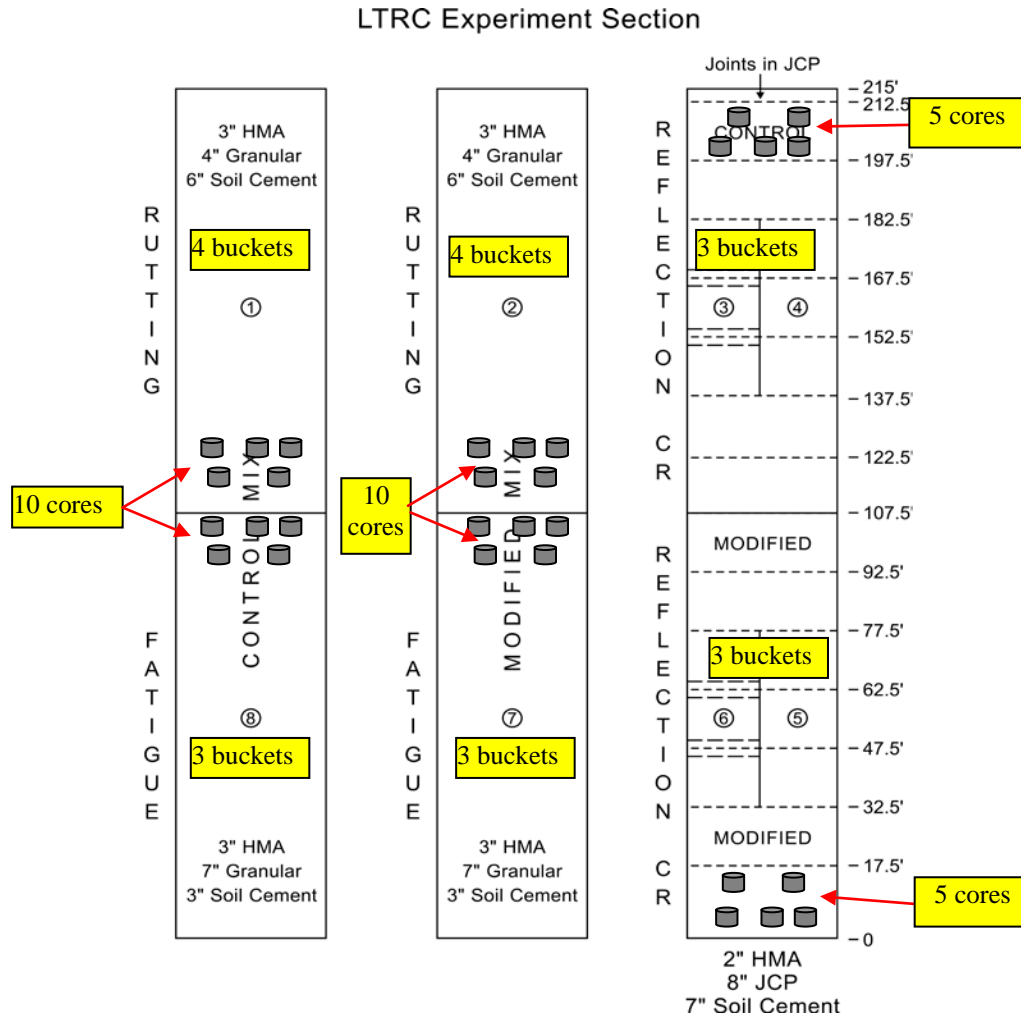
- 1) Compare the rutting performance of the control versus the modified mix.
- 2) Measure the change in air voids with load applications for both mixes under the wheel path and outside of the wheel path.

Up to 10,000 passes will be put on each section prior to moving the ALF to the adjacent section. The standard 5000 lb per tire and 100 psi will be utilized for the first 10 k ALF applications. The test plan is as follows.

**Table F-2. ALF Rutting Test Plan.**

<b>ALF Reps</b>	<b>Strain (1)</b>	<b>FWD</b>	<b>Rut</b>	<b>Density</b>
0 (2)	x	x	x	x
100	x		x	x
500			x	x
1000	x		x	x
5000			x	x
10000	x	x	x	x

## APPENDIX F: APT CONSTRUCTION DETAILS (CONTINUED)



**Figure F-2. Plant-Mix (Buckets) and Core Locations.**